ROLE OF TRANSLATION FACTOR eIF5A AND ITS HYPUSINE MODIFICATION IN SYNTHESIS OF POLYPROLINE PROTEINS

by
Erik Niko Espiritu Gutierrez

A dissertation submitted to Johns Hopkins University in conformity with the requirements for the degree of Doctor of Philosophy

Baltimore, Maryland
November 2014

© 2014 Erik E. Gutierrez
All Rights Reserved

Abstract

In addition to the small and large ribosomal subunits, aminoacyl-tRNAs, and mRNA, cellular protein synthesis is dependent on translation factors. Since its discovery nearly 40 years ago, eIF5A is one such factor that has remained a mystery. eIF5A was initially characterized based on its ability to stimulate methionyl-puromycin synthesis, a model assay for protein synthesis; however, the function of this factor in cellular protein synthesis has been difficult to resolve. Interestingly, eIF5A is the sole cellular protein to contain the post-translational hypusine modification. Hypusine formation requires the conserved enzymes deoxyhypusine synthase and deoxyhypusine hydroxylase for its biosynthesis. This dissertation focuses on the novel role of the translation factor eIF5A and its hypusine modification in the elongation phase of protein synthesis. Combining yeast genetic and biochemical techniques, we uncover new functional and mechanistic insights for the role of eIF5A and its hypusine modification in translation. Similar to its bacterial homolog EF-P, eIF5A stimulates the production of proteins containing runs of consecutive proline residues. In addition, genome-wide ribosome profiling studies reveal ribosomal pausing and drop-off on mRNA sequences encoding polyproline. Moreover, molecular analyses of eIF5A mutants dependent on the conserved hydroxyl group on hypusine demonstrate that the second step of hypusine synthesis contributes to the translation function of the factor. Taken together, these discoveries delineate the extraordinary role of eIF5A and its hypusine modification in the synthesis of polyproline sequences and reinforces the position of eIF5A as a crucial factor in translation elongation.

Thesis Committee

Dr. Orna Cohen-Fix	Cell Cycle Regulation and Nuclear Structure Section, NIDDK/NIH and CMDB/JHU
Dr. Thomas Dever	Advisor, Section on Protein Biosynthesis, NICHD/NIH
Dr. Nicholas Ingolia	Carnegie Institution of Science, CMDB/JHU
Dr. Daniel Masison	Protein Chaperones and Amyloid Section, NIDDK/NIH
Dr. Sarah Woodson	Department of Biophysics, CMDB/JHU

Readers

Drs. Thomas Dever and Sarah Woodson

Preface and Acknowledgements

First and foremost, I thank God for providing me with the strength and courage to pursue my dream. He has placed me in good company and amongst individuals who continue to show a selfless regard for others.

I am eternally grateful to my advisor, Dr. Thomas Dever, for his tireless mentorship and guidance over the years. His enthusiasm for science is contagious and his support for his graduate students and postdoctoral fellows is inspirational. He truly cares for the growth and development of his trainees. Tom will remain a lifelong mentor and friend.

I have been very fortunate to be a laboratory member of the Section on Protein Biosynthesis (Dever lab) for the past three and a half years. The lab is filled with dedicated, supportive and talented individuals who made it a pleasure to come to work everyday. I will be forever grateful for their contributions to my growth as a scientist. I would like to thank current and past lab members, including Dr. Cheryl Bolinger, Chune Cao, Dr. Ivaylo Ivanov, Dr. Margarito Jacinto-Rojas, Joo-Ran Kim, Jason Murray, Dr. Yvette Pittman and Dr. Meghna Thakur, with special thanks to Dr. Byung Shin for sharing his technical expertise and for providing valuable reagents.

I would like to extend my gratitude to current and past members of the Section on Nutrient Control of Gene Expression (Hinnebusch lab) especially Fan Zhang, for being the "glue" that kept the lab together, and Dr. Alan Hinnebusch for his advice and constructive criticism during my scientific lab meetings.

I would like to thank Dr. Ramanujan Hegde for his mentorship and support during the early years of graduate school. Manu has been an instrumental contributor to my development as a scientist.

I am gracious to my collaborators: Drs. Peter Backlund, Allen Buskirk, Rachel Green, Nicholas Guydosh and Christopher Woolstenhulme. Without their technical support and scientific expertise, it would have been nearly impossible to complete the necessary experiments to round out my story.

I would like to thank my thesis and examining committee members, including Drs. Sarah Woodson, Daniel Masison and Orna Cohen-Fix, and past member Dr. Nicholas Ingolia, for attending my progress reports, accommodating meeting schedules, reading my dissertation, and providing constructive feedback.

I thank my wife Nina, who with me, endured the agonies and challenges of my graduate school career. Despite the long days in the lab (which often led to negative experimental results), Nina has supported and encouraged me to continue the arduous journey of the PhD degree.

I would like to give heartfelt thanks to my parents, Meynardo and Crispina Gutierrez. My parents are first-generation immigrants from the Philippines. My father worked as a grade school teacher and my mother was an administrative worker for the city of Cambridge, MA. They raised my sister and I with a tremendous emphasis on the values of hard work and education.

Lastly, I would like to dedicate this work to my daughter Isabella who, at the time this was written, is two years old. Isabella, one day you may come across this body of work, attempt to read it, and toss it aside. I want you to know that God has put us here for

a reason. Always remember to find joy in asking questions and to hold on to a childlike curiosity and an emboldened passion in whatever it is that you do. Always remember that daddy loves you very much.

Table of Contents

1. Introduction 1

1.1 Protein synthesis requires dedicated translation machinery 2

1.2 The discovery of eIF5A and its bacterial homolog EF-P 7

1.3 Structural analysis of eIF5A/EF-P and EF-P bound to 70S ribosomes 10

1.4 Post-translational modifications of eIF5A and EF-P 15

1.4.1 Hypusination of eIF5A 15

1.4.2 Phosphorylation of eIF5A 22

1.4.3 β-lysinylation (lysylation) of EF-P 22

1.5 Yeast studies reveal a role for eIF5A in translation elongation 23

1.6 Thesis research objectives and significance of findings 27

2. Materials and Methods 31

2.1 Yeast strains 32

2.2 Polysome analysis 33

2.3 Plasmid and yeast strain construction 34

2.4 Dual luciferase assay 37

2.5 Peptide formation assay 41

2.6 Preparation of initiation and elongation factors 43

2.7 Preparation of wild-type and mutant eIF5A 45

2.8 Preparation of mRNA, tRNA, and ribosomes 47

2.9 Preparation of ribosome footprints and mRNA-Seq libraries for deep sequencing 49

3. eIF5A promotes translation of polyproline motifs 52

3.1 The significance and rationale for study 53

3.2 eIF5A stimulates translation through polyproline sequences *in vivo* 54

3.3 Expression of yeast polyproline-containing proteins requires eIF5A *in vivo* 65

3.4 eIF5A plays an essential role in polyproline peptide synthesis 67

3.5 Conclusion 71

4. Genome-wide profiling reveals ribosomal stalling during translation of polyproline sequences in a temperature-sensitive eIF5A mutant 73

4.1 The ribosome profiling strategy for the identification of translational targets of eIF5A 74

4.2 The preparation of ribosome footprint and total mRNA libraries 75

4.3 Ribosome profiling reveals widespread ribosomal pausing and drop-off around polyproline motifs 86

4.4 Conclusion 89

5. Identification and characterization of eIF5A mutants that require the hydroxyl group on hypusine 91

5.1 The significance and rationale for study 92

5.2 Isolation of randomly mutated *HYP2* alleles that confer a strong slow-growth phenotype in the absence of *LIA1* 93

5.3 *LIA1*-dependent mutations in *HYP2* are positioned in the N-terminal domain of eIF5A 98

5.4 *LIA1*-dependent eIF5A mutants exhibit altered polysome profiles 100

5.5 Loss of *LIA1* does not result in decreased levels of the eIF5A mutant proteins 103

5.6 *LIA1*-dependent eIF5A mutations do not promote the reversibility of the deoxyhypusine modification 105

5.7 Impaired stimulation of polyproline synthesis by deoxyhypusine forms of eIF5A mutants 109

5.8 Conclusion 119

6. Discussion 120

6.1 eIF5A and EF-P promote production of polyproline proteins 121

6.2 The requirement of the hypusine/β-lysyl-lysine modification for eIF5A/EF-P function in protein synthesis 129

6.3 eIF5A is the keymaster that presents hypusine to the ribosome active site 134

6.4 eIF5A/EF-P: the third universally conserved elongation factor 136

7. References 139

7.1 Appendix: Glossary of Abbreviations 140

7.2 Bibliography 141

8. Curriculum Vitae 166

8.1 Curriculum Vitae 167

8.2 Papers published as a member of the Ramanujan Hegde laboratory 170

List of Figures

Figure 1. Schematic of the translation elongation cycle. 4

Figure 2. Sequence alignment of eIF5A and EF-P. 12

Figure 3. Comparison of eIF5A and EF-P structures. 14

Figure 4. Structure of EF-P–70S ribosome co-complex. 15

Figure 5. Post-translational modification pathways for eIF5A and EF-P. 17

Figure 6. eIF5A stimulates translation of polyproline motifs *in vivo*. 56

Figure 7. Summary of the firefly to *Renilla* luminescence ratios for each of the reporters transformed into wild-type eIF5A and eIF5A-S149P mutant yeast strains grown at 33°C. 59

Figure 8. The *ts*$^{-}$ eIF5A-S149P mutant impairs yeast cell growth, protein expression, and translation elongation. 60

Figure 9. eEF2 and eEF3 mutants do not specifically impair polyproline synthesis. 62

Figure 10. Translation of three or more consecutive proline codons reveals eIF5A dependency. 64

Figure 11. Expression of polyproline-containing proteins requires eIF5A *in vivo*. 66

Figure 12. eIF5A stimulates synthesis of polyproline peptides.. 69ow turn off auto-update

Figure 13. Schematic of the ribosome footprinting protocol. 77

Figure 14. Sucrose density gradients for isolation of 80S monosomes in nuclease-treated lysates containing wild-type or mutant eIF5A. 79

Figure 15. Size selection of ribosome footprint and total mRNA fragments. 80

Figure 16. Linker ligation of footprint and total mRNA. 81

Figure 17. Reverse transcription products of footprint and total mRNA samples. 82

Figure 18. Isolation of PCR products for generation of cDNA library for deep sequencing. 84

Figure 19. BioAnalyzer profiles of cDNA deep-sequencing libraries. 85

Figure 20. Genome-wide ribosome pausing and drop-off at polyproline sequences in the eIF5A mutant strain. 88

Figure 21. Genetic screen to identify *LIA1*-dependent mutants of eIF5A in yeast. 95

Figure 22. eIF5A primary sequence and location of mutations in *LIA1*-dependent eIF5A mutants. 99

Figure 23. *LIA1*-dependent eIF5A mutants exhibit translation elongation defects and a loss of polysomes. 102

Figure 24. *LIA1*-dependent mutations in *HYP2* do not affect eIF5A protein levels. 104

Figure 25. MS analyses of *LIA1*-dependent eIF5A mutants purified from yeast. 107

Figure 26. Stimulation of polyproline synthesis by eIF5A both *in vivo* and *in vitro* requires the hydroxyl group on hypusine. 112

Figure 27. Post-translational modification pathway for EF-P. 131

Figure 28. Model of eIF5A stimulating polyproline synthesis. 135

1. Introduction

1.1 Protein synthesis requires dedicated translation machinery

The translation of mRNAs to generate proteins is a fundamental attribute of the central dogma of molecular biology and requires dedicated translation machinery to facilitate cellular protein synthesis. Composed of distinct initiation, elongation, termination, and recycling stages, protein synthesis is the process in which the ribosome, the protein-synthesizing engine of the cell, uses a template mRNA to guide the step-wise addition of amino acids to form polypeptides. In addition to mRNA, aminoacyl-tRNAs, and the small and large ribosomal subunits, translation factors are also required to promote the production of proteins. As translation factors are among the most abundant proteins in the cell, they are also prolific energy consumers as some factors bind guanosine-5'-triphosphate (GTP) to drive the different stages of protein synthesis.

Translation initiation is the first and typically rate-limiting stage of translation. In this phase of eukaryotic translation, initiation factors assist in: 1) the delivery of the initiator methionyl-tRNA (Met-$tRNA_i^{Met}$) to the 40S subunit, 2) the binding of the resulting 43S complex to an mRNA, and 3) the assembly of an 80S ribosome on a start codon (reviewed in Hinnebusch and Lorsch, 2012). Whereas translation initiation requires at least eleven factors in eukaryotes (eIFs), bacteria need only three initiation factors (IFs) (reviewed in Simonetti et al., 2009). The difference in factor requirements between eukaryotes and bacteria can be attributed to the direct targeting of the small ribosomal subunit to the translation start site in bacteria by the Shine-Dalgarno sequence versus the 5'-cap-dependent scanning mechanism in eukaryotes.

Once the eukaryotic 80S ribosome is positioned on an mRNA with a Met-$tRNA_i^{Met}$ anticodon base-paired with the start codon, the ribosome is ready for the

elongation phase of protein synthesis. At this stage, the 80S ribosome consists of three distinct sites for translation of the mRNA sequence: an A site, a P site, and an E site. The ribosomal A site is the destination for aminoacyl-tRNAs except for the first aminoacyl-tRNA which is bound to the P site. The aminoacyl-tRNA that enters the A site is the acceptor for the growing polypeptide chain during peptide bond formation. The P site is the location of the peptidyl-tRNA attached to the growing polypeptide chain. The E site contains a deacylated tRNA that is ready for exiting the ribosome.

While bacteria and eukaryotes have largely distinct mechanisms for translation initiation, the elongation phase is very similar in mechanism and highly conserved in factor requirements (reviewed in Dever and Green, 2012). In the elongation stage (Fig. 1), the eukaryotic elongation factors (eEFs) eEF1A (EF-Tu in bacteria) and eEF2 (EF-G in bacteria) have largely defined functions. With peptidyl-tRNA in the P site, the eEF1A ternary complex (eEF1A–GTP–aminoacyl-tRNA) binds the vacant ribosomal A site in a codon-dependent manner. Upon codon recognition by the tRNA, GTP is hydrolyzed resulting in release of eEF1A and accommodation of the aminoacyl-tRNA in the A site. As seen in bacterial ribosomes, it is thought that high fidelity decoding of the mRNA is dependent on the ability of the EF-Tu–GTP–aminoacyl-tRNA to bind the A site and to facilitate interactions with the 16S rRNA (reviewed in Schmeing et al., 2009; Schmeing et al., 2011).

After accommodation of the cognate aminoacyl-tRNA to the A site, the ribosome then catalyzes peptide bond formation between the peptidyl-tRNA in the P site and the aminoacyl-tRNA in the A site. This peptidyl transferase reaction is facilitated by rRNA through a nucleophilic attack of the α-amino group of the aminoacyl-tRNA on the

carbonyl carbon of the peptidyl-tRNA. The peptidyl transferase center (PTC) consists of highly conserved rRNA elements that promote this peptidyl transfer reaction.

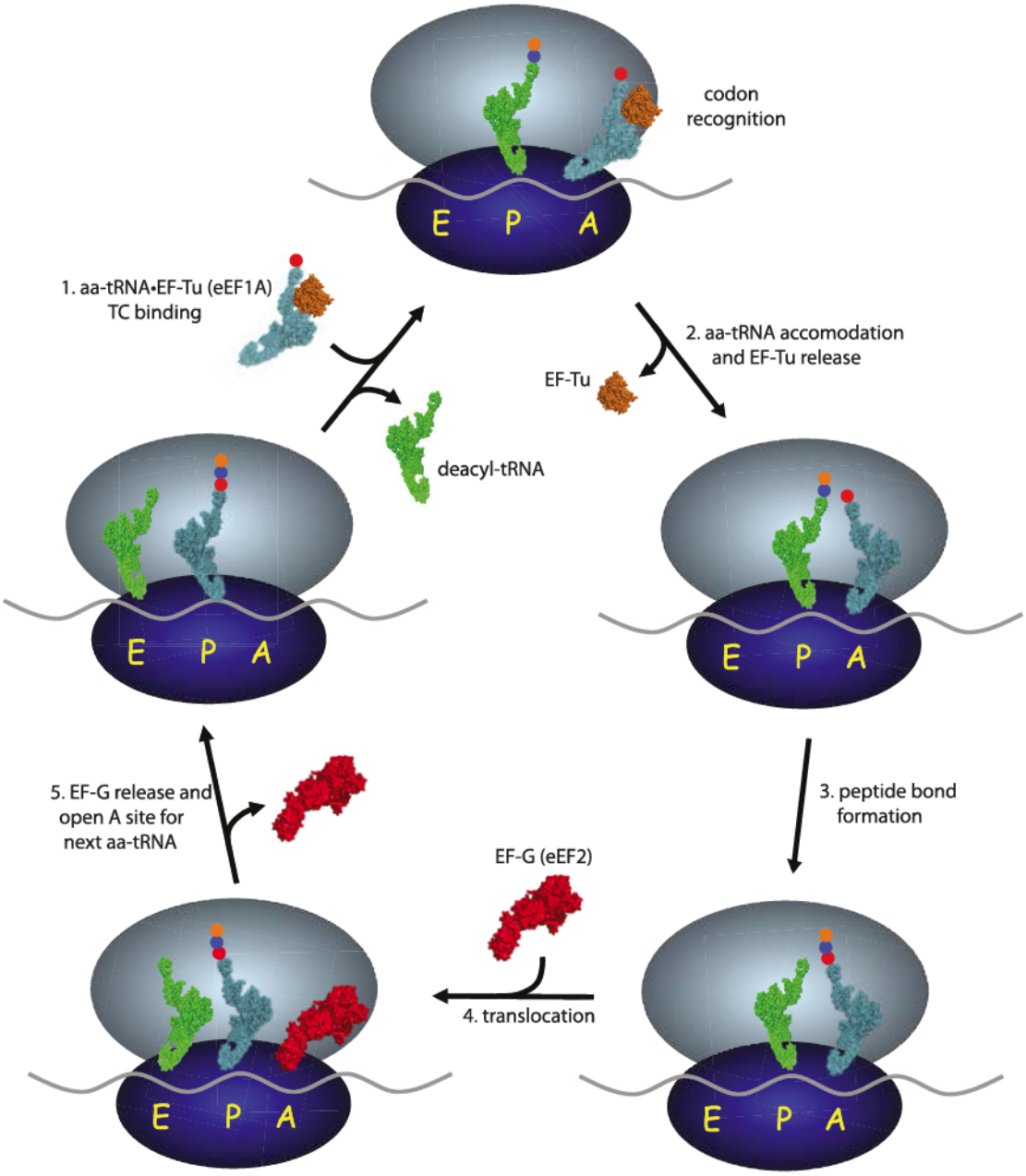

Figure 1. Schematic of the translation elongation cycle.

(Top) An EF-Tu(eEF1A)–GTP–aminoacyl(aa)-tRNA ternary complex (TC) binds aa-tRNA to the A site of the 70S (eukaryotic 80S) ribosome in a codon-dependent manner. (Middle right) Following release of EF-Tu–GDP, the aa-tRNA is accommodated into the A site. Peptide bond formation (lower right) is followed by binding of EF-G (eEF2)–GTP (lower left), which promotes translocation of the deacylated tRNA and peptidyl-tRNA into the canonical E and P sites, respectively. (Middle left) Following release of EF-G–GDP, the ribosome is ready for the next cycle of elongation.

Next, the large and small subunits assume a ratcheted state allowing for movement of the tRNAs into hybrid P/E and A/P states with the acceptor ends of the tRNAs in E and P sites and the anticodon loops at the P and A sites. The factor eEF2/EF-G promotes the translocation of the tRNAs and mRNA on the ribosome leaving the deacylated tRNA and the peptidyl-tRNA in the canonical E and P sites, respectively. It is thought that the GTPase eEF2/EF-G bound to GTP stabilizes the hybrid state and, upon binding the ribosome, results in GTP hydrolysis and inorganic phosphate (P_i) release. It is also presupposed that P_i release can de-ratchet the ribosome relieving the hybrid state conformation and allowing movement of the tRNAs and mRNA (Dever and Green, 2012). In the post-translocation state, eEF2/EF-G is released and the A site is open for delivery of the next eEF1A–GTP–aminoacyl-tRNA ternary complex for an additional round of elongation. When the ribosome encounters a stop codon (UAA, UGA, or UAG) in the A site, release factors bind the A site and promote hydrolysis of the peptidyl-tRNA linkage, releasing the completed polypeptide chain from the ribosome. Then, ribosome recycling factors promote the dissociation of the ribosome, tRNA and mRNA. Thus, by their

interactions with various components of the translation machinery, translation factors play essential roles in facilitating protein synthesis.

My thesis project focuses on the role of the translation factor eIF5A and its enigmatic hypusine modification in protein synthesis. eIF5A was first identified in the early 1970s when purified from rabbit reticulocyte lysates and found to stimulate methionyl-puromycin (Met-Pmn) peptide synthesis, a model assay for translation that monitors the transfer of a methionine from Met-tRNA in the ribosomal P site to puromycin, an aminoacyl-tRNA analog that binds in the A site. Based on this activity, this assay was interpreted as an indicator of first peptide bond formation and thus, eIF5A was linked to a role in translation initiation (Benne and Hershey, 1978). However, more recent genetic and biochemical studies on eIF5A demonstrate a prevalent role for the factor in the elongation phase of protein synthesis (Saini et al., 2009; Zanelli et al., 2006). In a cellular context, eIF5A has also been implicated in nucleocytoplasmic transport (Bevec et al., 1996; Hofmann et al., 2001; Ruhl et al., 1993) and mRNA stability (Schrader et al., 2006; Zuk and Jacobson, 1998). Furthermore, eIF5A has been linked to oncogenesis, diabetes, and HIV-1 infections (reviewed in Kaiser, 2012). Presumably, these cellular processes are regulated at the level of translation by eIF5A and, when dysfunctional, can result in disease.

In this thesis, I discuss the role of eIF5A and its hypusine modification in protein synthesis. First, I give a comprehensive overview of the field prior to the time I joined the Dever lab in early 2011. Next, I relate eIF5A to the translation field and present the outstanding questions circa 2011 and the objectives of my research. Then, I present my key findings and results. Finally, I end with a discussion on the major developments in

the field during my time in the Dever lab, the impact and implications of our work in the field, and propose future areas of research.

1.2 The discovery of eIF5A and its bacterial homolog EF-P

eIF5A and its bacterial ortholog EF-P were identified by their isolation from cellular extracts. Initially, *in vitro* reconstituted model assays were used to characterize the functions of these factors and to define their actions during discrete phases of translation. Purified from rabbit reticulocytes, eIF5A (originally named IF-M2Bα or eIF-4D) was identified as an abundant 17 kDa protein and shown to stimulate the overall yield of Met-Pmn synthesis in assays containing 80S ribosomes, the known complement of initiation factors (eIF2, eIF1A, eIF3, and eIF5) and the trinucleotide 5'-AUG-3' mRNA (Benne et al., 1978; Benne and Hershey, 1978; Kemper et al., 1976; Schreier et al., 1977). In this assay, 80S initiation complexes were first assembled with Met-$tRNA_i^{Met}$ in the P site. Then, the assay monitored the transfer of methionine to puromycin, a partial mimic of aminoacyl-tRNA that binds to the ribosomal A site. Interestingly, eIF5A did not affect other model assays for translation initiation such as 43S pre-initiation or 80S initiation complex formation (Benne and Hershey, 1978; Schreier et al., 1977). However, based upon the ability to stimulate Met-Pmn synthesis, but not other assays monitoring early steps of translation initiation, it was proposed that eIF5A functioned to promote formation of the first peptide bond or to facilitate the transition from the initiation to the elongation phase of protein synthesis (Benne and Hershey, 1978). It is also notable that puromycin is an aminonucleoside antibiotic and has been shown to be an imperfect substrate due to its poor positioning in the ribosome active site (Wohlgemuth et al., 2008;

Youngman et al., 2004). Nevertheless, the stimulation of Met-Pmn synthesis could indicate roles for eIF5A in first peptide bond synthesis, general translation elongation, and/or the reactivity of poor substrates, like puromycin, in the ribosome active site.

Along with its ability to stimulate Met-Pmn synthesis, eIF5A was found to stimulate the overall yield of polyphenylalanine (encoded by a polyU mRNA) synthesized by 80S ribosomes at low Mg^{2+} concentrations (Kemper et al., 1976). When assayed at 10 mM Mg^{2+}, synthesis of polyphenylalanine required only translation elongation factors; however, at low Mg^{2+} concentrations this assay also required the initiation factors eIF1A, eIF2A (now called eIF2D), eIF5B, and eIF5A (Merrick, 1979a), though the role of initiation factors in this assay was not clear. The 2-4–fold stimulatory activity of eIF5A in the polyphenylalanine and Met-Pmn synthesis assays, which both monitored the formation of a peptide bond, was consistent with the notion that eIF5A functions in translation elongation. However, when eIF5A was added to assays monitoring the synthesis of globin protein chains, it failed to stimulate globin synthesis. Arguably, this result was inconsistent with a role for eIF5A throughout translation elongation. While this apparent lack of activity might be attributed to the presence of eIF5A in the post-ribosomal supernatant and crude aminoacyl-tRNA synthetase preps used for the globin synthesis assays (Merrick, 1979b; Thomas et al., 1979), the addition of eIF5A did not stimulate the yield of globin synthesis in reconstituted assays using purified aminoacyl-tRNAs and thus lacking this proposed eIF5A contamination (Schreier et al., 1977). In additional *in vitro* experiments, eIF5A lowered the Mg^{2+} requirement for globin synthesis in assays lacking spermidine (Schreier et al., 1977). However, when similar assays were conducted in the presence of spermidine at the low Mg^{2+}

concentration, eIF5A did not exhibit a stimulatory effect. The authors proposed that eIF5A could have a role in protein synthesis aside from translation initiation, perhaps mimicking the role of polyamines during protein synthesis though the function of polyamines is unclear.

Concurrent with the discovery of eIF5A in rabbit reticulocytes and its characterization in model assays of protein synthesis, the bacterial ortholog of eIF5A called EF-P was purified from *E.* coli extracts with >90% in the post-ribosomal supernatant. EF-P was shown to stimulate formylmethionyl (fMet)-Pmn synthesis in an assay consisting of 70S ribosomes, [^{35}S]fMet-tRNA$_{Met}$, mRNA, and puromycin. Based upon this initial observation, EF-P was proposed to be an elongation factor that functioned to promote peptide bond synthesis on the ribosome (Glick and Ganoza, 1975). In a subsequent study, EF-P was found to differentially stimulate dipeptide synthesis between fMet-tRNA and the cytidyl-aminoacyladenosine (C-A) analogs of the acceptor ends of various aminoacyl-tRNAs. Interestingly, the EF-P stimulatory activity was most pronounced for the A-site substrates C-A-Gly, puromycin, and C-A-Ala, leading to the hypothesis that EF-P promoted the activity of poor substrates (smaller and/or less hydrophobic side chains) for peptidyl transfer (Ganoza and Aoki, 2000; Glick et al., 1979).

Intriguingly, eIF5A is the only known cellular protein to contain the amino acid hypusine (N^{ε}-(4-amino-2-hydroxybutyl)lysine) (Park et al., 1981). Hypusine was initially identified as a free and unattached amino acid isolated from bovine brain, and was later reported to be widely distributed in other tissues. Hypusine is highly basic and was named for its component parts: hydroxyputrescine and lysine (Shiba et al., 1971). When

cultured mammalian cells were grown in the presence of [^{3}H]spermidine, eIF5A was the single labeled protein resolved by two-dimensional gel electrophoresis (Cooper et al., 1982; Cooper et al., 1983; Park et al., 1981). The size (~17 kDa) and pI (~5.1) of the hypusine-containing protein, as well as the direct correlation of increased hypusine labeling with increased rates of protein synthesis in mammalian cells, led to the hypothesis that hypusine plays a critical role in cellular protein synthesis. Furthermore, the detection of hypusine in acid hydrolysates of highly purified eIF5A confirmed its identity as the sole hypusine-containing protein (Cooper et al., 1983). Finally, cloning of eIF5A and comparison of the predicted amino acid sequence from the cDNA with the observed sequence based on Edman degradation revealed that Lys50 was the site of the hypusine modification in mammalian eIF5A (Park et al., 1986; Smit-McBride et al., 1989a). Further genome sequencing efforts and spermidine labeling studies revealed that the hypusine (or at least deoxyhypusine) modification is conserved in all eukaryotic eIF5A and archaeal aIF5A proteins (Bartig et al., 1992; Bartig et al., 1990; Gordon et al., 1987a; Park et al., 1997). Moreover, despite the absence of hypusine in bacteria, amino acid sequence comparisons revealed that bacterial EF-P, eukaryotic eIF5A and archaeal aIF5A are homologs (Kyrpides and Woese, 1998). Given their common ability to stimulate Met-Pmn synthesis assays, it was reasonably proposed that eIF5A and EF-P perform similar functions in cellular protein synthesis (Saini et al., 2009).

1.3 Structural analysis of eIF5A/EF-P and EF-P bound to 70S ribosomes

Both yeast and humans express two eIF5A proteins, and the two forms of eIF5A within each organism share strong (80-90%) amino acid sequence identity. Moreover, the eIF5A

proteins in yeast, humans, and fruit fly consist of 153-159 residues and share >50% amino acid sequence identity with the highest degree of amino acid similarity existing near the site of the hypusine modification (Fig. 2). The archaeal aIF5A shows strong similarity to the eukaryotic factor, though archaeal aIF5A is truncated by around 10 residues at the N-terminus compared to the eukaryotic factor. Bacterial EF-P is around 30 residues longer than eIF5A (Fig. 2), and based on multiple sequence alignments these extra residues are inserted in the C-terminal half of the protein. It is noteworthy that the sequence flanking the site of hypusine modification K-x-G-Hyp-H-G-x-A-K is conserved among eukaryotes and archaea. Four of the residues in this motif (Lys, both Gly, and Ala) are also conserved in EF-P, while the His residue is not present in EF-P and the Lys residue that is modified to hypusine is conserved in EF-P from *E. coli* but substituted with Arg in *T. thermophilus* EF-P (Fig. 2).

The crystal structures of eIF5A and EF-P from several eukaryotes, archaea and bacteria have been solved and the proteins show significant structural similarity. aIF5A from *M. jannaschii* (Kim et al., 1998), *P. aerophilum* (Peat et al., 1998), and *P. horikoshii* (Yao et al., 2003), and eIF5A from human (Tong et al., 2009) and yeast (pdb code 3ER0) fold into a two domain structure with residues ~1-83 forming the N-terminal domain. This N-terminal domain consists of six β-strands that fold into a partially open β-barrel (Kim et al., 1998), while the C-terminal domain, consisting of 3-5 β-strands and 0-2 α-helices, resembles an OB-fold type of β-barrel domain (Kim et al., 1998; Peat et al., 1998; Yao et al., 2003) (Fig. 3). In all structures, the highly conserved residues flanking the site of hypusine modification are in a long unstructured loop (the hypusine loop) between strands β3 and β4 that protrudes from the N-terminal domain (Fig. 3).

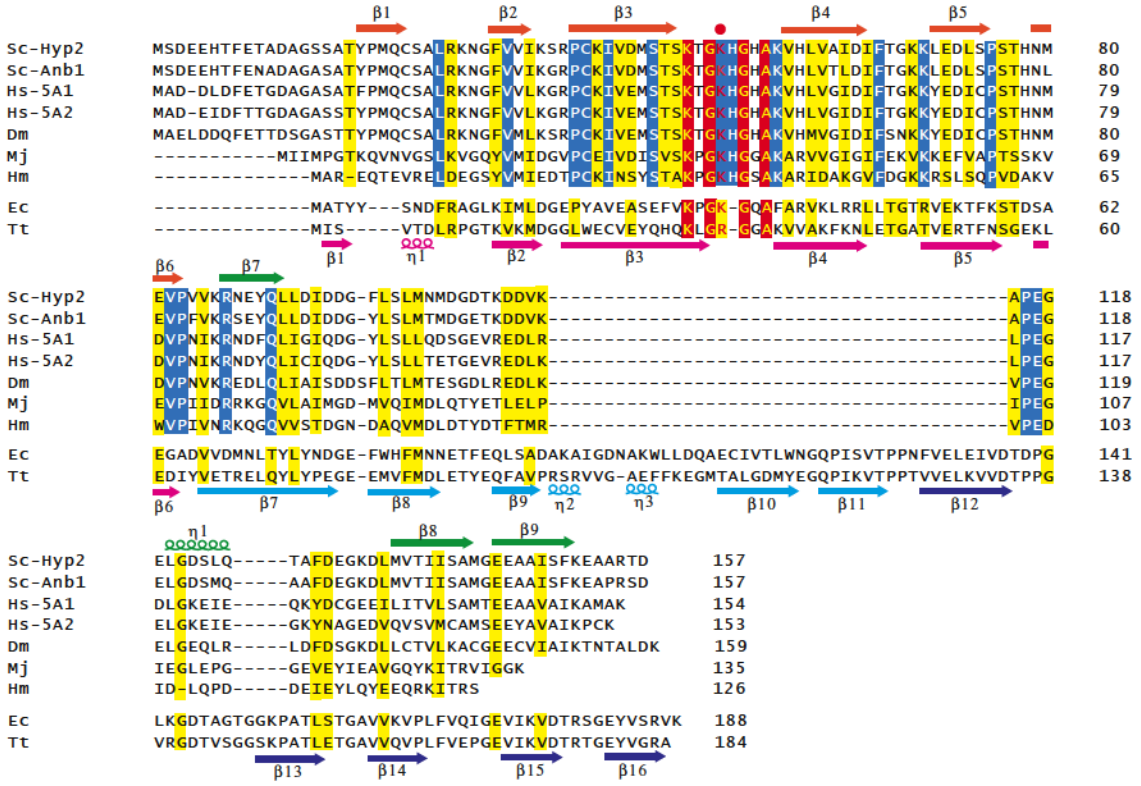

Figure 2. Sequence alignment of eIF5A and EF-P.

Multiple sequence alignment of yeast (*Saccharomyces cerevisiae*, Sc) Hyp2 (Tif51A; eIF5A1) and Anb1 (Tif51B, eIF5A2), human (Hs) eIF5A1 and eIF5A2, fly (*Drosophila melanogaster*, Dm) eIF5A, archaeal (*Methanococcus jannaschii*, Mj, and *Haloarcula marismortui*, Hm) aIF5A, and bacterial (*Escherichia coli*, Ec, and *Thermus thermophilus*, Tt) EF-P was performed using Clustal X (v2.0). Residues in red are identical in all eIF5A and EF-P proteins; residues in blue are identical only in eIF5A and aIF5A; and residues in yellow are conserved in eIF5A and EF-P. Secondary structure elements are shown at the top (eIF5A) and bottom (EF-P) of the sequences (arrow = β-strand, loops = α-helix). The lysine residue that is modified to hypusine in eIF5A and aIF5A and β-lysinylated in

E. coli EF-P is denoted by the red dot above the alignment. Figure is from Dever et al. (Dever et al., 2014).

In contrast to the two-lobed structure of eIF5A, EF-P is composed of three domains (Hanawa-Suetsugu et al., 2004) (Fig. 3). The N-terminal domain I of EF-P can be superimposed on the N-terminal domain of eIF5A, while domains II and III of EF-P share structural similarity with one another and with the C-terminal domain of eIF5A (Fig. 3). The three domains of free EF-P are arranged in an L-shaped configuration that resembles the structure of tRNA (Hanawa-Suetsugu et al., 2004). In support of this structural resemblance, the co-crystal structure of EF-P bound to the *T. thermophilus* 70S ribosome revealed that EF-P binds adjacent to the P-site tRNA in a location that partially overlaps the E site of the ribosome (Blaha et al., 2009) (Fig. 4). Domain I of EF-P binds near the acceptor stem of the P-site tRNA and contacts the large ribosomal subunit, while domain III of EF-P is located adjacent to the anticodon of the P-site tRNA and partially overlaps the E site of the small ribosomal subunit. Based on the extensive overlap of domain III of EF-P with the position of an E-site tRNA on the small subunit, EF-P binding is predicted to preclude binding of tRNA to the E site.

Although eIF5A lacks a structure corresponding to domain III of EF-P, it can be proposed that eIF5A binds to a similar region on the 80S ribosome. Accordingly, eIF5A would be positioned adjacent to the P-site tRNA and would overlap the ribosomal E site with the N-terminal domain of eIF5A lying close to the acceptor stem of the P-site tRNA. Interestingly, the Arg32 residue of *T. thermophilus* EF-P corresponds to Lys51 of *S. cerevisiae*, the site of hypusine modification. Modeling of hypusine in place of Arg32

(Blaha et al., 2009) indicates that the hypusine modification could extend into the PTC of the ribosome and influence peptide bond synthesis.

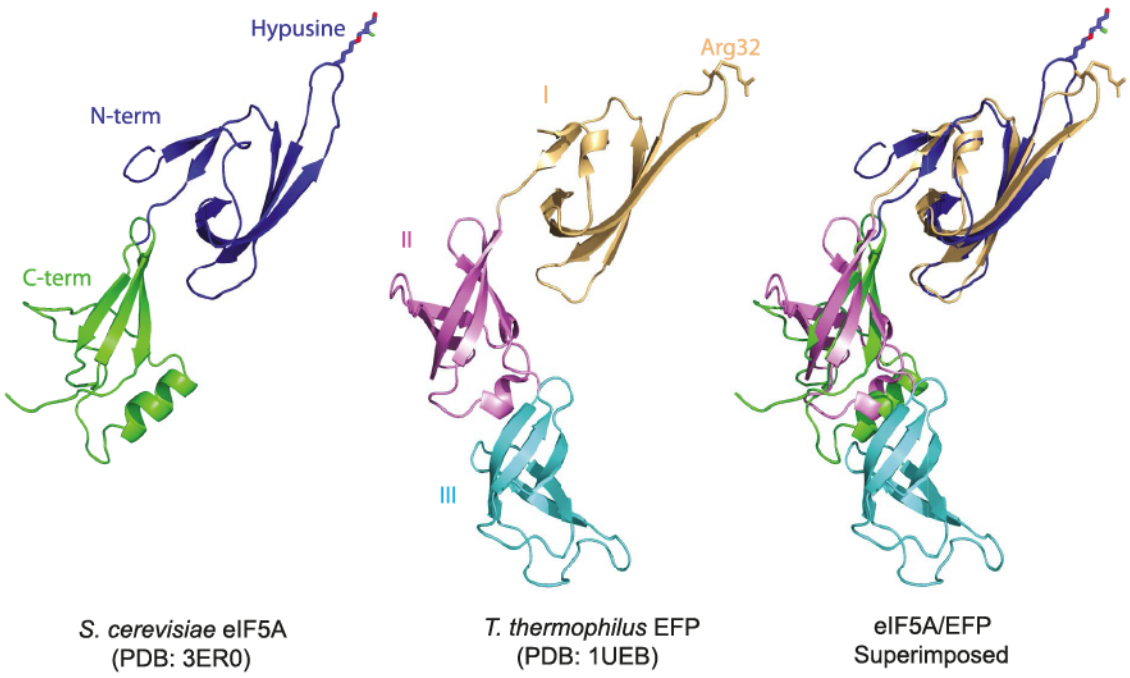

Figure 3. Comparison of eIF5A and EF-P structures.

Structures of *Saccharomyces cerevisiae* eIF5A (Left, PDB: 3ER0) and *Thermus thermophilus* EF-P (middle, PDB: 1UEB (Hanawa-Suetsugu et al., 2004)) are superimposed (right) using PyMOL software (PyMOL Molecular Graphics System, Version 1.5.0.4 Schrödinger, LLC). Colors are used to highlight the domains of eIF5A, N-terminal domain (blue) and C-terminal domain (green), and EF-P, domain I (gold), domain II (magenta), and domain III (cyan). The modeled hypusine residue of eIF5A and corresponding Arg32 residue of EF-P are shown as a stick representation.

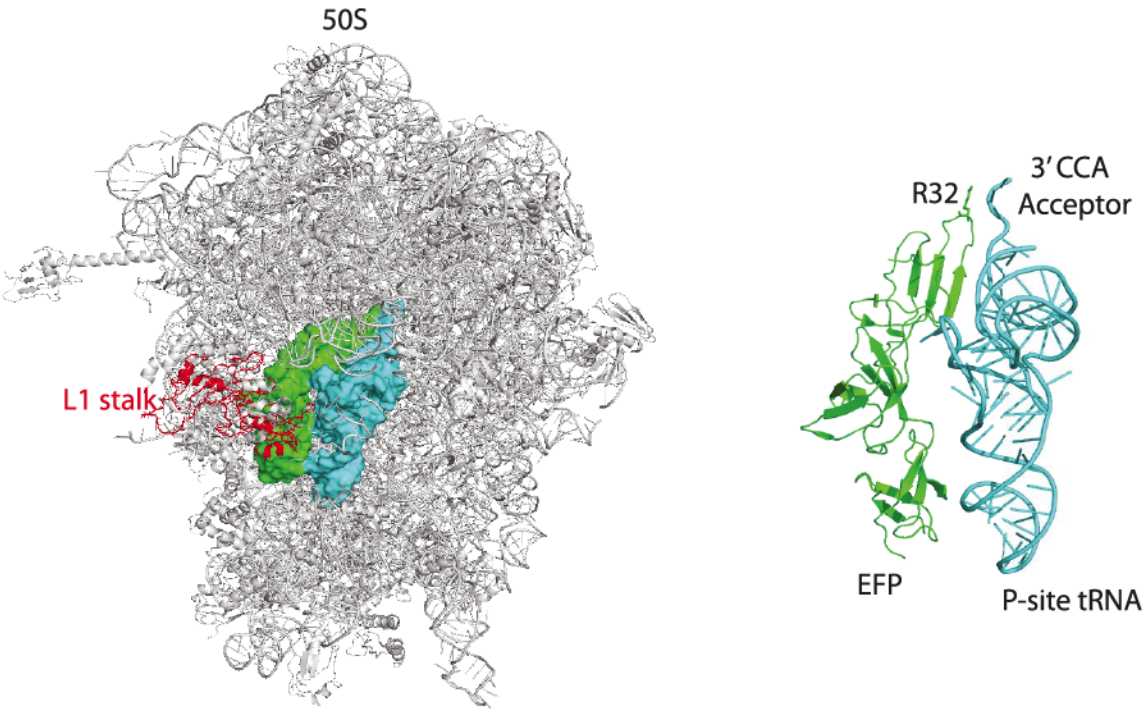

Figure 4. Structure of EF-P–70S ribosome co-complex.

(Left) EF-P–70S ribosome complex (PDB: 3HUW and 3HUX, (Blaha et al., 2009)). 70S ribosome is colored gray. EF-P is colored green and $tRNA_f^{Met}$ in the P site is colored cyan. (Right) Magnified view of EF-P and P-site $tRNA_f^{Met}$ structures.

1.4 Post-translational modifications of eIF5A and EF-P

1.4.1 Hypusination of eIF5A

As mentioned above, eIF5A is the only known protein to contain the amino acid hypusine. When cells are grown in the presence of [^{3}H]spermidine, eIF5A was the only protein that was labeled with [^{3}H] as monitored by two-dimensional gel electrophoresis (Park et al., 1981). The post-translational hypusine modification on eIF5A appeared to occur shortly after eIF5A synthesis with no pools of unmodified eIF5A except when the protein was

synthesized in cells depleted of spermidine (Murphey and Gerner, 1987; Park, 1987). Moreover, hypusine formation in eIF5A appeared to be constitutive with no evidence of turnover or reversion of the protein to the unmodified state (Duncan and Hershey, 1986; Gordon et al., 1987b). Interestingly, in spermidine-dependent mutants of yeast, the hypusine modification of eIF5A appeared to be limiting for cell growth, indicating that hypusine formation is a critical role of spermidine in cells (Chattopadhyay et al., 2008).

Hypusine biosynthesis is tightly controlled by two enzymes: deoxyhypusine synthase (DHS) and deoxyhypusine hydroxylase (DOHH) (Fig. 5A). First, DHS catalyzes the transfer of an *N*-butylamine group from spermidine to the ε-amino group of the conserved lysine on eIF5A (Lys50 in human eIF5A and Lys51 in yeast) to form deoxyhypusine. In a second step, DOHH converts the deoxyhypusine residue to hypusine by addition of a hydroxyl group (Park et al., 1981; Park et al., 2010) (Fig. 5A). This latter step involves a stereo-specific hydroxylation at C2 of the *N*-butylamine residue of deoxyhypusine (N^{ε}-(butylamine)lysine)) to form hypusine (N^{ε}-(4-amino-2-hydroxybutyl)lysine) (Abbruzzese et al., 1986; Park et al., 2006). Both genetic and biochemical studies demonstrated that the hypusine modification is critical for eIF5A function. While wild-type yeast or human eIF5A can complement a lethal eIF5A knockout in yeast, a conservative mutation that substituted Arg for Lys at the site of hypusination blocked the ability of yeast or human eIF5A to complement the lethal phenotype of a yeast mutant lacking eIF5A (Magdolen et al., 1994; Schnier et al., 1991). Consistent with these *in vivo* results, unmodified forms of eIF5A that were produced in bacteria or purified from a chinese hamster ovary (CHO) cell line grown in the presence

of 2-difluoromethylornithine, an inhibitor of spermidine biosynthesis, failed to stimulate Met-Pmn synthesis *in vitro* (Park, 1989; Park et al., 1991; Smit-McBride et al., 1989b).

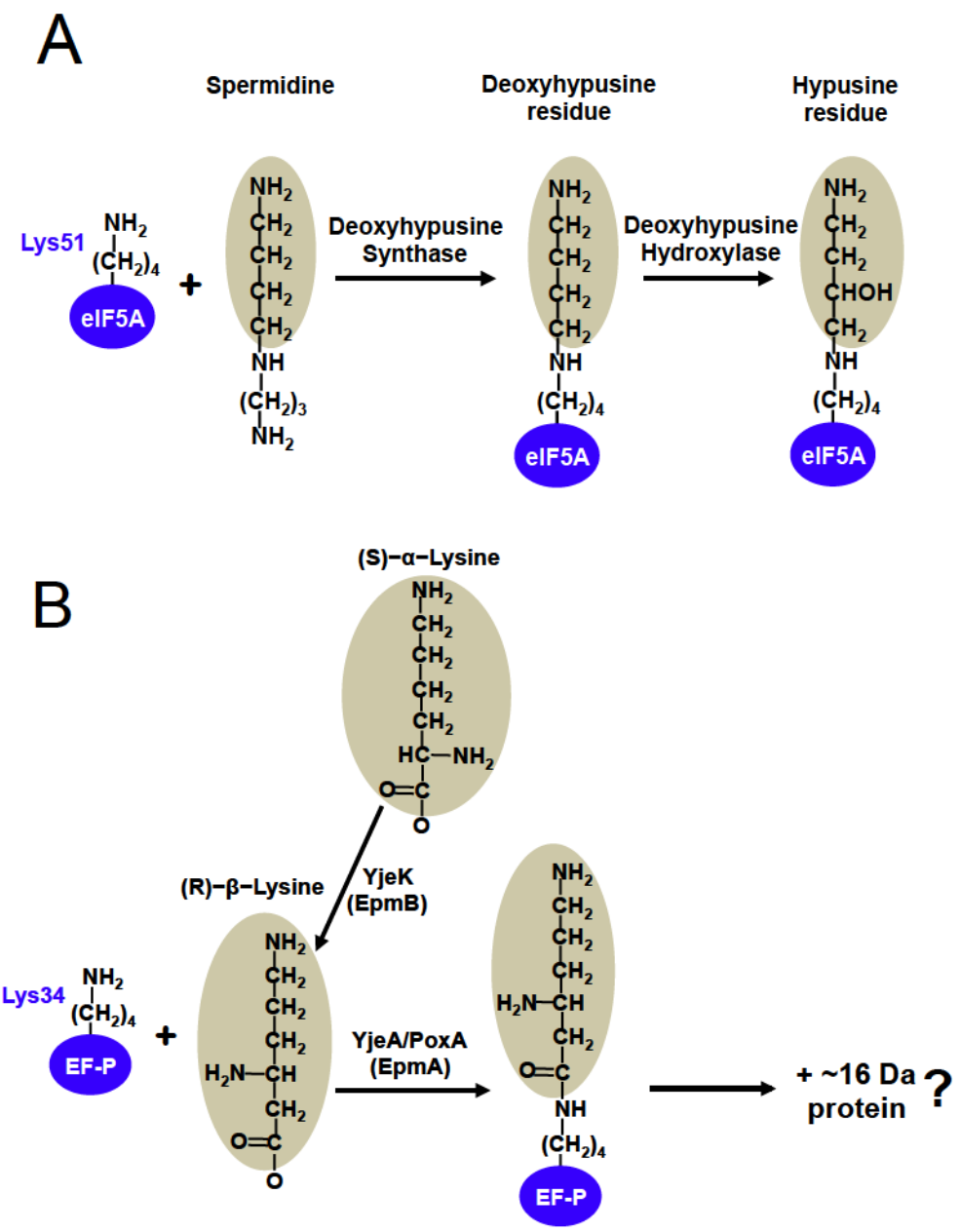

Figure 5. Post-translational modification pathways for eIF5A and EF-P.

(A) In eukaryotes and archaea, an *N*-butylamine moiety is transferred from spermidine to the ε-amino group of the specific lysine residue (Lys50 in human eIF5A and Lys51 in

yeast) by the enzyme DHS. Next, DOHH adds a hydroxyl group to convert deoxyhypusine to hypusine.

(B) In bacteria, β-lysinylation of EF-P occurs in two known steps catalyzed by YjeK (EpmB) and YjeA/PoxA (EpmA). First, YjeK, a lysine aminomutase, converts lysine to β-lysine. Next, YjeA/PoxA catalyzes the addition of β-lysine onto the specific lysine residue (Lys34 on *E. coli* EF-P). It was controversial whether the EF-P post-translational β-lysinylation pathway produces a ~128 or a ~144 Da modification.

In contrast to the lack of function of unmodified eIF5A, the partially modified deoxyhypusine form of eIF5A is functional. Purified DHS was readily able to add deoxyhypusine to recombinant eIF5A, but not to recombinant eIF5A-K51R (Park et al., 1991), indicating that Arg is not an acceptor for deoxyhypusine and consistent with the failure of the K51R mutant to function *in vivo*. The deoxyhypusinated recombinant eIF5A stimulated Met-Pmn synthesis, though not as robustly as native eIF5A purified from HeLa cells (Park et al., 1991). While this result could have indicated that full hypusine modification was required for eIF5A function, more recent experiments using recombinant eIF5A produced in bacteria co-expressing DHS or DHS plus DOHH revealed nearly equivalent abilities of the deoxyhypusine and hypusine forms of eIF5A to stimulate Met-Pmn synthesis (Park et al., 2011). Consistent with this latter result, it was noteworthy that yeast strains lacking the *LIA1* gene encoding yeast DOHH were viable and grow only slightly slower than wild-type strains (Park et al., 2006; Park, 2006).

The enzymes for hypusine synthesis, DHS and DOHH, are conserved in eukaryotes and show high specificity for eIF5A (Park et al., 1997). The DHS enzyme

from yeast was identified based on the sequence of tryptic peptides from purified rat DHS (Kang et al., 1995). The cloned *DYS1* gene in yeast encodes a protein of 387 amino acids that possesses DHS activity, and biochemical studies revealed yeast DHS to be a homotetramer of the ~43 kDa subunits (Kang et al., 1995). Consistent with the deoxyhypusine requirement for eIF5A stimulation of Met-Pmn and peptide synthesis, and with the inability of eIF5A-K51R to function *in vivo*, the *DYS1* gene is essential for yeast viability (Park et al., 1998; Sasaki et al., 1996). Deoxyhypusine synthesis proceeds through a multistep process including spermidine cleavage, a DHS-imine intermediate, and then transfer of the *N*-butylamine moiety from the enzyme to eIF5A (Wolff et al., 1997; Wolff et al., 1995; Wolff et al., 1990). Interestingly, the DHS reaction required NAD (Chen and Dou, 1988; Wolff et al., 1990), and the NAD cofactor as well as N1-guanyl-1,7-diaminoheptane (GC7), a spermidine analog and inhibitor of DHS, were observed in crystal structures of human DHS (Liao et al., 1998; Umland et al., 2004).

Yeast DOHH was initially identified based on its interaction with eIF5A in a yeast two-hybrid assay (Thompson et al., 2003). The protein was named LIA1 to signify that it was a LIgand of eIF5A. Subsequently, Park and colleagues screened a yeast GST-open reading frame (ORF) expression library for DOHH activity and identified LIA1 (Park et al., 2006). Consistent with this biochemical assignment, deletion of the *LIA1* gene blocked the production of hypusine, but not deoxyhypusine in yeast (Park et al., 2006). Sequence analysis of the DOHH enzyme suggests that the 325 amino acid protein contains eight HEAT repeats with conserved His-Glu motifs present in four of the repeats (Park et al., 2006). DOHH contains 2 molecules of iron, thought to be present in a diiron active site, per enzyme (Kim et al., 2006), and mutation of the conserved His-Glu motifs

impaired Fe and/or eIF5A binding to DOHH (Kang et al., 2007). In contrast to the non-essential nature of DOHH in budding and fission yeast (Park et al., 2006; Weir and Yaffe, 2004), loss of DOHH is recessively lethal in *C. elegans* (Sugimoto, 2004) and *Drosophila* (Patel et al., 2009), suggesting perhaps that the hydroxyl group on hypusine is more critical for eIF5A function in metazoan cells. While the function of the hydroxyl group on hypusine is unknown, it is noteworthy that the yield of hypusinated (Hyp)-eIF5A in bacteria co-expressing eIF5A, DHS and DOHH is greater than the yield of deoxyhypusinated (dHyp)-eIF5A in bacteria co-expressing eIF5A and DHS (Park et al., 2011). As the DHS reaction is reversible *in vitro* (Park et al., 2003), it is possible that hydroxylation of deoxyhypusine to hypusine blocks this back reaction and thus stabilizes the hypusine modification. Interestingly, DOHH orthologs have not been identified in archaea (Park et al., 2006). This lack of DOHH was consistent with the presence of deoxyhypusine rather than hypusine in some archaea (Bartig et al., 1990). Moreover, the presence of hypusine in a few archaeal species that grew in the absence of oxygen indicated that a distinct mechanism of hydroxylation has been adopted (Bartig et al., 1990).

Genetic and biochemical studies have provided insights into the recognition of eIF5A by DHS and DOHH. *In vitro* assays with purified DHS and truncated derivatives of human eIF5A identified the fragment from residues 10-90 as the smallest efficient substrate, while the highly conserved region consisting of residues Phe^{30} to Asp^{80} was the minimal fragment required for deoxyhypusine biosynthesis (Joe and Park, 1994). Point mutations in the conserved hypusine loop sequence G-Hyp-H-G-H-K immediately flanking the site of hypusine formation impaired DHS modification of human or yeast

eIF5A expressed in yeast cells (Cano et al., 2008; Dias et al., 2008). Taken together, these results indicated that DHS recognizes the N-terminal domain and residues flanking the modified Lys residue when forming hypusine on eIF5A. The DOHH recognition of dHyp-eIF5A is likewise mediated through the N-terminal domain of eIF5A. Residues 20-90 of eIF5A were sufficient for binding to DOHH and for hydroxylation *in vitro* (Kang et al., 2007); and similar to the requirements for deoxyhypusine synthesis, mutation of Lys47 and His51 flanking the Lys50 site of modification impaired hydroxylation of human eIF5A expressed in yeast (Cano et al., 2008). Thus, modification of eIF5A by both DHS and DOHH is dependent on recognition of the N-terminal domain of the factor and specific residues within the hypusine loop.

Despite evidence supporting the essential nature of the eIF5A Lys residue that is modified to hypusine, the precise function of hypusine in protein synthesis remains unknown. As stated above, Arg cannot substitute for the modified Lys residue in eIF5A; however, partially modified eIF5A containing deoxyhypusine retained the ability to stimulate Met-Pmn synthesis (Park, 1989) and maintained yeast viability (Park et al., 2006). Interestingly, a structural mimic of eIF5A containing homodeoxyhypusine [N^{ε}-(5-aminopentyl)lysine] was unable to stimulate Met-Pmn synthesis (Park et al., 1991). In contrast to hypusine, which contains an *N*-butylamine group from spermidine, homodeoxyhypusine contains an aminopentyl moiety from *N*-(3-aminopropyl)-cadaverine (Park et al., 1991). Thus, the side chain of homodeoxyhypusine is one methyl group longer than the side chain of hypusine. The observation that homodeoxyhypusine-modified eIF5A was unable to stimulate Met-Pmn synthesis indicated a precise length

and structural restriction on the hypusine side chain, perhaps reflecting a critical contact between hypusine and other components in the eukaryotic translation complex.

1.4.2 Phosphorylation of eIF5A

In addition to its hypusine modification, yeast eIF5A is also phosphorylated. The phosphorylation was mapped to the Ser2 residue of the protein (Klier et al., 1993). As mutation of this residue to Ala did not affect yeast cell growth and the phosphorylated and unphosphorylated forms of the factor were equally active in stimulating Met-Pmn synthesis in assays with mammalian factors and ribosomes, the phosphorylation of eIF5A, unlike its hypusine modification, did not appear to be important for the factor's function (Kang et al., 1993; Klier et al., 1993).

1.4.3 β-lysinylation (lysylation) of EF-P

Alignment of the EF-P sequence from *E. coli* with the sequence of eIF5A showed conservation of the Lys residue that is modified to hypusine in eIF5A (Fig. 2). However, the absence of DHS and DOHH homologs in *E. coli* (Park et al., 2011), the absence of spermidine labeling of proteins in bacteria, and the substitution of this Lys residue in *E.coli* EF-P by Arg in several bacteria including *Thermus thermophilus* led to the notion that EF-P was not modified like eIF5A. However, several studies demonstrated that EF-P, at least in some bacteria, is modified. Mass spectrometry (MS) analyses of tryptic peptides from native EF-P purified from *E. coli* revealed that Lys34 was modified, and that the modification contributed an extra mass of ~144 Da (Aoki et al., 2008). Based on comparative genomics analyses including gene clustering and phylogenetic conservation,

it was hypothesized that the *E. coli* genes *yjeA* and *yjeK*, encoding a truncated lysyl-tRNA synthetase-related protein and a protein related to lysine aminomutase, respectively, function in a pathway to modify EF-P (Bailly and de Crecy-Lagard, 2010). Consistent with the hypothesis that these genes were acting in the same pathway, mutation of *yjeA* (also known as *poxA*, *genX*, and *epmA*) and *yjeK* (*epmB*) in *Salmonella enterica* had equivalent and non-additive negative impacts on *S. enterica* virulence and resistance to antibiotics (Navarre et al., 2010). Biochemical studies demonstrated that YjeA/PoxA could lysinylate (lysylate) EF-P *in vitro* (Navarre et al., 2010; Yanagisawa et al., 2010), and this activity was dependent on the conserved Lys34 residue which corresponds to the site of hypusine modification in eIF5A (Navarre et al., 2010). *In vitro* and co-expression studies revealed that YjeA/PoxA could add a Lys residue to EF-P, increasing the mass by ~128 Da (Navarre et al., 2010; Yanagisawa et al., 2010). Notably, this mass is ~16 Da less than the ~144 Da modification detected by Aoki et al. (Aoki et al., 2008). In the co-expression studies, enhanced levels of EF-P modification were observed in the presence of *yjeK*, encoding a homolog of lysine-2,3-aminomutase that catalyzed the isomerization of α-lysine to β-lysine, and it was thus concluded that EF-P is modified to a β-lysyl-lysine form (Yanagisawa et al., 2010) (Fig. 5B). Until now, it is not known whether EF-P is modified in bacterial species that lack Lys at residue 34, such as *T. thermophilus* in which Lys34 is substituted by Arg.

1.5 Yeast studies reveal a role for eIF5A in translation elongation

Molecular genetic and biochemical studies of yeast eIF5A have provided novel insights into the function of the factor. Using the human eIF5A cDNA in comparative

hybridization techniques, Schnier et al. identified two genes encoding eIF5A in the yeast *Saccharomyces cerevisiae* (Schnier et al., 1991). The yeast genes *HYP2* and *ANB1* encode 157-residue proteins that shared 90% amino acid sequence identity with one another and >60% identity with human eIF5A (Schnier et al., 1991) (Fig. 2). Though *HYP2* and *ANB1* differ by only 15 residues, it was not entirely clear why yeast retain these two isoforms. Nevertheless, further studies by several laboratories revealed that expression of *HYP2* and *ANB1* was reciprocally regulated by oxygen. Whereas *ANB1*, also known as *HYP1* or *TIF51B*, is expressed exclusively under anaerobic conditions, *HYP2*, also known as *TIF51A*, was preferentially expressed under aerobic conditions (Lowry et al., 1983; Magdolen et al., 1994; Mehta et al., 1990; Schwelberger et al., 1993). Consistent with these expression patterns, *HYP2* was essential for growth under aerobic conditions, but dispensable for anaerobic growth (Schnier et al., 1991; Schwelberger et al., 1993; Wohl et al., 1993). In contrast, *ANB1* was dispensable for growth under aerobic conditions (Schnier et al., 1991). These growth phenotypes can be attributed to the expression patterns of *HYP2* and *ANB1* and not to functional differences between the protein isoforms, as expression of HYP2 or ANB1 protein from a heterologous promoter was able to restore growth of a yeast strain lacking the *HYP2* gene (Magdolen et al., 1994; Schwelberger et al., 1993; Wohl et al., 1993). Moreover, expression of human, alfalfa, or slime mold eIF5A protein was able to complement the growth defect in the strain lacking *HYP2*, demonstrating the functional equivalence of eIF5A across eukaryotes (Magdolen et al., 1994; Schwelberger et al., 1993; Wohl et al., 1993).

To gain further insights into eIF5A function, several groups have examined the impact of depleting eIF5A in yeast. By placing *HYP2* expression under the control of a

galactose-regulated promoter, eIF5A expression was turned off by changing growth conditions. In initial experiments, depletion of eIF5A resulted in a significant inhibition of cell growth but only a 30% reduction in total protein synthesis rates, as measured by [^{35}S]Met incorporation, and a small change in polysome profiles (Kang and Hershey, 1994). This discrepancy between the impact of eIF5A depletion on cell growth versus protein synthesis raised the possibility that eIF5A was required for the translation of only a subset of mRNAs whose protein products were critical for cell growth. Further studies with the same eIF5A degron revealed a more substantial impairment in general translation with up to a 4-fold decrease in translation rates upon depletion of eIF5A in rich medium (Henderson and Hershey, 2011). Consistent with this latter study, analysis of an independent eIF5A degron revealed a pronounced defect in total protein synthesis upon depletion of eIF5A (Saini et al., 2009). Likewise, total protein synthesis was impaired when an eIF5A temperature-sensitive (*ts*$^{-}$) mutant was shifted to the restrictive temperature (Dias et al., 2008).

While these eIF5A degron studies revealed that eIF5A promotes general protein synthesis, the role of the factor in translation was not resolved. Polysome profile analyses are commonly used to assess translation function in yeast. In this technique, cells were treated with cycloheximide (CHX) to freeze ongoing translation elongation and crude extracts were fractionated on sucrose gradients. While one study reported a loss of larger polysomes and accumulation of smaller polysomal species and 80S monosomes upon depletion of eIF5A, indicative of a translation initiation defect (Henderson and Hershey, 2011), this polysome loss was not detected in other studies. Zanelli et al. reported that polysomes were maintained upon shifting two different eIF5A *ts*$^{-}$ mutants to the

restrictive temperature (Zanelli et al., 2006). Moreover, polysome analyses performed by Saini and co-workers indicated a defect in translation elongation upon depletion or inactivation of eIF5A (Saini et al., 2009). Whereas omission of CHX during analysis of strains expressing wild-type eIF5A resulted in the expected loss of polysomes due to continued translation elongation and release of the ribosomes from mRNAs during extract preparation, polysomes were maintained in the absence of CHX upon depletion of eIF5A (Saini et al., 2009). This retention of polysomes in the absence of CHX in the eIF5A mutant mimicked the effect of CHX addition to the wild-type strain. Thus loss of eIF5A, like addition of CHX, impaired translation elongation.

Though the extended incubations required to fully deplete eIF5A in the degron strains might have allowed secondary effects resulting in the apparent elongation defect, similar polysome retention in the absence of CHX was observed in an eIF5A ts^- mutant after shifting for a short time to the restrictive temperature (Saini et al., 2009). Interestingly, polysome analyses in *Drosophila* and mammalian cells likewise indicated a role for eIF5A in translation elongation. Knockdown of eIF5A expression in *Drosophila* S2 cells resulted in the accumulation of polysomes (Patel et al., 2009), and whereas treatment of mammalian cells with arsenite caused impaired translation initiation and polysome loss, knockdown of eIF5A was reported to block this disassembly of polysomes in arsenite-treated cells (Li et al., 2010). In further support of the notion that loss or inactivation of eIF5A impaired translation elongation, two studies reported that eIF5A mutations caused an increase in the average ribosomal transit time, the time it takes for a ribosome following initiation to synthesize and release a completed polypeptide (Gregio et al., 2009; Saini et al., 2009). It is noteworthy that both the

polysome profile analyses and ribosomal transit time measurements assessed global translation. Thus, these data indicate that loss of eIF5A impairs translation elongation on a substantial fraction of the mRNAs in yeast cells.

Consistent with the results of the yeast genetic studies, *in vitro* assays have provided additional evidence that directly link yeast eIF5A to translation elongation. First, the translation defect in crude extracts prepared from eIF5A-depleted or mutant extracts was rescued by addition of purified eIF5A in a hypusine-dependent manner (Henderson and Hershey, 2011; Saini et al., 2009). Hyp-eIF5A, and not the unmodified eIF5A-K51R mutant, stimulated the rate of Met-Phe-Phe (M-F-F) tripeptide synthesis in reconstituted *in vitro* translation assays employing recombinant or highly purified translation factors and ribosomes (Saini et al., 2009). In further support of these studies that directly link eIF5A to translation elongation, other reports indicate eIF5A association with ribosomes or polysomes in whole-cell extracts (WCEs) from yeast (Jao and Chen, 2006; Saini et al., 2009; Zanelli et al., 2006) and are consistent with earlier studies of an eIF5A mutant that suppresses nonsense-mediated mRNA decay (Zuk and Jacobson, 1998). Taken together, the results of these various *in vivo* and *in vitro* studies indicate that eIF5A is a translation elongation factor.

1.6 Thesis research objectives and significance of findings

After nearly 40 years of genetic and biochemical work, eIF5A has heretofore remained an enigma. However, based upon previous work attributing a role for eIF5A in translation elongation (Saini et al., 2009; Zanelli et al., 2006) and the structure of bacterial EF-P bound to 70S ribosomes, which places the hypusine loop in close

proximity to the CCA acceptor stem of the P-site tRNA (Blaha et al., 2009), eIF5A/EF-P, at the time that I joined the lab, was poised for new functional and mechanistic insights into its role in translation. Given the substantial promise for new eIF5A discoveries, the primary focus of my thesis research was to delineate the requirements for eIF5A and its hypusine modification in protein synthesis. We hypothesized that eIF5A bound the ribosome and functioned to present hypusine to the ribosome active site to promote peptide bond formation. Combining yeast genetics, biochemistry, and ribosome profiling techniques, we uncovered a specialized role for eIF5A in promoting the translation of polyproline motifs, and also defined the requirements for hydroxylation of hypusine as mediated by *LIA1*. Ultimately, our data reinforce the critical function of eIF5A in translation elongation and reveal a specialized role for incorporation of specific amino acids in proteins.

First, we explored the possibility that eIF5A promotes amino acid-specific peptide bond synthesis. We initially proposed that eIF5A may have a function similar to reports made by Glick et al., who demonstrated *in vitro* that EF-P stimulated peptide bond formation of particular amino acid dipeptides (Glick et al., 1979). Concurrent with my studies on eIF5A impacts on synthesis of proteins containing homopolymeric runs of specific amino acids, Ude and colleagues (Ude et al., 2013) and Doerfel and co-workers (Doerfel et al., 2013) reported that *E. coli* EF-P enhanced the synthesis of proteins containing runs of consecutive proline codons. Given this finding, I focused my efforts on asking whether eIF5A had a similar function in eukaryotic cells.

In collaboration with other members of the Dever lab and with Chris Woolstenhulme and Allen Buskirk of Brigham Young University, we used *in vivo* assays

in yeast and *in vitro* reconstituted translation assays to reveal a specific requirement for eIF5A to promote peptide bond formation between consecutive proline residues. We found that addition of eIF5A relieves ribosomal stalling during translation of three consecutive proline residues *in vitro*, and loss of eIF5A function impairs translation of polyproline-containing proteins *in vivo*. Moreover, in collaboration with the Rachel Green lab at Johns Hopkins Medical Institute, results from genome-wide ribosome profiling studies revealed ribosomal pausing and/or drop-off during translation of consecutive proline residues. Thus, we proposed that eIF5A, like its bacterial ortholog EF-P, functions to promote the peptidyl transferase activity of the ribosome and facilitates the reactivity of poor substrates like proline during peptide bind formation.

To investigate the functional role of hypusine and its hydroxyl group, I identified a distinct class of eIF5A mutants that require *LIA1* for efficient cell growth. Using a yeast genetic screen, I found a collection of eIF5A mutants that elicit synthetic phenotypes when deoxyhypusine is unable to mature to hypusine. I identified three eIF5A mutants eIF5A-C23Y,V60D, eIF5A-S74F, and eIF5A-N79I that modestly impact cell growth on their own, but that are severely impaired or inviable in the absence of *LIA1*. Another mutant, eIF5A-H52A, identified in a candidate-based screen by mutational analysis of residues surrounding the hypusine modification, also showed exacerbated phenotypes in the absence of *LIA1*. As the mutant proteins were expressed well in the absence or presence of *LIA1*, and loss of *LIA1* did not result in accumulation of unmodified eIF5A versus the deoxyhypusine form, we concluded that the hydroxyl group on hypusine does not function to prevent the back reaction of the deoxyhypusine-containing to unmodified form of the eIF5A mutants. Using reconstituted yeast translation assays, I found that the

dHyp forms of these eIF5A mutants were defective in synthesis of a polyproline-containing peptide. Thus, analysis of these mutants has revealed that the hydroxyl group on hypusine has a direct role in promoting protein synthesis. Altogether, our research has provided new insights into the functional requirements of the hypusine modification on eIF5A and established its role in translation elongation and specifically in promoting the translation of polyproline motifs.

2. Materials and Methods

2.1 Yeast strains

Strain	Description	Source
H1511	*MATα ura3-52 leu2-3 leu2-112 trp1-Δ63*	(Foiani et al., 1991)
J696	*MATα trp1-Δ63 ura3-52 leu2-3 leu2-112 gcn2Δ anb1::NAT hyp2::KANMX4* p[*HYP2, URA3*]	(Saini et al., 2009)
J697	*MATα trp1-Δ63 ura3-52 leu2-3 leu2-112 gcn2Δ anb1::NAT hyp2::KANMX4* p[*HYP2, LEU2*]	(Saini et al., 2009)
J699	*MATα trp1-Δ63 ura3-52 leu2-3 leu2-112 gcn2Δ anb1::NAT hyp2::KANMX4* p[*hyp2-S149P, LEU2*]	(Saini et al., 2009)
J1005	*MAT*a *trp1-Δ63 ura3-52 leu2-3 leu2-112 GAL2*$^{+}$ *gcn2Δ hyp2*::*HPHMX4 anb1*::*NAT* p[*HYP2, URA3*]	This study
J1058	*MAT*a *trp1-Δ63 ura3-52 leu2-3 leu2-112 GAL2*$^{+}$ *gcn2Δ hyp2*::*HPHMX anb1*::*NAT GAL-LIA1*::*KANMX4* p[*HYP2, URA3*]	This study
J1119	*MAT*a *trp1-Δ63 ura3-52 leu2-3 leu2-112 GAL2*$^{+}$ *gcn2Δ hyp2*::*HPHMX anb1*::*NAT lia1*::*KANMX4* p[*HYP2, URA3*]	This study
TKY597	*MATα leu2-3 leu2-112 ura3-52 trp1-7 yef3*::*LEU2 lys2 his4-713 met2-1* p[*YEF3, TRP1*]	(Anand et al., 2003)
TKY599	*MATα leu2-3 leu2-112 ura3-52 trp1-7 yef3*::*LEU2 lys2 his4-713 met2-1* p[*yef3-F650S, TRP1*]	(Anand et al., 2003)

TKY675	*MATa ade2 leu2 ura3 his3 trp1 eft1*::*HIS3* *eft2*::*TRP1* p[*EFT2-6xHis, LEU2*]	(Jorgensen et al., 2002)
TKY702	*MATα leu2-3 leu2-112 ura3-52 trp1-7 yef3*::*LEU2* *lys2 his4-713 met2-1* p[*YEF3-6xHis, TRP1*]	(Anand et al., 2003)
TKY742	*MATa ade2 leu2 ura3 his3 trp1 eft1*::*HIS3* *eft2*::*TRP1* p[*eft2-6xHis-H699N*, *LEU2*]	(Ortiz et al., 2006)
TKY825	*MATa ade2 leu2 ura3 his3 trp1 eft1*::*HIS3* *eft2*::*TRP1* p[*eft2-6xHis-H696A*, *LEU2*]	(Ortiz et al., 2006)
YRP840	*MATa leu2-3 leu2-112 his4-539 trp1 ura3-52* *cup1*::*LEU2/PGK1pG/MFA2pG*	(Hatfield et al., 1996)

2.2 Polysome analysis

Yeast cultures were either treated with 50 µg/mL CHX for 5 min before collection or left untreated, transferred to a 500 mL centrifuge bottle containing shaved ice, pelleted, and washed with 10 mL Buffer A (20 mM Tris-HCl [pH 7.5], 50 mM KCl, 10 mM $MgCl_2$, 1 mM DTT, Complete protease inhibitor cocktail [EDTA-free, Roche]). In all subsequent steps, the CHX-treated cells were treated with 50 µg/mL CHX. Cell pellets were suspended in 300-500 µL Buffer A, mixed with an equal volume of glass beads, and then cells were broken by 5 cycles of vigorous mixing on a vortex for 1 min followed by 1 min on ice. Following clarification, ten OD_{254} units of the WCE were layered on 4.5-45% sucrose gradients prepared in Buffer A, and then subjected to centrifugation in a Beckman SW41 rotor for 2.5 h at 260,000 × g. Gradients were fractionated on a Teledyne ISCO Density Gradient Fractionator while monitoring absorbance at OD_{254}.

2.3 Plasmid and yeast strain construction

Yeast strain J1005 was constructed by swapping a hygromycin-resistance (*HPHMX4*^{R}) cassette in place of a kanamycin-resistance (*KANMX4*^{R}) cassette in the yeast strain J696 as described previously (Goldstein and McCusker, 1999). First, plasmid pAG32 containing the *HPHMX4*^{R} cassette was digested with *Bam*HI and *Spe*I [Roche]. The digested plasmid was PCR-purified, then transformed into J696 using the lithium acetate procedure (Gietz et al., 1995). Yeast cells were allowed to recover in 1 mL yeast peptone dextrose (YPD) for 90 min at 30°C while shaking, then plated on YPD containing 0.5 µg/mL hygromycin. Those colonies that grew in the presence of hygromycin were streaked on YPD plates. Individual colonies were patched and prepared for replica printing to confirm the markers. Colonies that grew in the presence of hygromycin (*Hph*$^+$) and nourseothricin (*Nat*$^+$) due to the presence of *anb1::NAT* allele, but failed to grow on medium containing kanamycin (*Kan*$^-$), were checked by PCR for the gain of *HPH*^{R} cassette, retention of *NAT*^{R} cassette, and loss of *KAN*^{R} cassette.

Using the parent yeast strain J1005, strain J1058 was constructed by inserting a galactose-inducible promoter upstream of the chromosomal *LIA1* gene. First, a DNA fragment containing the inducible *GAL1* promoter and an upstream kanamycin selectable marker was amplified by PCR using the plasmid pFA6a-KANMX6-PGAL1 (Longtine et al., 1998) as a template. The PCR amplification was conducted using primers that contain 50 nucleotide complementarity to the promoter (P1) or start of the *LIA1* ORF (P2) and 20 nucleotide complementarity to the plasmid:

P1 5'-AATCCAGTGAATACACGTGTATATTTGACGGTAGGTTTAGGTTAGA-

3’ (forward)

P2 5’-AGAGTGCATTCATCGACGTTTTCTTGGAAATGTTTTTCAAAGTTAGT

AGACATTTTGAGATCCGGGTTTT-3’ (reverse)

The PCR product was gel-purified and used to transform J1005 using the lithium acetate procedure (Gietz et al., 1995). Cells were plated on YPD containing G418 to select for the *KANMX6*^{R} cassette. Those colonies that grew in the presence of G418 were kanamycin resistant (*Kan*$^{+}$) and were streaked on YPD. Individual colonies were patched and prepared for replica printing to check the markers. Colonies displaying hygromycin resistance (*Hph*$^{+}$), nourseothricin resistance (*Nat*$^{+}$), and kanamycin resistance (*Kan*$^{+}$) were checked by PCR for the presence of the *HPH*^{R} cassette, the *NAT*^{R} cassette, and the *KAN*^{R} cassette. Expression of *GAL-LIA1* in galactose-containing medium and repression of *GAL-LIA1* in glucose-containing medium was checked by RT-PCR.

Strain J1119 was constructed by deletion of the chromosomal copy of *LIA1* and replacement with a *KANMX4*^{R} cassette in strain J1005. Using the primers

P3 5’-AGAACAAAAGGTGAGGTCAACGAGAACTCTG-3’ (forward)

P4 5’-GCACCTGGTAGACCGTTAAATTCGTCAAATC-3’ (reverse),

which are complementary to sequences 500 bp 5’ and 500 bp 3’, respectively, of the *LIA1* locus, the *lia1Δ::KANMX4*^{R} cassette was amplified using chromosomal DNA from the *lia1*Δ strain from the Yeast ORF deletion collection [Open Biosystems] as a template. The PCR product was used to transform strain J1005, selecting for *Kan*$^{+}$ colonies. Candidate transformants were tested for hygromycin (*Hph*$^{+}$) and nourseothricin (*Nat*$^{+}$) resistance by replica test, and the replacement of *LIA1* by *lia1*Δ*::KANMX4* was confirmed by PCR.

To construct a *HYP2* mutant library, error-prone PCR using a low-fidelity DNA polymerase [Agilent Tecnologies] was used to amplify the *HYP2* gene in plasmid pC3287 (Saini et al., 2009). The following primers were used to amplify the *HYP2* ORF:

P5 5'-GATCCGCTCGAGACAATGTCTGACGAAGAACATACCTTTG-3' (forward)

P6 5'-GATCTCGGCCGTGATGTTAACCGGTTTAATCGGTTCTAGC-3' (reverse)

The PCR product was purified and sub-cloned between the *Eag*I and *Xho*I sites in the plasmid pC3292 (Saini et al., 2009). The ligation products were transformed into *E.coli* by electroporation and approximately 10,000 independent colonies were collected. The *HYP2* mutant plasmid library was amplified by inoculating the pooled colonies into LB + ampicillin medium, and the plasmids were isolated using a Qiagen Midiprep kit.

Site-directed mutagenesis of the *HYP2* gene was performed using the QuikChange II XL kit [Stratagene]. The following primers were used to introduce the point mutations:

C23Y

P7 5'-CCACCTACCCAATGCAATATTCTGCCTTGAGAAAGA-3' (forward)

P8 5'-TCTTTCTCAAGGCAGAATATTGCATTGGGTAGGTGG-3' (reverse)

V60D

P9 5'-CACGCTAAAGTCCATTTGGATGCCATTGATATCTTCACT-3' (forward)

P10 5'-AGTGAAGATATCAATGGCATCCAAATGGACTTTAGCGTG-3' (reverse)

S74F

P11 5'-TCACTGGTAAGAAGTTGGAAGATTTGTTTCCATCTACTCACA-3'

(forward)

P12 5’-TGTGAGTAGATGGAAACAAATCTTCCAACTTCTTACCAGTGA-3’ (reverse)

N79I

P13 5’-GTCTCCATCTACTCACATCATGGAAGTTCCAGTTG-3’ (forward)

P14 5’-CAACTGGAACTTCCATGATGTGAGTAGATGGAGAC-3’ (reverse)

H52A

P15 5’-CACTTCTAAGACTGGTAAGGCCGGTCACGCTAAAGTCCAT-3’ (forward)

P16 5’-ATGGACTTTAGCGTGACCGGCCTTACCAGTCTTAGAAGTG-3’ (reverse)

S149P

P17 5’-GAAGAAGCCGCCATCCCCTTCAAGGAAGCTG-3’ (forward)

P18 5’-CAGCTTCCTTGAAGGGGATGGCGGCTTCTTC-3’ (reverse)

The *HYP2* mutant plasmids, which bear a *LEU2* selectable marker, were substituted in place of the wild-type *HYP2,URA3* plasmid in *hyp2Δ* strains by plasmid shuffling (Boeke et al., 1987).

2.4 Dual luciferase assay

Dual luciferase reporter constructs containing 10 codon repeats at amino acid 314 between the in-frame *Renilla* and firefly luciferase ORFs were obtained from Beth Grayhack (Letzring et al., 2010). Constructs with insertions of variable numbers of Pro or Phe codons between the two luciferase ORFs were generated by cloning PCR products

between the unique *Sal*I, located prior the insert, and *Pst*I, located after the firefly luciferase ORF, restriction sites of the parental dual luciferase plasmid pDL202:

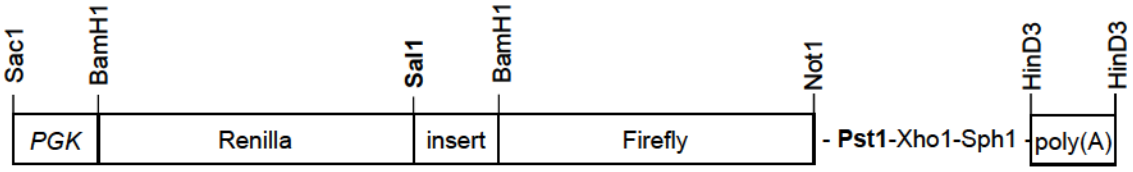

The following primers were used to introduce the consecutive Pro or Phe codons:

Single Pro Insert

P19 5'-CCCCCCGTCGACG**CCA**TTCGGATCCTTCAACTTCCCTGAGCTCGA-3' (forward)

P20 5'-CGAAAAGCTTGCATGCCTCGAGCTGCAGGCG-3' (reverse)

Single Phe Insert

P21 5'-CCCCCCGTCGACG**TTC**TTCGGATCCTTCAACTTCCCTGAGCTCGA-3' (forward)

P20 5'-CGAAAAGCTTGCATGCCTCGAGCTGCAGGCG-3' (reverse)

Two Pro Insert

P22 5'-CCCCCCGTCGACG**CCACCA**TTCGGATCCTTCAACTTCCCTGAGCTC GA-3' (forward)

P20 5'-CGAAAAGCTTGCATGCCTCGAGCTGCAGGCG-3' (reverse)

Two Phe Insert

P23 5'-CCCCCCGTCGACG**TTCTTC**TTCGGATCCTTCAACTTCCCTGAGCTCG A-3' (forward)

P20 5'-CGAAAAGCTTGCATGCCTCGAGCTGCAGGCG-3' (reverse)

Three Pro Insert

P24 5’-CCCCCCGTCGACG**CCACCACCA**TTCGGATCCTTCAACTTCCCTGAG CTCGA-3’ (forward)

P20 5’-CGAAAAGCTTGCATGCCTCGAGCTGCAGGCG-3’ (reverse)

Three Phe Insert

P25 5’-CCCCCCGTCGACG**TTCTTCTTC**TTCGGATCCTTCAACTTCCCTGAGC TCGA-3’ (forward)

P20 5’-CGAAAAGCTTGCATGCCTCGAGCTGCAGGCG-3’ (reverse)

Four Pro Insert

P26 5’-CCCCCCGTCGACG**CCACCACCACCA**TTCGGATCCTTCAACTTCCCT GAGCTCGA-3’ (forward)

P20 5’-CGAAAAGCTTGCATGCCTCGAGCTGCAGGCG-3’ (reverse)

Four Phe Insert

P27 5’-CCCCCCGTCGACG**TTCTTCTTCTTC**TTCGGATCCTTCAACTTCCCTG AGCTCGA-3’ (forward)

P20 5’-CGAAAAGCTTGCATGCCTCGAGCTGCAGGCG-3’ (reverse)

Six Pro Insert

P28 5’-CCCCCCGTCGACG**CCACCACCACCACCACCA**TTCGGATCCTTCAA CTTCCCTGAGCTCGA-3’ (forward)

P20 5’-CGAAAAGCTTGCATGCCTCGAGCTGCAGGCG-3’ (reverse)

Six Phe Insert

P29 5’-CCCCCCGTCGACG**TTCTTCTTCTTCTTCTTC**TTCGGATCCTTCAACT TCCCTGAGCTCGA-3’ (forward)

P20 5’-CGAAAAGCTTGCATGCCTCGAGCTGCAGGCG-3’ (reverse)

Eight Pro Insert

P30 5’-CCCCCCGTCGACG**CCACCACCACCACCACCACCACCA**TTCGGATC CTTCAACTTCCCTGAGCTCGA-3’ (forward)

P20 5’-CGAAAAGCTTGCATGCCTCGAGCTGCAGGCG-3’ (reverse)

Eight Phe Insert

P31 5’-CCCCCCGTCGACG**TTCTTCTTCTTCTTCTTCTTCTTC**TTCGGATCC TTCAACTTCCCTGAGCTCGA-3’ (forward)

P20 5’-CGAAAAGCTTGCATGCCTCGAGCTGCAGGCG-3’ (reverse)

Ten Pro Insert

P32 5’-CCCCCCGTCGACG**CCACCACCACCACCACCACCACCACCACCA**TT CGGATCCTTCAACTTCCCTGAGCTCGA-3’ (forward)

P20 5’-CGAAAAGCTTGCATGCCTCGAGCTGCAGGCG-3’ (reverse)

Ten Phe Insert

P33 5’-CCCCCCGTCGACG**TTCTTCTTCTTCTTCTTCTTCTTCTTCTTC**TTC GGATCCTTCAACTTCCCTGAGCTCGA-3’ (forward)

P20 5’-CGAAAAGCTTGCATGCCTCGAGCTGCAGGCG-3’ (reverse)

To measure luciferase activities, individual yeast transformants were grown in Synthetic Dextrose (SD) medium containing required nutrients to OD_{600} = 0.8-1.0, harvested, and the cell pellets were resuspended in 300 µL Breaking Buffer L (20 mM Tris-HCl [pH 7.5], 100 mM KCl, 5 mM $MgCl_2$, 0.1 mM EDTA, Complete protease inhibitor cocktail [EDTA-free, Roche]), and vigorously mixed with 1 vol glass beads on a vortex for 1 min at 4°C. Lysates were cleared by centrifugation at 9,400 × *g* for 5 min at 4°C, and aliquots of the supernatant were assayed for firefly luciferase activity using a

microplate luminometer [Berthold] and the Dual Luciferase Reporter 1000 Assay System [Promega]. Next, *Renilla* luciferase activity was measured following addition of Stop and Glo reagent [Promega].

The ratio of firefly to *Renilla* activity was measured for each of the reporters tested and those values were normalized to the firefly to *Renilla* ratio for the no insert control (pDL202), which was pre-set to a value of 1.0. For error calculations, the propagation of error analysis for three independent transformants was used:

$$\delta R = |R| \bullet \sqrt{\left(\frac{\delta X}{X}\right)^2 + \left(\frac{\delta Y}{Y}\right)^2}$$

where *R is* the average of the reporter firefly to *Renilla* ratio over the average of no insert firefly to *Renilla* ratio, δX is the standard deviation of the reporter firefly to *Renilla* ratio, X is the average of the reporter firefly to *Renilla* ratio, δY is the standard deviation of the no insert firefly to *Renilla* ratio, Y is the average of the no insert firefly to *Renilla* ratio.

2.5 Peptide formation assay

Initiation complexes were prepared in 1× Recon Buffer A (30 mM Hepes-KOH [pH 7.4], 100 mM KCl, 2.5 mM magnesium acetate, 2 mM DTT) based on the protocol described by Acker et al. (Acker et al., 2007) and contained the following components: 4 nM [^{35}S]Met-tRNA$_i^{Met}$, 0.4 µM eIF2, 1 µM eIF1, 1 µM eIF1A, 0.4 µM 40S, 1 µM mRNA (5'-AUGCCACCACCAAAAUAA-3') encoding 5'-M-P-P-P-K-Stop-3', 1 µM eIF5 and 0.5 µM eIF5B. All reactions were performed at 26°C. Following assembly of initiation complexes, reactions were layered on 0.8 mL 1M sucrose cushion in 1× Recon Buffer A and then pelleted by centrifugation at 260,000 × *g* for 1 h. Ribosomal pellets were

dissolved in 1× Recon Buffer B (30 mM Hepes-KOH [pH 7.4], 100 mM KCl, 1 mM magnesium acetate, 2 mM $MgCl_2$, 1 mM spermidine, 2 mM DTT, and aliquots were stored at -80°C.

Peptide formation assays contained 2 nM initiation complex, 2 µM eEF1A, 1 µM eEF2, 1 µM eEF3, 10 nM to 5 µM eIF5A, 1 µM Pro-tRNA$^{Pro}_{UGG}$, 1 µM Lys-tRNA$^{Lys}_{UUU}$, 1 mM GTP and 1 mM adenosine-5'-triphosphate (ATP) in 1× Recon Buffer B. The elongation assay components were pre-incubated for 15 min on ice before adding the initiation complex, and then reactions were incubated at 26°C. Progress of peptide formation was examined by electrophoretic thin-layer chromatography (TLC) as described previously (Eyler and Green, 2011). Briefly, elongation reactions were quenched at different times by mixing with an equivalent vol of 0.2 N KOH to hydrolyze the peptidyl-tRNA product, and then 0.5 µL was spotted on a cellulose TLC plate [EMD Chemicals]. The spot was dried using a heat gun, then the TLC plate was briefly equilibrated with pyridine acetate buffer (200 mL glacial acetic acid and 5 mL pyridine in 1 L, pH 2.8) before electrophoresis at 1,000 V for 20 min in the same pyridine acetate buffer. Following electrophoresis, the TLC plate was dried using a heat gun, and peptide spots were detected by phosphorimage analysis. The fractional yield of the peptides and free [^{35}S]Met in each reaction at different times were quantified and fit using KaleidaGraph [Synergy Software] to the single exponential equation: $y = Y_{max} (1-\exp(-k_{obs}t))$, where Y_{max} is the maximum fraction of peptide formed and k_{obs} is the observed rate constant.

2.6 Preparation of initiation and elongation factors

Initiation factors eIF1 and eIF1A were expressed in *E. coli* BL21 CodonPlus (DE3)-RIL cells [Agilent Technologies] and purified using the IMPACT Protein Purification System [New England Biolabs] as described previously (Shin et al., 2011). eIF5 was kindly provided by Byung Shin and purified as in Shin et al. (Shin et al., 2011). Initiation factor eIF5B was purified from yeast using Glutathione Sepharose 4B affinity chromatography as described previously (Shin and Dever, 2007) with minor modification. Briefly, yeast strain H1511 harboring the expression vector pEG-KT-eIF5B$^{397\text{-}1002}$ (Shin and Dever, 2007) was grown in S-raffinose medium (0.145% yeast nitrogen base (YNB), 0.5% ammonium sulfate and 2% raffinose plus required supplements) until $OD_{600} = 0.5$, and GST-eIF5B$^{397\text{-}1002}$ expression was induced by adding galactose to final 2% (v/v) and incubating the culture with shaking at 30°C for 14 h. Cells were harvested and the cell pellet was suspended in an equivalent volume of Lysis Buffer A (1× phosphate-buffered saline (PBS) solution containing Complete protease inhibitor cocktail [EDTA-free, Roche], 0.5 mM 4-(2-aminoethyl) benzenesulfonyl fluoride hydrochloride (AEBSF), 5 µg/mL pepstatin). Cells were broken by adding 50% (v/v) glass beads to the cell suspension and then mixing vigorously on a vortex for 5 min at 4°C. Following removal of the glass beads and unbroken cells by centrifugation at 1,900 × *g* for 10 min, the extract was clarified by centrifugation at 27,000 × *g* for 30 min, and then mixed with 1 mL of a 50% slurry of Glutathione Sepharose 4B [GE Healthcare] at 4°C for 2 h. The resin was then washed extensively with 20-fold excess volume of 1× PBS buffer, and eIF5B was eluted by adding 40 U/mL thrombin in 1× PBS buffer and incubating at room temperature for 2 h and then overnight at 4°C. The supernatant containing released eIF5B

was dialyzed against Storage Buffer A (20 mM Hepes-KOH [pH 7.5], 100 mM potassium acetate, 2.5 mM magnesium acetate, 2 mM DTT, and 10% glycerol) and aliquots were stored at -80°C.

Elongation factor eEF1A was purified from YRP840 (Hatfield et al., 1996). Cells were grown in 2.5 L YPD to OD_{600} = 2.0, harvested, and broken in 150 mL Lysis Buffer B (60 mM Tris-HCl [pH 7.5], 50 mM KCl, 5 mM $MgCl_2$, 0.1 M EDTA [pH 8.0], 10% glycerol, 1 mM DTT, 0.2 M AEBSF) using glass beads as described above. After removal of unbroken cells by centrifugation at 7,600 × *g* for 30 min, the supernatant was clarified by centrifugation at 150,000 × *g* for 3 h, and then mixed gently with 10 mL DE52 resin (Whatman, pre-equilibrated with Lysis Buffer B) for 1 h at 4°C. The unbound fraction containing eEF1A was isolated by pouring the mixture into a column and collecting the elute, which was then applied to a HiTrap CM Sepharose column (GE Healthcare), and eEF1A was eluted with a linear gradient to 500 mM KCl. Fractions containing eEF1A were identified by SDS-PAGE, pooled, dialyzed against Storage Buffer A and stored at -80°C.

Poly-histidine tagged versions of elongation factors eEF2 and eEF3 were purified from yeast strains TKY675 and TKY702, respectively, using published protocols (Andersen et al., 2004; Ortiz et al., 2006) with some modifications. Cells were grown in 5 L YPD to OD_{600} = 1.5, harvested, and then suspended in Lysis Buffer C (20 mM Tris-HCl [pH 7.6], 300 mM KCl, 1 mM DTT, 1 mM AEBSF, 10 mM imidazole, and 1× Complete protease inhibitor cocktail [EDTA-free, Roche]). After the cells were broken with glass beads as described above, the lysate was cleared of unbroken cells by centrifugation at 17,000 × *g* for 30 min, clarified by centrifugation at 180,000 × *g* for 80

min, and then gently mixed with 1 mL Ni-NTA resin for 2 h at 4°C. The resin was then washed with 5 vol of the Lysis Buffer C containing 20 mM imidazole, and the His_6-tagged proteins were eluted in Buffer E containing 500 mM imidazole. eEF2 or eEF3 were identified by SDS-PAGE then concentrated and dialyzed against Storage Buffer B (20 mM Tris-HCl [pH 7.5], 100 mM potassium acetate, 0.1 mM magnesium acetate, 2 mM DTT, 10% glycerol) and then stored at -80°C.

2.7 Preparation of wild-type and mutant eIF5A

The polycistronic expression system developed by Song Tan (Tan, 2001) was used to produce unmodified or modified (dHyp or Hyp) forms of eIF5A in *E. coli*. As produced by Byung Shin and Joo-Ran Kim, an N-terminally His_6-tagged version of the *HYP2* ORF was cloned between the *Nde*I and *Bam*HI sites of the vector pET3a Trm, and then moved as an *Xba*I-*Bam*HI fragment to the expression vector pST39 generating the plasmid pC4181. The *DYS1* and *LIA1* ORFs were cloned into pET3a Trm using *Nde*I-*Hin*dIII and *Nde*I-*Mlu*I sites, respectively, and then sequentially transferred to pST39 using *Eco*RI-*Hin*dIII and *Bsp*EI-*Mlu*I sites, respectively, to make the plasmid pC4183. Plasmid pC4182 contains N-terminally His_6-tagged *HYP2* and *DYS1* ORFs cloned into pST39 sequentially using *Xba*I-*Bam*HI and *Eco*RI-*Hin*dIII sites, respectively.

To purify eIF5A, *E. coli* strain BL21 CodonPlus(DE3)-RIL [Agilent Tecnologies] or BL21(DE3)pLysS [Agilent Technologies] for toxic byproducts was transformed with pC4181, pC4182, or pC4183, or mutant derivatives and cells were grown in 0.5 L LB medium containing 100 µg/mL ampicillin at 37°C to OD_{600} = 0.5. Then, 0.5 mM IPTG was added and the culture was incubated at 25°C for 14 h or 37°C for 3-6 h for mutants.

Following harvesting, the cell pellet was suspended in 40 mL Lysis Buffer D (50 mM Tris-HCl [pH 7.5], 300 mM KCl, 10 mM imidazole) and cells were broken by sonication using a microtip (5 cycles of 30 sec pulse followed by 30 sec cooling at 4°C). The cell lysate was cleared by centrifugation at 27,000 × *g* for 30 min and then mixed gently with 1 mL Ni-NTA resin [Qiagen] at 4°C for 2 h. The resin was transferred to a disposable column [Qiagen], washed sequentially with 10 mL Lysis Buffer D and then 10 ml Lysis Buffer D containing 20 mM imidazole, and then protein was eluted in 2 mL Lysis Buffer D containing 0.5 M imidazole. Samples were then dialyzed against Storage Buffer C (30 mM Hepes-KOH (pH 7.5), 150 mM potassium acetate, 2 mM DTT and 10% glycerol).

The eIF5A proteins were purified from yeast as well. 2.5 L YPD cultures of yeast strains J1005 and J1119, expressing single copy C-terminal FLAG-tagged eIF5A proteins, were grown to OD_{600} 3.0, washed with 1× Tris-buffered saline (TBS), and broken with glass beads. The lysate was cleared of unbroken cells by centrifugation at 1,900 × *g* for 10 min, the extract was clarified by centrifugation at 27,000 × *g* for 30 min, and then mixed with 1 mL of anti-FLAG-M2 affinity gel (50% slurry) [Sigma]. The gel was washed with 10 mL of 1× TBS containing 0.1% Triton X-100, and then bound eIF5A was eluted with 200 μg/mL FLAG peptide in 1× TBS. eIF5A proteins were dialyzed against Storage Buffer D (30 mM Hepes-KOH [pH 7.5], 150 mM KCl, 2 mM DTT, 10% glycerol).

The modification (unmodified, dHyp, or Hyp) status of eIF5A was assessed by ElectroSpray-Ionization Quadrupole-Time-of-Flight Mass Spectrometry (ESI QTOF MS, [Agilent Tecnologies]) by Dr. Peter Backlund (Section on Mass Spectrometry and Metabolism, NICHD).

2.8 Preparation of mRNA, tRNA, and ribosomes

A model 5'-AUGCCACCACCAAAAUAA-3' encoding 5'-M-P-P-P-K-Stop-3' was purchased [Integrated DNA Technologies] and used for preparation of elongation complexes.

The UGG isoacceptor of $tRNA^{Pro}$ was purified from bulk *S. cerevisiae* tRNA [Roche] using the biotinylated oligo 5'-CCAAAGCGAG AATCATACCA CTAGAC-3' (BioTEG) as follows (Yokogawa et al., 2010): 400 µL streptavidin beads [Pierce] were washed three times with 400 µL 10 mM Tris-HCl (pH 7.5), bound to 8 nmol biotinylated oligonucleotide at 25°C for 30 min, and then washed twice with 10 mM Tris-HCl (pH 7.5). The beads were pelleted by centrifugation for 30 sec at 1000 × *g* after each wash to remove the supernatant. Bulk yeast tRNA [Sigma, R5636] (180 nmol in 300 µL) was mixed with an equal volume of 2 M TMA buffer (20 mM Tris-HCl [pH 7.5], 1.8 M tetramethylammonium chloride, 0.2 mM EDTA), incubated with the streptavidin beads at 65°C for 10 min to denature the tRNA, and then the mixture was slowly cooled to 25°C over ~10 min to allow annealing. The beads were then washed eight times with 400 µL 10 mM Tris-HCl (pH 7.5) to remove unbound tRNA. The $tRNA^{Pro}_{UGG}$ was melted off the beads by heating to 65°C for 5 min and then eluted by centrifugation of the beads in a new tube pre-loaded with 2 µL 1M magnesium acetate. After repeating this melting and elution process, the two eluted fractions were combined and precipitated with ethanol. The tRNA was then resuspended in 50 µL water and quantified by measuring the OD_{254}. The purified $tRNA^{Pro}_{UGG}$ was further treated with nucleotidyl transferase (CCA-adding enzyme) to increase the proline charging efficiency. For the CCA-adding reaction, 20 µM

$tRNA^{Pro}_{UGG}$ was mixed with 10 mM ATP, 10 mM cytidine-5'-triphosphate (CTP), and 6 μM CCA-adding enzyme in 1× CCA Buffer (50 mM Tris-HCl [pH 7.5], 20 mM $MgCl_2$, 0.5 mM DTT), and then incubated at 37°C for 30 min. The CCA-adding enzyme was purified from *E.coli* BL21(DE3) containing pET22-CCA-His_6 (from Allen Buskirk). For aminoacylation, 5 μM $tRNA^{Pro}_{UGG}$ was mixed with 2 mM ATP-Mg^{2+}, 0.3 mM proline, and 100 μM ProRS in 1× Reaction Buffer (40 mM Tris-HCl [pH 7.6], 10 mM magnesium acetate, 1 mM DTT), and then incubated at 30°C for 30 min. The reaction was purified from unbound nucleotides by using ProbeQuant micro columns [GE Healthcare]. $tRNA^{Pro}_{UGG}$ was extracted by phenol-chloroform and ethanol-precipitated. The *S. cerevisiae* His_6-tagged ProRS was purified as described (SternJohn et al., 2007) and obtained from Byung Shin. Yeast Lys-$tRNA^{Lys}$ was obtained from tRNA Probes, College Station, TX.

Ribosomal subunits were prepared from the yeast strain YAS2488 as described previously (Shin et al., 2007). YAS2488 cells were grown in a total of 10 L YPD medium at 30°C to OD_{600} = 1.0. Following harvesting, the cell pellet was suspended in 100 mL of Lysis Buffer E (20 mM Hepes-KOH [pH 7.4], 100 mM potassium acetate, 2.5 mM magnesium acetate, 1 mg/mL heparin, 2 mM DTT, Complete protease inhibitor cocktail [EDTA-free, Roche], 0.4 mM AEBSF) and the cells were broken with glass beads in the cold room on a bead beater (5 cycles of 1 min followed by 1 min cooling on ice). The cell lysate was cleared by centrifugation at 1,900 × *g* for 5 min followed by 27,000 × *g* for 30 min. A sucrose cushion (20 mM Hepes-KOH [pH 7.4], 100 mM potassium acetate, 2.5 mM magnesium acetate, 0.5 M KCl, 1 M sucrose, 2 mM DTT) was prepared and layered with yeast ribosomal extract. Samples were subjected to ultracentrifugation in a Beckman

Type 70 rotor for 3 h at 165,000 × *g*. Following removal of the supernatant, the ribosome pellet was dissolved in 5 mL Subunit Separation Buffer (50 mM Hepes-KOH [pH 7.4], 2 mM $MgCl_2$, 0.5 M KCl, 2 mM DTT) and mixed by rotation in the cold room for 1 h. Puromycin (10 µL of 100 mM puromycin for 1 mL sample) was added to the sample, which was then incubated on ice for 15 min, followed by 10 min at 37°C, and then 10 min on ice. Samples were then layered on a 5-20% sucrose gradient in 50 mM Hepes-KOH [pH 7.4], 5 mM $MgCl_2$, 2 mM DTT, 0.5 M KCl. Following centrifugation in a Beckman SW32 rotor for 6 h at 175,000 × *g*, samples were fractionated using a Teledyne ISCO Density Gradient Fractionator while monitoring OD_{254}. Fractions containing the 40S and the 60S ribosomal subunits were pooled separately, layered on a 1 M sucrose cushion and subjected to centrifugation in a Beckman Type70 rotor for 24 h at 60,000 × *g*. After decanting the supernatant, the subunit pellet was dissolved in 20 mM Hepes-KOH [pH 7.4], 100 mM potassium acetate, 2.5 mM magnesium acetate, and the ribosome concentration was determined by measuring the OD_{254}.

2.9 Preparation of ribosome footprints and mRNA-Seq libraries for deep sequencing

Ribosome footprints were prepared as previously described (Ingolia et al., 2012; Ingolia et al., 2009) with minor modifications (Guydosh and Green, 2014). Yeast strains J697 and J699, expressing wild-type eIF5A or eIF5A-S149P mutant, respectively, were grown in 1 L synthetic complete (SC) media at 25°C to OD_{600} = 0.5 then shifted to non-permissive 37°C (pre-warmed media exchange) for 2 h to inactivate expression of eIF5A in the mutant strain. Yeast cells were vacuum-filtered rapidly and frozen in liquid

nitrogen. Frozen pellets were mixed in Lysis Buffer F (20 mM Tris [pH 8.0], 140 mM KCl, 1.5 mM $MgCl_2$, 1% Triton X-100, and 0.1 mg/mL CHX) then lysed using a freezer mill [Spex]. Lysates were clarified and treated with 15 U of RNase I [Ambion] per OD_{254} unit for 1 h at room temperature while gently rotating on a mixer. Next, 80S monosomes were separated and fractionated by 10-50% sucrose density ultracentrifugation as described in the polysome profiling method above (Section 2.2). Collected fractions representing the 80S monosome peak were pooled then mRNA footprints were extracted by phenol-chloroform. Following isolation of mRNA footprint samples, footprints were resolved on a 15% 7 M urea-TBE gel and fragments between 25-34 nucleotides were extracted and eluted. For subsequent gel extraction precipitation steps, RNA was eluted with 300 mM sodium acetate [pH 5.5], 1 mM EDTA, 0.1 U/µL SUPERaseIn [Ambion]. As detailed by Ingolia et al. (Ingolia et al., 2012), RNA samples containing ribosome-protected mRNA footprints were dephosphorylated by treatment with T4 polynucleotide kinase [New England Biolabs] then ligated to a preadenylylated linker-1 [Integrated DNA Technologies]: 200 U T4 RNA ligase 2 truncated [New England Biolabs], 1 µg/µL linker-1 in a buffer containing 10% PEG 50, 10% DMSO, and 20 U SUPERaseIn and heated at 37°C for 2.5 h. Following linker ligation, the reverse transcription, circularization, rRNA subtraction and PCR amplification steps were performed as described previously (Ingolia et al., 2012) except rRNA subtraction oligos were each used at 3.75-7.5 µM. The oligos for yeast rRNA subtraction were:

1b 5'-biotin-$(CH_2)_6$-GGTGCACAATCGACCGATC-3'

2b 5'-biotin-$(CH2)_6$-GTTTCTTTACTTATTCAATGAAGCGG-3'

3b 5'-biotin-$(CH_2)_6$-TATAGATGGATACGAATAAGGCGTC-3'

4 5'-biotin-$(CH_2)_6$-TTGTGGCGTCGCTGAACCATAG-3'

5 5'-biotin-$(CH_2)_6$-CAGGGGGCATGCCTGTTTGAGCGTCAT-3'

6 5'-biotin-$(CH_2)_6$-CGGTGCCCGAGTTGTAATTT-3'

DNA was eluted from TBE gels with 300 mM sodium chloride, 1 mM EDTA, and 10 mM Tris [pH 8.0]. After PCR amplification, cDNA libraries were sequenced on an Illumina HiSeq2000 at the UC Riverside Sequencing facility.

In parallel with the ribosome footprints, mRNA-Seq samples were prepared by purification of total RNA extracted from cells as described (Guydosh and Green, 2014). After phenol-chloroform extraction, total RNA was subjected to polyA pulldown with oligo-dT dynabeads [Life Technologies]. Then, the RNA was fragmented by treatment in a solution containing 2 mM EDTA, 10 mM sodium carbonate, and 100 mM sodium bicarbonate [pH 9.2] for 20 min at 95°C. Following fragmentation, the RNA was precipitated and size-selected on a 15% 7 M urea-TBE gel. Unlike the ribosome footprint samples, 40-60 nucleotide fragments were extracted from the denaturing gel and eluted. All subsequent steps for total RNA samples were performed similar to the steps taken during ribosome footprint generation.

Data Analysis of deep sequencing libraries was performed by Nicholas Guydosh, a member of the Rachel Green lab at Johns Hopkins Medical Institute and Howard Hughes Medical Institute.

3. eIF5A promotes translation of polyproline motifs

3.1 The significance and rationale for study

A common misperception is that the ribosome is a monolithic machine that catalyzes peptide bonds at equivalent rates regardless of the amino acid. In fact, certain residues including the imino acid proline are poor substrates for peptide bond formation (Pavlov et al., 2009; Wohlgemuth et al., 2008). At the time of my preliminary studies regarding the function of eIF5A in protein synthesis, it was shown that the translation elongation factor EF-P is essential for translation of polyproline sequences by bacterial ribosomes (Doerfel et al., 2013; Ude et al., 2013); however, it was still unclear how eukaryotic ribosomes managed to synthesize peptide bonds with poor substrates. In this collaborative study, we aimed to determine the requirements for eIF5A in peptide bond synthesis for particular amino acids.

In addition to the canonical elongation factors eEF1A and eEF2, eIF5A has also been linked to translation elongation. Depletion of eIF5A *in vivo* or inactivation of a *ts*$^{-}$ mutant of yeast eIF5A impaired translation elongation and stabilized polysomes in the absence of CHX (Saini et al., 2009) and increased the average ribosomal transit time *in vivo* (Gregio et al., 2009; Saini et al., 2009). Moreover, addition of eIF5A resulted in a two-fold stimulation in the rate of (Met-Phe-Phe) M-F-F tripeptide synthesis using a reconstituted yeast *in vitro* translation system (Saini et al., 2009). Taken together, these data revealed a role for eIF5A in translation elongation as opposed to the previously held notion that eIF5A functioned during translation initiation. However, it was difficult to rationalize the essential requirement for eIF5A in yeast with the modest two-fold stimulation of M-F-F tripeptide synthesis, suggesting that eIF5A may have a more specialized and critical requirement in translation elongation.

eIF5A is of particular interest because it is the only protein that contains the modified amino acid hypusine and because eIF5A and hypusine have been linked to tumorigenesis and cancer (Scuoppo et al., 2012; Silvera et al., 2010). Earlier studies revealed that the impact of bacterial EF-P on dipeptide synthesis varied for different aminoacyl analogs (Ganoza and Aoki, 2000; Glick et al., 1979), suggesting that EF-P, and by extension eIF5A, may facilitate the reactivity of certain amino acids and/or tRNAs in peptide bond synthesis. Consistent with these findings, and during my preliminary analysis of eIF5A function in specific amino acid or tRNA reactivity using dual luciferase reporters, reports showed that EF-P enhances the synthesis of proteins containing stretches of consecutive proline residues (Doerfel et al., 2013; Ude et al., 2013). In our follow-up analysis, we addressed whether eIF5A has a similar function in yeast. In our paper (Gutierrez et al., 2013), we used *in vivo* assays in yeast and *in vitro* reconstituted translation assays to reveal a specific requirement for eIF5A in promoting peptide bond formation between consecutive proline residues. Addition of eIF5A relieved ribosomal stalling during translation of three consecutive proline residues *in vitro* (Gutierrez et al., 2013), and loss of eIF5A function impaired translation of polyproline-containing proteins *in vivo*. Thus, we proposed that eIF5A, like its bacterial ortholog EF-P, stimulates the peptidyl transferase activity of the ribosome and facilitates the reactivity of poor substrates like proline.

3.2 eIF5A stimulates translation through polyproline sequences *in vivo*

To further define the role of eIF5A in translation elongation and to determine whether eIF5A, like EF-P, stimulates translation of specific amino acid motifs, I monitored the

expression of a set of dual luciferase reporters in isogenic yeast strains expressing wild-type eIF5A or the *ts*⁻ eIF5A-S149P mutant (Saini et al., 2009; Zuk and Jacobson, 1998). These dual luciferase reporters, developed by Beth Grayhack and colleagues to examine codon bias in translation (Letzring et al., 2010), express a single mRNA in which the 5' *Renilla* luciferase and 3' firefly luciferase ORFs are joined in-frame by sequences encoding repeats of 10 identical codons for each of the 20 amino acids (Fig. 6A). For the initial analysis, the inserted sequences repeated the optimal codon for each amino acid (Letzring et al., 2010). As shown in Fig. 6B (top panel), and as previously observed (Letzring et al., 2010), the ratio of firefly to *Renilla* luciferase activity varied depending on the repeated codon. While the ratios for most constructs were similar to the no insert control, low ratios were observed for the ArgAGA and CysUGU reporters (Fig. 6B, top panel); whereas, high ratios were observed with GluGAA and PheUUC codon insertions (Fig. 7). These eIF5A-independent effects might reflect codon or aminoacyl-tRNA abundance or impacts of the inserted amino acids on luciferase activity in the bifunctional *Renilla*-firefly luciferase fusion protein.

If eIF5A stimulates the translation of specific amino acids, then the ratio of firefly to *Renilla* luciferase activity is expected to decrease when these reporters are analyzed in the strain expressing eIF5A-S149P when grown at the semi-permissive temperature (33°C). As shown in Fig. 8A, the slow-growth phenotype of the eIF5A-S149P mutant at 30°C is exacerbated at 33°C, and the mutant strain fails to grow at 37°C. The impaired growth at 33°C is marked by reduced levels of eIF5A (Fig. 8B) and by retention of polysomes in the absence of CHX (Fig. 8C), indicative of a general translation elongation defect in the strain. Analysis of all 20 luciferase reporter constructs revealed that only the

A

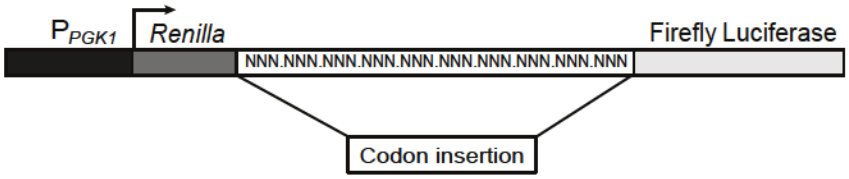
P PGK1
Renilla
Firefly Luciferase
NNN.NNN.NNN.NNN.NNN.NNN.NNN.NNN.NNN.NNN
Codon insertion

B

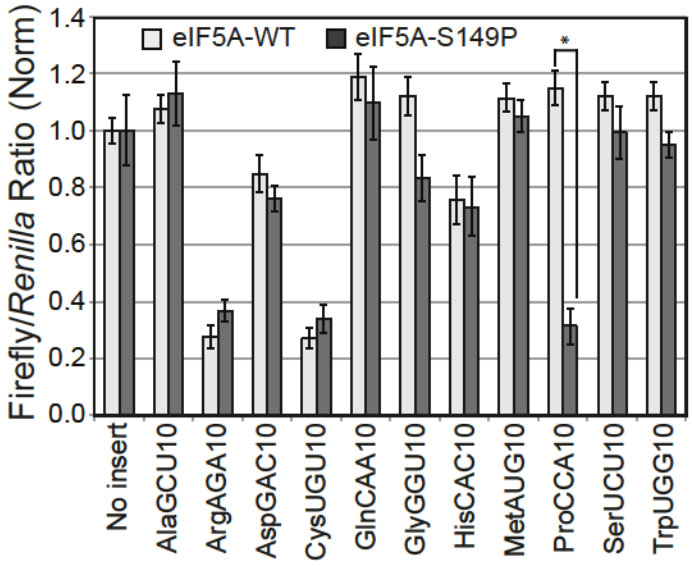
eIF5A-WT
eIF5A-S149P
*
Firefly/Renilla Ratio (Norm)
1.4
1.2
1.0
0.8
0.6
0.4
0.2
0.0
No insert
AlaGCU10
ArgAGA10
AspGAC10
CysUGU10
GlnCAA10
GlyGGU10
HisCAC10
MetAUG10
ProCCA10
SerUCU10
TrpUGG10

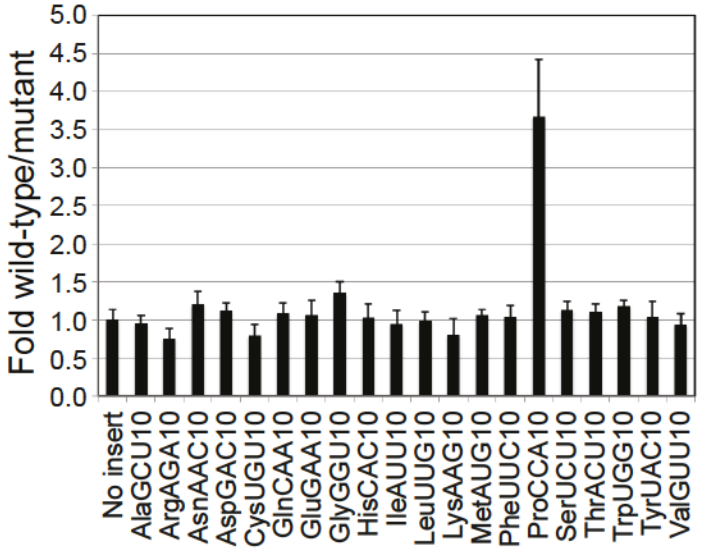
Fold wild-type/mutant
5.0
4.5
4.0
3.5
3.0
2.5
2.0
1.5
1.0
0.5
0.0
No insert
AlaGCU10
ArgAGA10
AsnAAC10
AspGAC10
CysUGU10
GlnCAA10
GluGAA10
GlyGGU10
HisCAC10
IleAUU10
LeuUUG10
LysAAG10
MetAUG10
PheUUC10
ProCCA10
SerUCU10
ThrACU10
TrpUGG10
TyrUAC10
ValGUU10

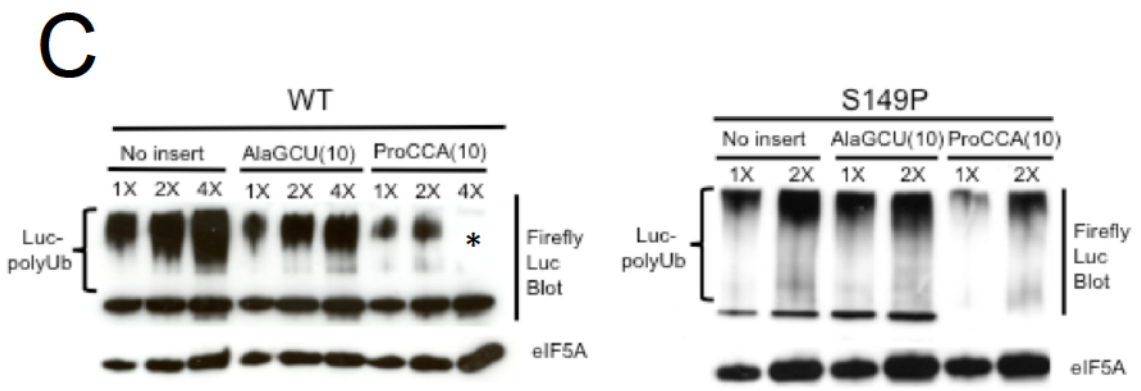

Figure 6. eIF5A stimulates translation of polyproline motifs *in vivo*.

(A) Schematic of *Renilla*-firefly luciferase reporter construct. Codon repeats were inserted in-frame between the *Renilla* and firefly luciferase ORFs (Letzring et al., 2010).

(B) Dual luciferase reporter constructs containing 10 repeats of the indicated codon were introduced into isogenic yeast strains expressing wild-type eIF5A or *ts*⁻ eIF5A-S149P. (Top panel) Following growth at semi-permissive 33°C, luciferase activities were determined, and the firefly to *Renilla* luciferase ratio for each construct was normalized to the ratio obtained from controls in which the reporter contained no insert between the ORFs. (Bottom panel) The fold difference in luciferase ratios between cells expressing wild-type eIF5A and eIF5A-S149P was quantitated and then normalized to the values obtained from the no insert control. *Statistical significance for ProCCA(10) was measured by student's t-test with a p-value <0.05. Error bars were calculated as propagated standard errors of the mean for three independent transformants.

(C) Dual luciferase reporters containing no insert or 10 repeats of AlaGCU or ProCCA were introduced into isogenic yeast strains expressing wild-type eIF5A (Left panel) or *ts*⁻ eIF5A-S149P (Right panel). Cells were grown at semi-permissive 33°C to OD_{600} 0.5 and 20 uM MG132 was added to inhibit the proteasome. Cells were broken with glass beads

in the presence of 10% trichloroacetic acid (TCA), and different amounts of each extract differing by a factor of 2 were loaded in successive lanes and subjected to immunoblot analysis using polyclonal anti-firefly luciferase [Thermo Scientific] or polyclonal anti-yeast eIF5A antiserum. *The unexpected absence of the higher molecular weight polyubiquitinated species (polyUb) in ProCCA(10) 4X lane for eIF5A-WT may be due to a blotting error.

Pro codon insertions demonstrated a strong dependence on eIF5A (Fig. 6B, bottom panel). For the ProCCA reporter, the ratio of firefly to *Renilla* luciferase in the strain expressing wild-type eIF5A was ~3.7-fold greater than the ratio observed in the strain expressing eIF5A-S149P (Fig. 6B, bottom panel), whereas this normalized ratio ranged from 0.75 (ArgAGA) to 1.35 (GlyGGU) for reporters containing any of the other 19 codon insertions. To validate the reporter activity, western blot analysis was performed for the firefly luciferase protein. Whereas the *Renilla*-firefly luciferase fusion proteins (expected size of ~99 kDa) were largely intact for constructs containing the AlaGCU or ProCCA codon inserts in the wild-type strain, expression of firefly luciferase was defective for the ProCCA, but not the AlaGCU, construct in the eIF5A-S149P mutant strain grown at 33°C (Fig. 6C). These results support the reporter activity data and suggest that translation of the 3' firefly luciferase ORF requires the eIF5A-dependent translation of the ProCCA insert.

	Firefly/*Renilla* Ratio	
Amino Acid(10)	**eIF5A-WT (SD)**	**eIF5A-S149P (SD)**
no insert	3.09 (0.10)	6.91 (0.61)
SerUCU	3.47 (0.11)	6.85 (0.23)
HisCAC	2.34 (0.25)	5.07 (0.54)
GlnCAA	3.68 (0.22)	7.59 (0.58)
ThrACU	3.66 (0.13)	7.42 (0.05)
AsnAAC	3.97 (0.33)	7.38 (0.53)
AspGAC	3.01 (0.27)	7.17 (0.63)
GlyGGU	3.47 (0.18)	5.74 (0.23)
ProCCA	3.55 (0.15)	2.16 (0.39)
no insert	8.45 (0.27)	11.46 (0.27)
PheUUC	23.26 (0.97)	30.42 (4.11)
TrpUGG	9.46 (0.28)	10.86 (0.44)
ArgAGA	2.34 (0.35)	4.21 (0.42)
MetAUG	9.42 (0.28)	12.01 (0.58)
LysAAG	2.03 (0.50)	3.43 (0.34)
CysUGU	2.27 (0.29)	3.89 (0.57)
no insert	2.25 (0.08)	2.66 (0.12)
LeuUUG	7.22 (0.48)	8.69 (0.78)
TyrUAC	7.71 (0.81)	8.77 (1.38)
IleAUU	8.12 (1.03)	10.15 (1.35)
ValGUU	12.70 (0.82)	16.03 (2.13)
AlaGCU	2.42 (0.07)	3.00 (0.27)
GluGAA	228.98 (16.00)	254.67 (38.64)

Figure 7. Summary of the firefly to *Renilla* luminescence ratios for each of the reporters transformed into wild-type eIF5A and eIF5A-S149P mutant yeast strains grown at 33°C.

Ratios of firefly to *Renilla* luciferase activity were determined for three independent transformants of each construct, and the average ratio (x 10^3) and standard deviation (SD) are presented. The values in Figure 6 were obtained by normalizing the ratios to the respective no insert control for each of the three sets of constructs.

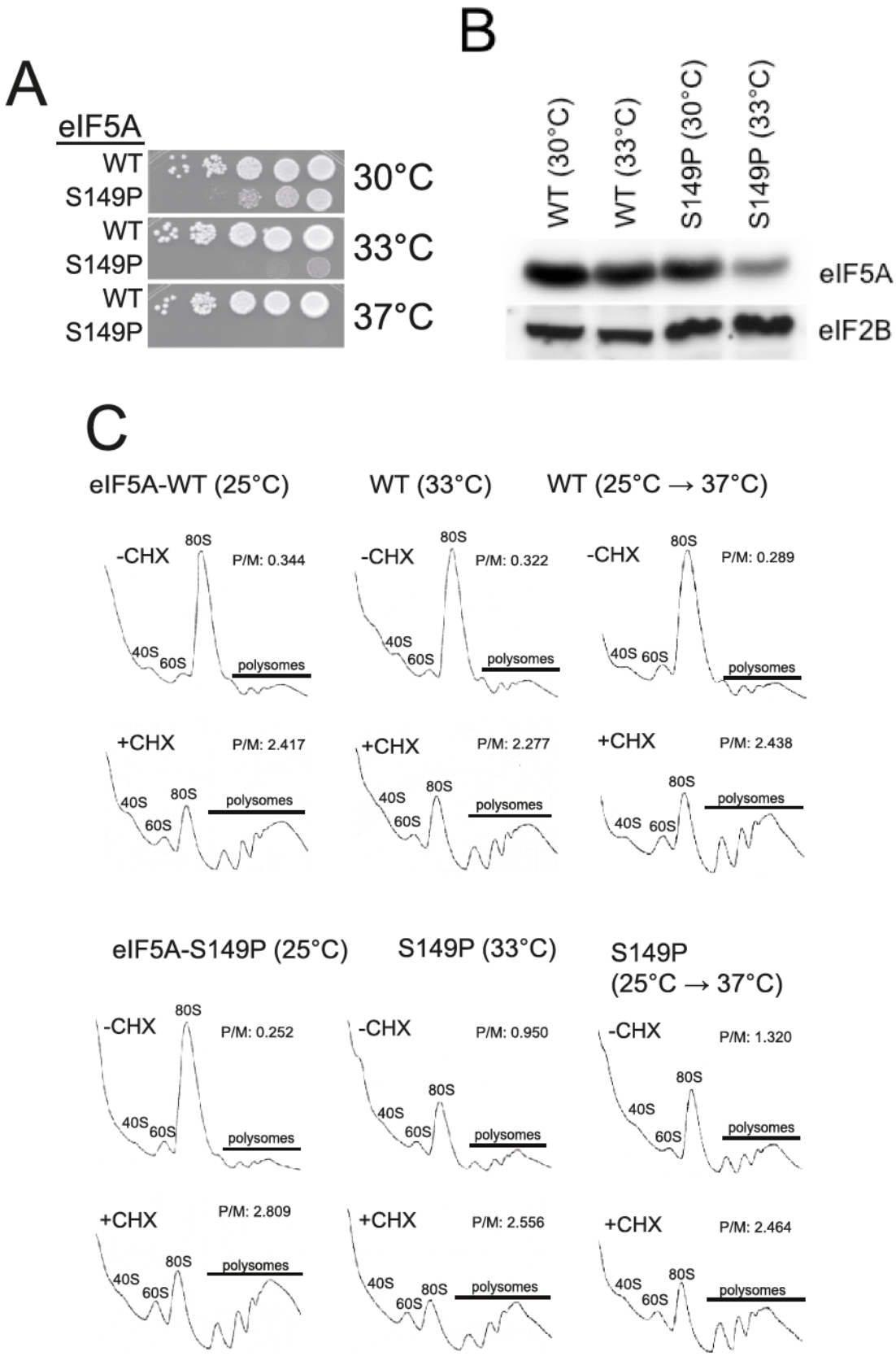
A
eIF5A
WT
S149P
30°C
WT
S149P
33°C
WT
S149P
37°C
B
WT (30°C)
WT (33°C)
S149P (30°C)
S149P (33°C)
eIF5A
eIF2B
C
eIF5A-WT (25°C)
WT (33°C)
WT (25°C → 37°C)
-CHX
P/M: 0.344
80S
40S
60S
polysomes
-CHX
P/M: 0.322
80S
40S
60S
polysomes
-CHX
P/M: 0.289
80S
40S
60S
polysomes
+CHX
P/M: 2.417
40S
80S
60S
polysomes
+CHX
P/M: 2.277
40S
80S
60S
polysomes
+CHX
P/M: 2.438
80S
40S
60S
polysomes
eIF5A-S149P (25°C)
S149P (33°C)
S149P
(25°C → 37°C)
-CHX
P/M: 0.252
80S
40S
60S
polysomes
-CHX
P/M: 0.950
80S
40S
60S
polysomes
-CHX
P/M: 1.320
80S
40S
60S
polysomes
+CHX
P/M: 2.809
40S
80S
60S
polysomes
+CHX
P/M: 2.556
40S
80S
60S
polysomes
+CHX
P/M: 2.464
40S
80S
60S
polysomes

Figure 8. The *ts*⁻ eIF5A-S149P mutant impairs yeast cell growth, protein expression, and translation elongation.

(A) Isogenic wild-type and eIF5A-S149P mutants strains were grown to saturation, and 4-µL volumes of serial dilutions (OD_{600} = 1.0, 0.1, 0.01, 0.001, and 0.0001) were spotted on YPD medium and incubated for 2 days at 30°C, 33°C, and 37°C.

(B) WCEs from yeasts strains expressing wild-type eIF5A or eIF5A-S149P and grown at permissive (30°C) and semi-permissive (33°C) temperatures were subject to immunoblot analysis using antisera specific for eIF5A or eIF2B.

(C) Polysome profiles were analyzed from wild-type and eIF5A-S149P mutant strains grown under permissive (25°C) or semi-permissive (33°C) conditions, or following a temperature-shift from 25°C to 37°C for 2 h, were treated with 50 µg/mL CHX (+CHX) or left untreated (-CHX), and WCEs were separated on sucrose gradients and fractionated to visualize polysomes and the indicated ribosomal species. Polysome to monosome (P/M) ratios were calculated by comparing the areas under the polysome and 80S peaks.

To test whether the impaired expression of firefly luciferase from the construct containing the ProCCA codon repeats was specific to the mutation of eIF5A, mutants of two other translation elongation factors were evaluated. No significant differences in firefly to *Renilla* luciferase ratios were observed when constructs containing proline or alanine codon insertions were examined in strains expressing *ts*⁻ mutants of translation elongation factors eEF2 or eEF3 (Fig. 9A-B). Thus, polyproline peptide bond formation shows a unique dependence on eIF5A. Alternatively, this result could reflect a specific requirement for eIF5A to promote decoding of the ProCCA codon by $tRNA^{Pro}_{UGG}$. As the

Pro-tRNA^{Pro} is composed of an amino acid residue and its cognate tRNA, either Pro or the accommodating tRNA could impose a requirement for eIF5A. Consistent with the hypothesis that eIF5A functions to promote polyproline peptide bond formation, reporters containing 10 repeats of the Pro codons CCA, CCG or CCU displayed a strong requirement for eIF5A, whereas no Ala codon insertions conferred a dependence on eIF5A (Fig. 9C). While these data are not definitive, as the yeast tRNA$^{Pro}_{UGG}$ has been reported to decode all four proline codons (Johansson et al., 2008), they suggest that the amino acid proline rather than the tRNA likely determine the requirement for eIF5A.

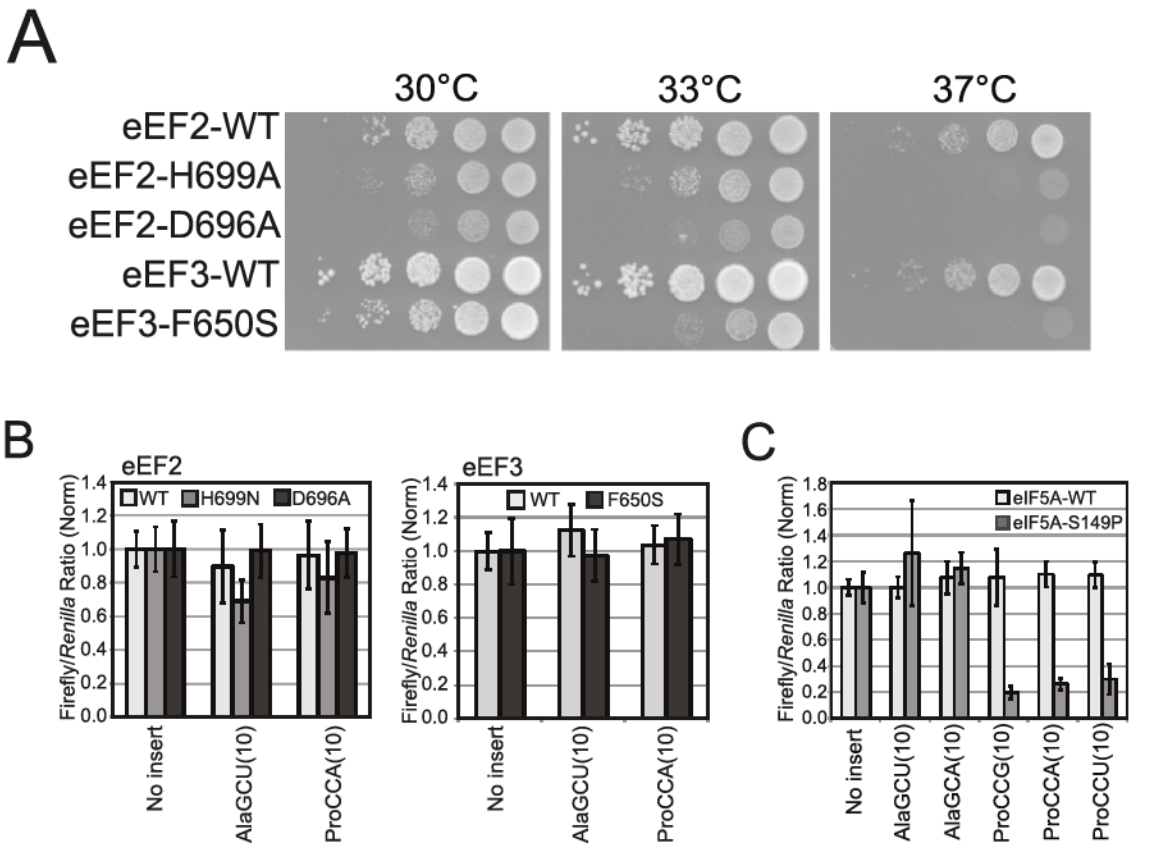

Figure 9. eEF2 and eEF3 mutants do not specifically impair polyproline synthesis.

(A) Yeast strains expressing the indicated *ts*$^{-}$ mutant of eEF2 or eEF3, or their respective isogenic strain expressing the wild-type factor, were grown to saturation, and 4-μL

volumes of serial dilutions (OD_{600} = 1.0, 0.1, 0.01, 0.001, and 0.0001) were spotted on YPD medium and incubated for 2 days at 30°C, 33°C, and 37°C.

(B) Dual luciferase reporter constructs containing 10 repeats of AlaGCU or ProCCA codons were introduced into the respective wild-type and eEF2 (left panel) or eEF3 (right panel) mutant strains, and luciferase activities were determined following growth at semi-permissive 33°C. Results were quantitated as described for Figure 6B.

(C) Dual luciferase reporters containing 10 consecutive repeats of the indicated Ala or Pro codons were assayed in wild-type or eIF5A-S149P mutant strains and the data was normalized to the no insert control as described in Fig. 6. Error bars were calculated as propagated standard deviations for three independent transformants.

To define the number of consecutive proline residues needed to impose a requirement for eIF5A, the dual luciferase reporters were modified to contain one, two, three, four, six, eight or ten consecutive ProCCA or PheUUC codons. As shown in Fig. 10, luciferase ratios for the Phe codon insertion constructs were the same in the wild-type and eIF5A-S149P mutant strains (fold wild-type/mutant = ~1.0). Likewise, insertion of one or two proline codons did not significantly impact luciferase ratios in the eIF5A mutant strain compared to the wild-type control. In contrast, insertion of four proline codons resulted in reduction of the luciferase ratio in the eIF5A-S149P mutant strain. (A modest reduction may be evident with insertion of three Pro codons as well.) Insertion of six, eight or ten proline codons further exacerbated the defect, and the normalized ratio of firefly to *Renilla* luciferase in the strain expressing wild-type eIF5A was ~3-4.5–fold greater than the ratio observed in cells expressing eIF5A-S149P. These results indicate

that at least four (or perhaps three) consecutive proline codons are needed to impose an eIF5A-dependency on protein synthesis. The data also reveal a significant decrease in the firefly to *Renilla* ratio between wild-type and mutant cells when the number of consecutive Pro codons is increased from 8 to 10. This unexpected lessening of eIF5A dependence is due to a gradual increase in the firefly to *Renilla* luciferase ratio of the mutant as the number of codons is increased from 6 to 10 (data not shown). At this point, it is unclear how translation occurs for reporters containing longer (>6 Pro codons) Pro stretches when eIF5A is slightly inactivated in the S149P mutant.

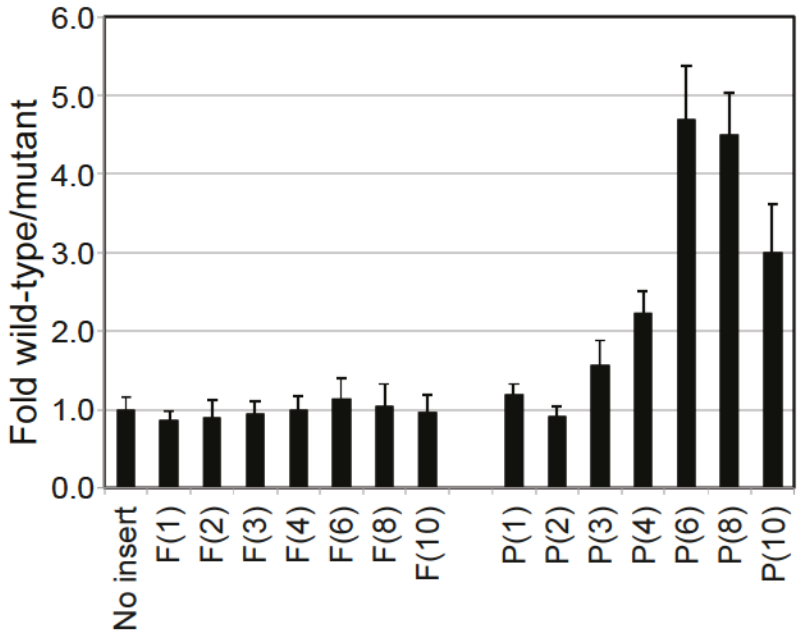

Figure 10. Translation of three or more consecutive proline codons reveals eIF5A dependency.

Dual luciferase reporters containing 1, 2, 3, 4, 6, 8, or 10 consecutive PheUUC (F) or ProCCA (P) codons were assayed in wild-type or eIF5A-S149P mutant strains grown at a semi-permissive temperature (33°C) and the fold difference in luciferase ratios were

quantitated and normalized to the no insert control as described in Fig. 6.

3.3 Expression of yeast polyproline-containing proteins requires eIF5A *in vivo*

Analysis of the *Saccharomyces cerevisiae* genome identified 549 proteins (out of 5886 ORFs) that contain polyproline motifs with at least three consecutive proline residues. To test whether expression of yeast proteins containing polyproline motifs is dependent on eIF5A, selected plasmids from the Yeast ORF Collection were introduced into isogenic strains expressing wild-type eIF5A or the *ts*$^-$ mutant eIF5A-S149P. Transformants were grown at the semi-permissive temperature of 33°C to partially inactivate eIF5A-S149P and in galactose medium to induce the *GAL1* promoter used to drive ORF expression. In experiments performed by Joo-Ran Kim, a member of the Dever lab, protein expression was monitored by Western analysis using antibodies to detect the HA-tag incorporated at the C-terminus of each ORF (Gelperin et al., 2005). Expression of LDB17, a regulator of endocytosis and containing a 9 consecutive polyproline motif, was dramatically reduced in the eIF5A mutant strain relative to the wild-type eIF5A strain and to the loading control eIF2α (no polyproline motifs) (Fig. 11A). Other yeast proteins, including EAP1 (two 6 Pro, one 3 Pro motif), and VRP1 (multiple polyproline sequences including one 9 Pro, one 8 Pro, one 6 Pro, four 5 Pro, three 4 Pro, and two 3 Pro motifs), also exhibited reduced protein levels in the eIF5A mutant strain (Gutierrez et al., 2013). Stable expression of TIF11 (eIF1A, no polyproline motifs) from a Yeast ORF Collection plasmid in the wild-type and mutant eIF5A strains indicates that the eIF5A-sensitive expression of the polyproline-containing proteins is not due to impacts on the expression system (e.g. the *GAL1* promoter, growth at 33°C) (Fig. 11A). In addition, substituting Ala

in place of the nine Pro residues in the C-terminal 9 Pro motif restored LDB17 expression in the eIF5A-S149P mutant (Fig. 11B), directly linking eIF5A function to the synthesis of polyproline motifs *in vivo*.

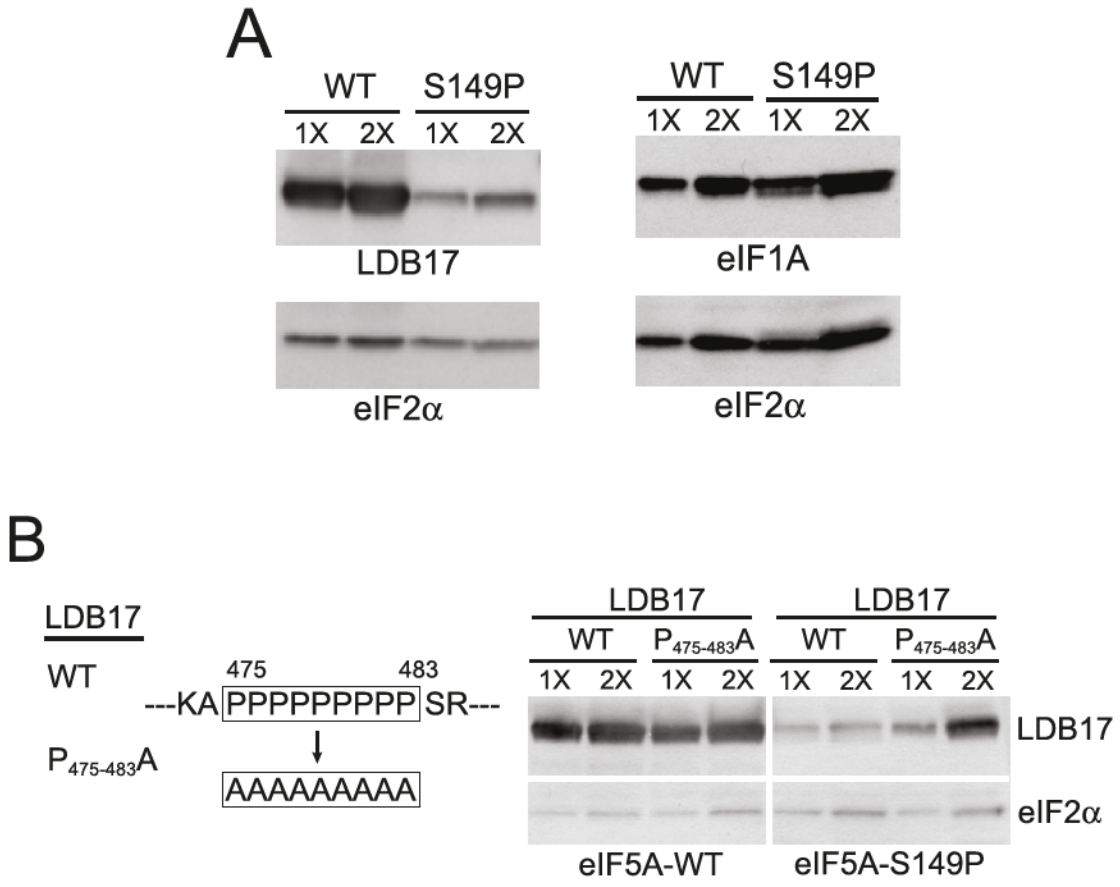

Figure 11. Expression of polyproline-containing proteins requires eIF5A *in vivo.*

(A) Plasmids expressing HA-tagged forms of the yeast proteins LDB17 or eIF1A under the control of the yeast *GAL1* promoter were introduced into isogenic strains expressing wild-type eIF5A or eIF5A-S149P. Cells were grown at semi-permissive 33°C in galactose medium, broken with glass beads in the presence of 10% TCA, and two volumes of each extract differing by a factor of two were loaded in successive lanes and

subjected to immunoblot analysis using monoclonal anti-HA or polyclonal anti-yeast eIF2α antiserum.

(B) The experiment in panel A was repeated using an LDB17 construct in which Ala codons were substituted for the nine Pro codons in the polyproline motif.

*Experiments for Panels A and B were conducted by Joo-Ran Kim.

3.4 eIF5A plays an essential role in polyproline peptide synthesis

To confirm the requirement for eIF5A in polyproline synthesis, Byung Shin, a staff scientist in the Dever lab, performed *in vitro* reconstituted yeast translation assays to directly examine the role of eIF5A in polyproline peptide bond synthesis. As shown in Figure 12A, minimal translation initiation (48S) complexes containing unstructured model mRNAs encoding polyproline or polyphenylalanine were assembled with [^{35}S]Met-tRNA$_i^{Met}$ in the P site of the ribosome. Following ribosomal subunit joining, the 80S initiation complexes were pelleted through a sucrose cushion to remove initiation factors and unbound Met-tRNA$_i^{Met}$. Next, elongation factors and the necessary aminoacyl-tRNAs were added to the purified 80S complexes in the absence or presence of excess recombinant eIF5A. As described in more detail in Chapter 5, the recombinant Hyp-eIF5A was prepared from *E. coli* that co-expresses eIF5A, *DYS1* and *LIA1*. The peptide synthesis activity in the assays was monitored by electrophoretic TLC (Eyler and Green, 2011; Youngman et al., 2004).

The Met-Phe (M-F), M-F-F, and M-F-F-F peptides resolved well on electrophoretic TLC (Gutierrez et al., 2013) and were synthesized in the absence or presence of eIF5A with less than a two-fold stimulation in the fraction of maximal yield

(Y_{max}) for formation of the peptides in the presence of eIF5A (Fig. 12B-C). These results are consistent with the previously reported ~2-fold stimulation of M-F-F synthesis upon adding eIF5A to the reconstituted system (Saini et al., 2009). In preliminary experiments, the proline-containing peptides Met-Pro (M-P), M-P-P and M-P-P-P were not resolved as discrete spots on the TLC (Gutierrez et al., 2013). However, incorporation of a lysine residue at the C-terminus of the proline peptides enabled resolution of the peptides by TLC and facilitated their quantitation. The fraction of maximum peptide yield for Met-Pro-Lys (M-P-K) peptide synthesis was increased ~1.3-fold by adding eIF5A (Y_{max} = 0.36 in the absence of eIF5A and 0.48 in the presence of eIF5A) (Fig. 12B-C). Thus, the presence of a single Pro residue conferred a modest eIF5A dependency for peptide synthesis. In contrast, synthesis of the M-P-P-K peptide containing two prolines was significantly impaired in the absence of eIF5A (Y_{max} = 0.06 ±0.03); and an 8.3-fold stimulation of Y_{max} was observed upon adding eIF5A (Y_{max} = 0.49 ±0.02) (Fig. 12B-C). Similar to reports made by Doerfel and colleagues (Doerfel et al., 2013), the large difference in reaction endpoints for the proline-containing peptides in the presence versus the absence of eIF5A suggests that variable and competing reactions are likely occurring (e.g. peptidyl-tRNA drop-off). Since the observed rates reflect both peptide bond formation and these competing reactions, the analysis was limited to the reaction endpoint differences and not the observed rates. Remarkably, no detectable formation of the M-P-P-P-K peptide, containing three consecutive proline residues, occurred in the absence of eIF5A during the time course of the experiments. The addition of eIF5A efficiently restored M-P-P-P-K synthesis stimulating the Y_{max} at least 39-fold (Y_{max} = 0.58 ±0.1) (Fig. 12C). Thus, consistent with the results of the *in vivo* assays, eIF5A is

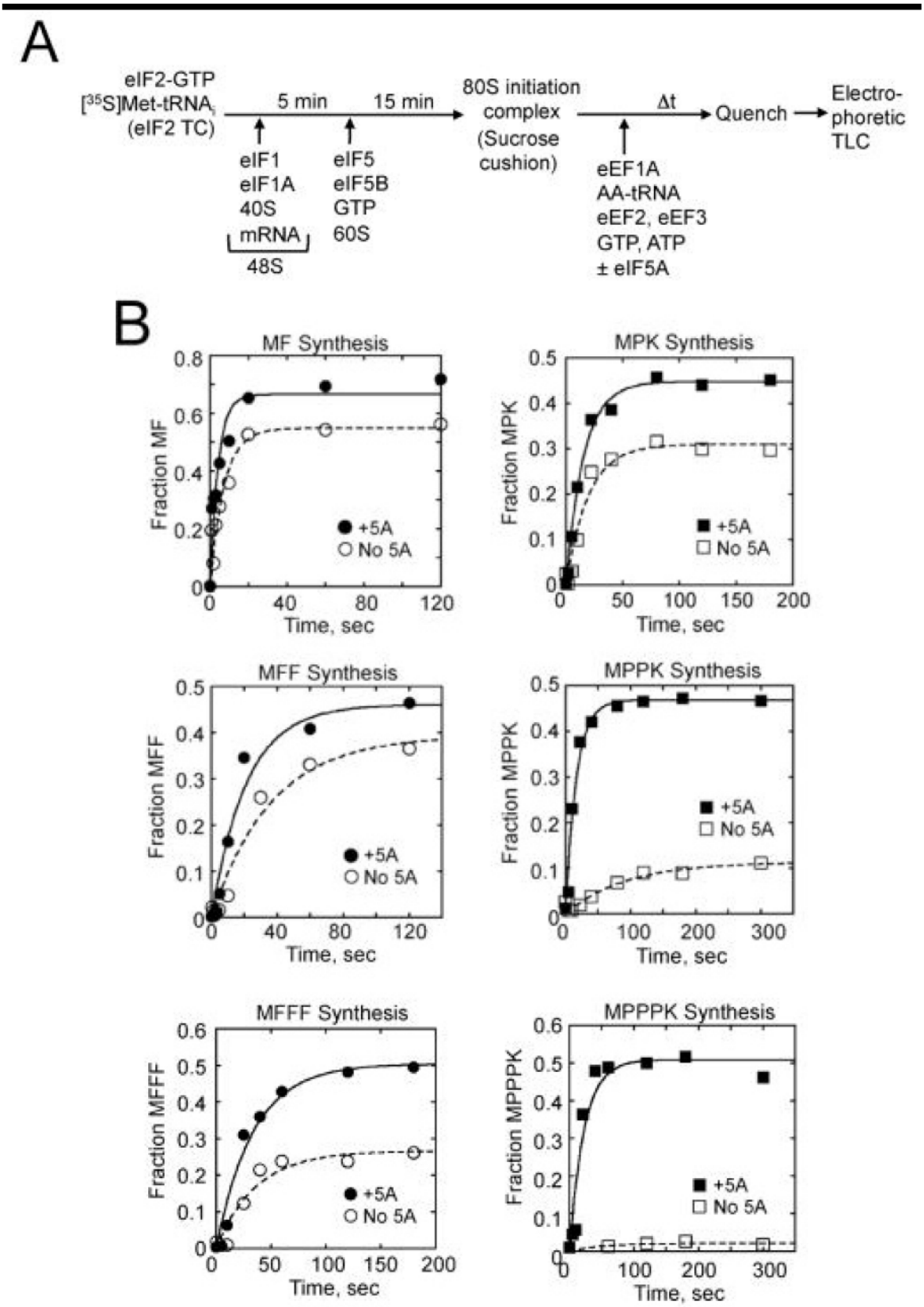
A
eIF2-GTP
[35S]Met-tRNAi
(eIF2 TC)
5 min
15 min
eIF1
eIF1A
40S
mRNA
48S
eIF5
eIF5B
GTP
60S
80S initiation complex (Sucrose cushion)
Δt
eEF1A
AA-tRNA
eEF2, eEF3
GTP, ATP
± eIF5A
Quench
Electro-phoretic TLC
B
MF Synthesis
Fraction MF
Time, sec
+5A
No 5A
MPK Synthesis
Fraction MPK
MFF Synthesis
Fraction MFF
MPPK Synthesis
Fraction MPPK
MFFF Synthesis
Fraction MFFF
MPPPK Synthesis
Fraction MPPPK

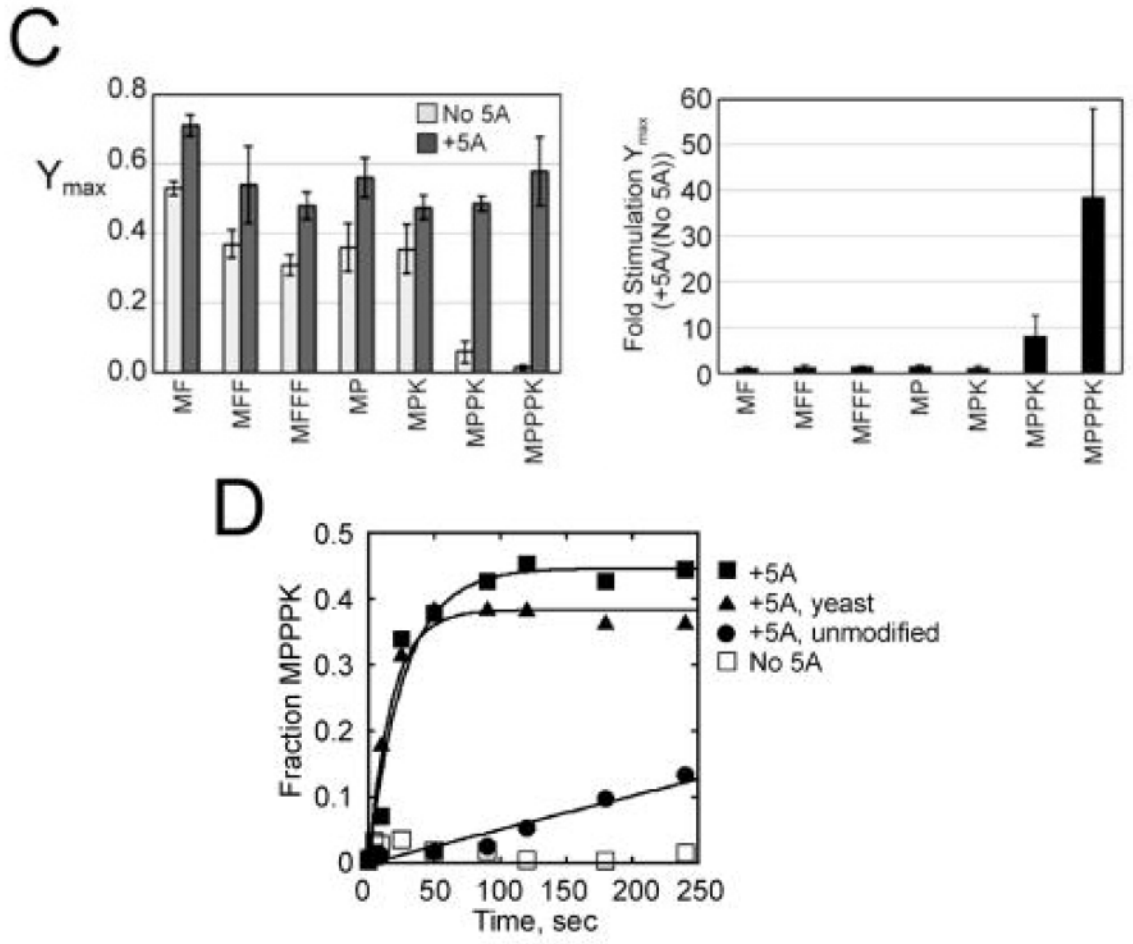

Figure 12. eIF5A stimulates synthesis of polyproline peptides.

(A) Scheme for *in vitro* reconstituted translation elongation assay.

(B) Fractions of M-F, M-F-F, M-F-F-F (left column) or M-P-K, M-P-P-K, and M-P-P-P-K (right column) synthesis in elongation assays performed in the absence (open symbols) or presence of eIF5A (closed symbols) were plotted and fit to a single exponential equation.

(C) Summary of maximum fractions of peptide synthesis (Y_{max}, left panel) and fold stimulation of Y_{max} by adding eIF5A (right panel) calculated from the data in panel B. Error bars are (left panel) standard deviations from at least three independent experiments and (right panel) calculated propagated errors.

(D) Effect of eIF5A hypusine modification on peptide synthesis. Fraction of M-P-P-P-K synthesis in reactions lacking eIF5A, containing unmodified eIF5A (no hypusine), or containing Hyp-eIF5A prepared from *E. coli* or purified from yeast (+5A, yeast) was plotted and fit to a single exponential equation.

*Experiments for these assays were performed by Byung Shin.

---

required for synthesis of peptides containing consecutive Pro residues. Moreover, these *in vitro* experiments demonstrate that eIF5A is acting directly to promote polyproline synthesis.

To assess the importance of the hypusine modification on eIF5A, M-P-P-P-K synthesis was analyzed using different forms of the factor. As shown in Fig. 12D, no M-P-P-P-K synthesis was detected in the absence of eIF5A and very little synthesis was detected in assays that included unmodified eIF5A prepared from *E. coli*. In contrast, hypusine-modified eIF5A, prepared either from yeast or from *E. coli* co-expressing the hypusine modification enzymes, readily stimulated M-P-P-P-K synthesis (Y_{max} = 0.38 ±0.02 for yeast eIF5A; and Y_{max} = 0.45 ±0.02 for recombinant eIF5A). Thus, the hypusine modification of eIF5A is necessary for efficient polyproline synthesis *in vitro*.

3.5 Conclusion

Our data indicate that eIF5A promotes the translation of homopolyproline sequences and are consistent with recent reports on bacterial EF-P (Doerfel et al., 2013; Ude et al., 2013). Partial inactivation of eIF5A-S149P in yeast, like deletion of the *efp* gene in *E. coli* (Ude et al., 2013), impaired expression of reporters or native proteins containing

polyproline sequences *in vivo*. Moreover, peptide synthesis assays demonstrated that eIF5A (Gutierrez et al., 2013) and EF-P (Doerfel et al., 2013) are critical for the *in vitro* synthesis of polyproline peptides. Additionally, in collaboration with Chris Woolstenhulme and Allen Buskirk at Brigham Young University, we performed toe-printing analyses to monitor ribosome stalling during *in* vitro translation of mRNAs encoding polyproline motifs (Gutierrez et al., 2013). In these experiments, ribosomes translating in the absence of eIF5A stalled with diproline bound to the P-site tRNA and a Pro codon in the A site (presumably bound by Pro-tRNA^{Pro}). These data corroborate the reporter and peptide synthesis assays, and together suggest that eIF5A and, likewise, EF-P are required to promote synthesis of the proline-proline peptide bonds in higher-ordered polyproline sequences.

4. Genome-wide profiling reveals ribosomal stalling during translation of polyproline sequences in a temperature-sensitive eIF5A mutant

4.1 The ribosome profiling strategy for the identification of translational targets of eIF5A

A large proportion of cellular mRNAs are targets for protein production by the ribosome. To facilitate protein synthesis, ribosomes must locate to the appropriate start codon, decode the mRNA, catalyze the synthesis of peptide bonds between a peptidyl-tRNA and aminoacyl-tRNA, and release the completed polypeptide chain. However, strong secondary structure elements or rare codons in the mRNA, truncated coding sequences, low tRNA availability, or interactions between the nascent peptide and the ribosomal exit tunnel can perturb the synthesis of peptide bonds. To overcome these challenges, translation factors facilitate protein synthesis by maintaining translation start site fidelity, ensuring the delivery of the proper aminoacyl-tRNA in a codon-specific manner, and promoting the release of the polypeptide chain upon encountering a stop codon. Moreover, some translation factors, rather than stimulating general protein synthesis, have specialized roles in enhancing the translation of specific mRNAs or the incorporation of specific amino acids, such as selenocysteine (Lobanov et al., 2010).

Polysome profile analyses indicated a general elongation defect when eIF5A was depleted in yeast (Saini et al., 2009). Because polysome profile analyses of WCEs examine translation of all mRNAs in the cell, the polysome retention in the absence of CHX in the eIF5A degron strain indicates that translation of most cellular mRNAs is impaired in the absence of eIF5A. However, although the polysome profile technique is quite useful for identifying general translation defects, the technique provides limited resolution and the results are biased toward examining the most abundant cellular mRNAs.

The ribosome profiling strategy involves the deep sequencing of ribosome-protected mRNA fragments and is a powerful tool to visualize ribosome positions throughout a transcriptome (Ingolia et al., 2012). Unlike polysome profile analyses, ribosome profiles provide a single nucleotide-level snapshot of ribosome occupancies, which correlates with the relative amount of time a ribosome resides on a given mRNA site. In addition to mapping ribosome positions within ORFs, ribosome profiling has uncovered ribosomal occupancies on large intergenic noncoding RNAs (Guttman et al., 2013), and in the 3' untranslated region (UTR) (Guydosh and Green, 2014) and upstream ORFs (Brar et al., 2012; Ingolia et al., 2009) of mRNAs. Ribosomal stalling induced by a particular peptide (Ingolia et al., 2011), mRNA or codon sequence (Li et al., 2012), or co-translationally by a bound chaperone (Oh et al., 2011) has also been revealed by ribosome profiling. Here, in collaboration with Nicholas Guydosh and Rachel Green of Johns Hopkins Medical Institute and Howard Hughes Medical Institute and Allen Buskirk and Christopher Woolstenhulme of Brighman Young University, we used ribosome profiling to identify the cellular targets of eIF5A in yeast. Consistent with our studies described in the previous chapter (Gutierrez et al., 2013), we identified prevalent ribosomal pausing along mRNA regions encoding polyproline sequences in a yeast strain expressing the *ts*$^{-}$ eIF5A-S149P mutant, supporting the notion that eIF5A functions to promote the translation of polyproline-containing proteins.

4.2 The preparation of ribosome footprint and total mRNA libraries

cDNA libraries were prepared for deep sequencing as described in the Materials and Methods Chapter and by Ingolia and colleagues (Ingolia et al., 2012) with minor

modifications. The schematic in Fig. 13 outlines the steps for generation of ribosome footprint cDNA libraries. In parallel with ribosome footprints, I prepared total mRNA samples, and then randomly fragmented the RNA for total abundance measurements by RNA-Seq. Normalizing ribosomal footprint sequences to total mRNA abundance measurements reveals sites of enhanced ribosome occupancy and avoids errors due to altered mRNA levels or recoveries.

To analyze eIF5A activity, polysome analyses on yeast strains expressing wild-type eIF5A or the *ts*⁻ eIF5A-S149P mutant were performed (Saini et al., 2009; Zuk and Jacobson, 1998). As shown in the previous chapter, the eIF5A-S149P mutant confers a semi-permissive growth phenotype at 33°C and is non-permissive for growth at 37°C (Saini et al., 2009) (Fig. 8A). In contrast to the wild-type strain, inactivation of eIF5A in the S149P mutant strain caused retention of polysomes in the absence of CHX. As shown in Fig. 8C, a ~4-5−fold higher P/M ratio was observed in the mutant compared to the wild-type strain. This result suggests that a large proportion of cellular mRNAs are subject to translational control by eIF5A during translation elongation. Therefore, when ribosome profiling the eIF5A-S149P strain, we expected to detect enhanced ribosome occupancies across many mRNAs.

To apply a stringent shut-off of eIF5A function in the mutant strain, cells were grown at permissive 25°C to mid-log phase (OD_{600} = 0.5) and then shifted the cultures to 37°C for two hours. To avoid possible complications associated with treating cells with CHX to freeze polysomes, including an accumulation of ribosomes at the start codon (Ingolia et al., 2012), cells were harvested by filtration, quickly frozen in liquid nitrogen, and then mixed with lysis buffer containing CHX to prevent polysome run-off during cell

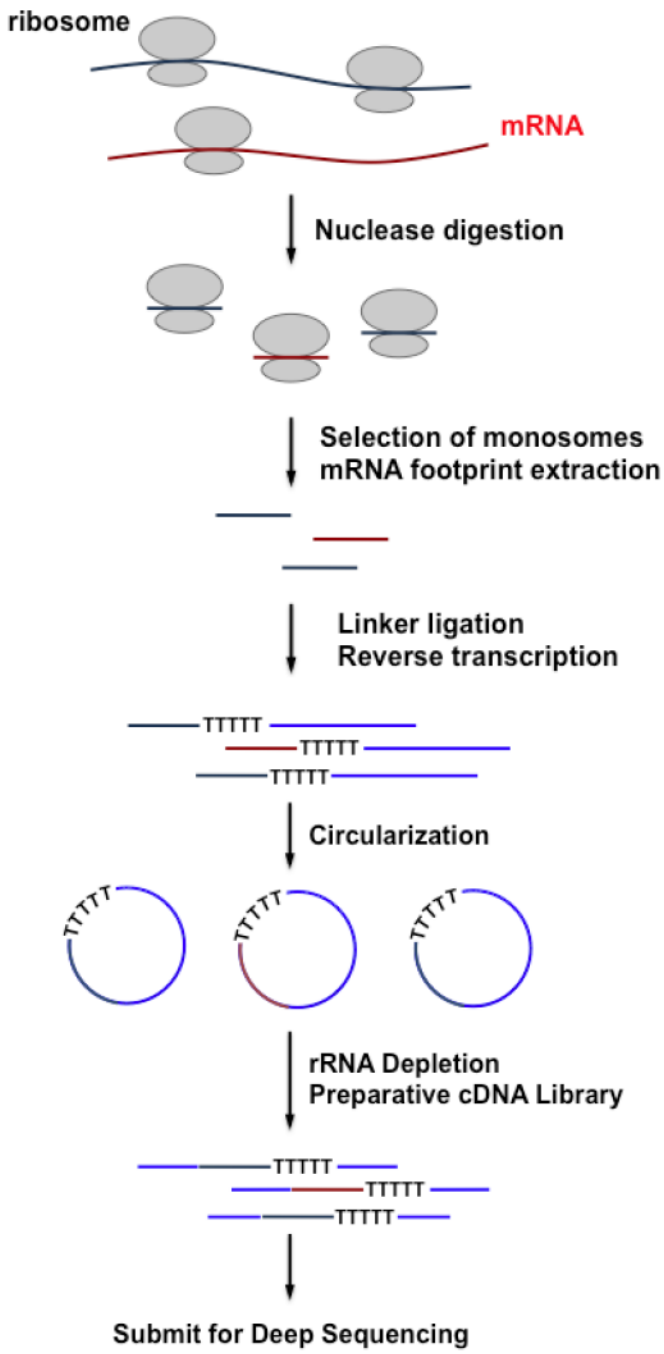

Figure 13. Schematic of the ribosome footprinting protocol.

Ribosome footprint cDNA libraries were prepared from yeast extracts for deep sequencing (Ingolia et al., 2009). The runs of polyT represent the conversion from the polyA tail in the mRNA after reverse transcription.

lysis and extract preparation. Notably, as shown in the polysome profiles of the mutant, adding CHX approximately five min prior to harvesting increased the P/M ratio (Fig. 8C) indicating a general enhancement of mRNAs bound to elongating polysomes. Therefore, in order to enrich for ribosome-protected mRNA fragments within ORFs and to avoid artifacts associated with CHX treatment, we included CHX in the lysis step after quickly freezing the cells (Guydosh and Green, 2014).

The WCEs containing polysomes were treated with RNase I as described by Ingolia and colleagues (Ingolia et al., 2012) with the expectation that unprotected tRNAs, rRNA and mRNA fragments would be digested, including the mRNA fragments within ORFs that reside between elongating ribosomes. After nuclease treatment, sucrose density centrifugation was used to separate and resolve 80S monosome fractions from both the wild-type and eIF5A-S149P mutant samples (Fig. 14). Importantly, no polysomes were detected in either sample, indicating that the nuclease treatment effectively digested the mRNA segments that were unprotected by polysomes.

RNA from ribosome footprint or total RNA samples were purified following phenol-chloroform extraction of proteins. The polyadenylated mRNA in the total RNA sample was isolated using oligo-dT Dynabeads, and then the RNA was fragmented by incubation with an alkaline solution consisting of sodium carbonate, sodium bicarbonate and EDTA [pH 9.2] at 95°C for 20 min (Ingolia et al., 2009). Both the ribosome-protected mRNA and fragmented total RNA samples were subjected to denaturing gel electrophoresis and a wide spectrum of RNA species were observed (Fig. 15). Knowing that the ribosome protects an approximately 30-nucleotide mRNA fragment (Steitz, 1969), RNA fragments from the ribosome footprint samples migrating between the 25

and 34 base markers were isolated for further analysis. For analysis of the total mRNA samples, RNA fragments between 40 and 60 nucleotides in length were selected.

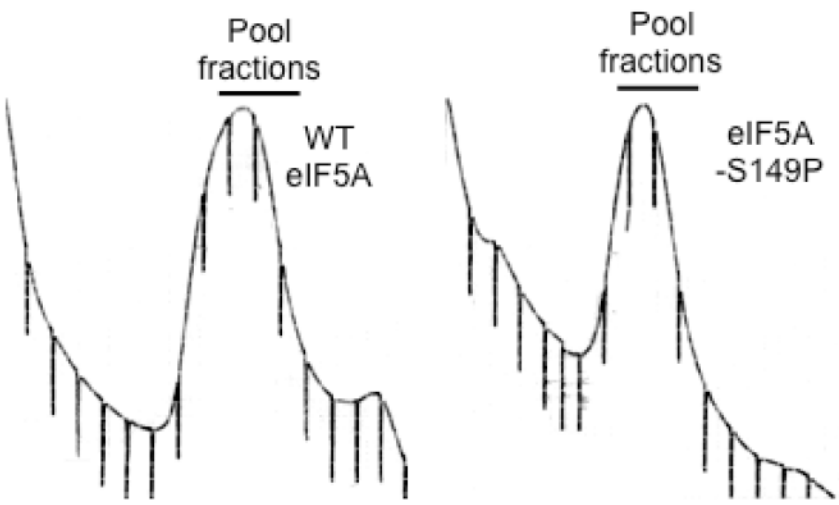

Figure 14. Sucrose density gradients for isolation of 80S monosomes in nuclease-treated lysates containing wild-type or mutant eIF5A.

Isogenic wild-type (left panel) and eIF5A-S149P mutant (right panel) strains were grown under permissive (25°C) conditions then shifted to 37°C for 2 h. WCEs were treated with RNase I as described, separated on 10-50% sucrose gradients, and fractionated to visualize ribosomal species. Fractions within the 80S monosome peak were pooled for preparation of protected mRNA fragment libraries.

Following dephosphorylation of the purified mRNA fragments, the 19-nucleotide universal linker-1 [Integrated DNA Technologies] (Lau et al., 2001), which is compatible for ligation with T4 RNA ligase 2 [New England Biolabs] (Ingolia et al., 2012), was ligated to the 5' end of each fragment. This polyadenylated linker will serve as the template for the subsequent reverse transcription reaction. After ligation, the RNA

fragments were subjected to denaturing urea-PAGE and the properly sized products (~34-45 bases for the ribosome-protected fragments, and ~60-100 bases for the total mRNA samples) were excised from the gel (Fig. 16). RNA fragments consisting of ~60-100 bases were excised for the total mRNA samples to differentiate samples from the smaller ribosome-protected mRNA samples. RNA fragments consisting of ~60-100 bases were excised for the total mRNA samples to differentiate them from the smaller ribosome-protected mRNA samples.

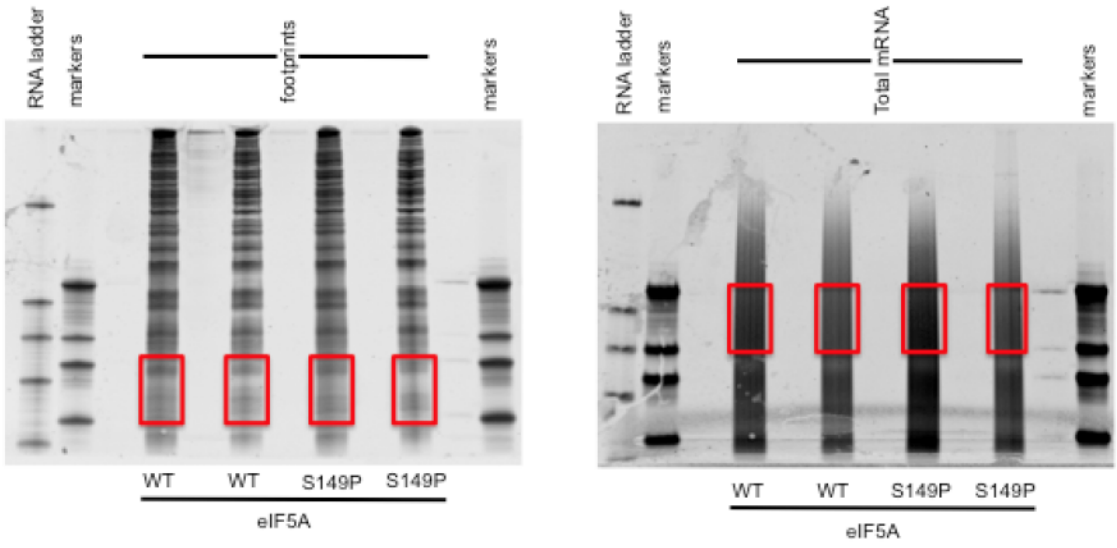

Figure 15. Size selection of ribosome footprint and total mRNA fragments.

Duplicate samples (from individual cultures) for isogenic strains expressing wild-type or mutant eIF5A were separated by denaturing urea-PAGE. For these gels and subsequent preparative gels, alternating lanes were intentionally left empty to prevent potential contamination from adjacent lanes. Ribosome footprint (left panel) and total mRNA (right panel) fragments (10 µg) were electrophoresed together with the RNA ladder [Abnova] (from top to bottom: 100, 50, 40, 30, and 20 nucleotide single-stranded RNAs), and RNA markers (from top to bottom: 60, 40, 34, and 25 bases). Following

electrophoresis, the gel was stained with SYBR Gold [Invitrogen], and then the regions denoted by the red boxes were excised and prepared for RNA extraction.

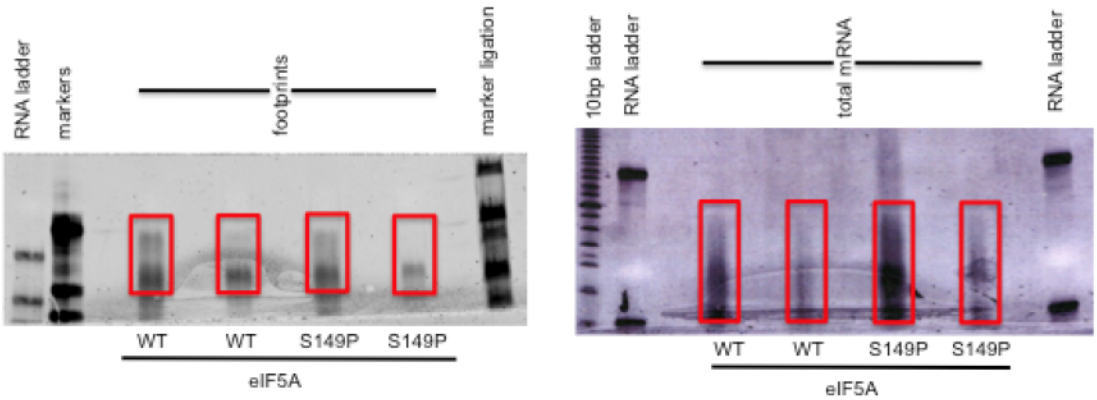

Figure 16. Linker ligation of footprint and total mRNA.

Duplicate samples of ribosome-protected footprint (left panel) and total mRNA (right panel) fragments from isogenic strains expressing wild-type or mutant eIF5A-S149P were separated by denaturing urea-PAGE [Invitrogen]. For the footprint library (left panel), the unligated markers in lane 2 (from top to bottom: 60, 40 and 34 bases) and the marker ligation in the far right lane, consisting of markers that were ligated to linker-1 (from top to bottom: ~80, 60, 54 and 45 bases) are used to demarcate boxes for excision. For the total mRNA library (right panel), the RNA ladder contains 100 and 50 base fragments. Following electrophoresis, the gel was stained with SYBR Gold [Invitrogen], and then the regions denoted by the red boxes were excised and prepared for RNA extraction.

As mentioned above, the attached linker-1 serves as the primer site for reverse transcription of the RNA fragments. The reverse transcription primer consists of two

elements: 1) sequences that are complementary to the linker, and 2) Illumina indexing sequences (Ingolia et al., 2012) that will enable multiplexed sequencing. Following reverse transcription, the resulting first-strand cDNA contains the reverse complement of the ribosome footprint (or fragmented RNA in total RNA prep), the universal linker, and the Illumina indexing sequences. The reverse transcription products were separated and resolved by urea-PAGE (Fig. 17).

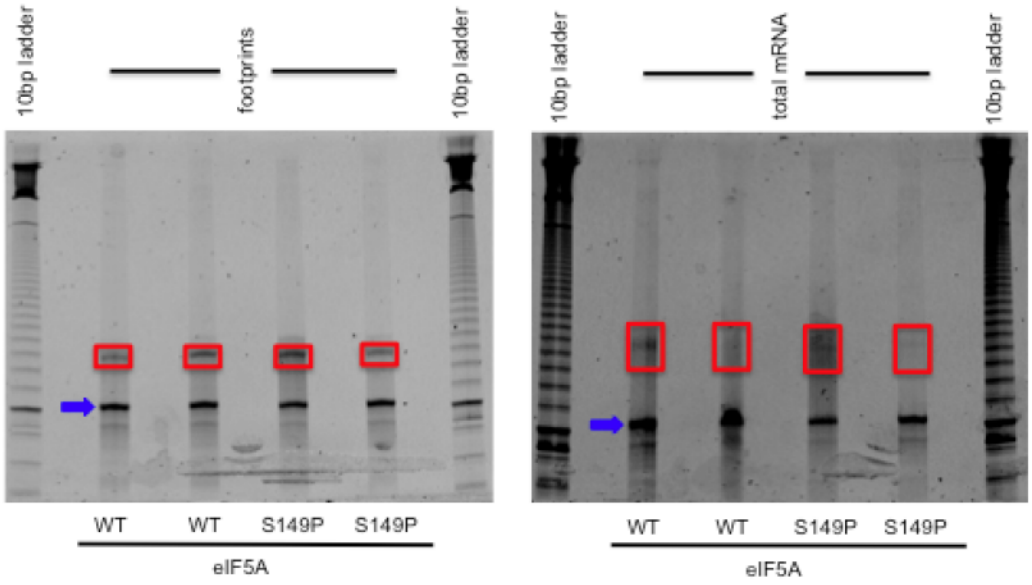

Figure 17. Reverse transcription products of footprint and total mRNA samples.

Duplicate samples originating from the linker ligation step were reverse transcribed to create single-stranded cDNAs. Ribosome footprint (left panel) and total mRNA (right panel) fragments were separated and resolved by urea-PAGE. The blue arrow indicates the unextended ~145-nucleotide reverse transcription primer. The prominent band of ~175 nucleotides within the red box in the left panel represents the reverse transcription primer plus the ~30-nucleotide footprint. For the total mRNA fragments (right panel), a

region slightly greater than ~175 nucleotides was excised, consistent with the earlier selection of larger fragments from total mRNA samples.

Circularization and ligation of the single-stranded cDNA reverse transcription product is required to produce a 5' and 3' sequence adapter flanking the ribosome footprint, or total mRNA, fragment (see schematic in Fig. 13). The 5' adapter end serves as the site for a forward primer in preparation for the deep-sequencing library. Moreover, ligation of the circularized cDNA template and introduction of the 5' adapter reduces the sequence-specific biases associated with RNA ligases, such as the T4 ligase used during the linker ligation step. Biases, like these, have been reported to distort the profiling data during analysis (Ingolia et al., 2009; Jayaprakash et al., 2011).

rRNA accounts for nearly 95% of total RNA in the cell and can severely impact the depth of coverage for mRNA in the profiling data. To enrich the ribosome profiling dataset with ribosome-protected mRNA footprints, rRNA contaminants were removed from the footprint samples. Biotinylated oligonucleotides with complementarity to yeast rRNA were first incubated with circularized DNA samples and then bound to streptavidin-coupled magnetic beads [Life Technologies]. This depletion removed ~40-60% of the rRNA contaminants (data not shown). Next, PCR was performed using barcoded and indexing primers annealed to the circularized DNA template to generate a deep-sequencing library (Fig. 18).

To assess the quality of the PCR-generated deep-sequencing library, BioAnalyzer profiles were obtained [Agilent Technologies] (Fig. 19). A single peak of 172-173 nucleotides was evident in the analysis of the ribosome footprints generated from the

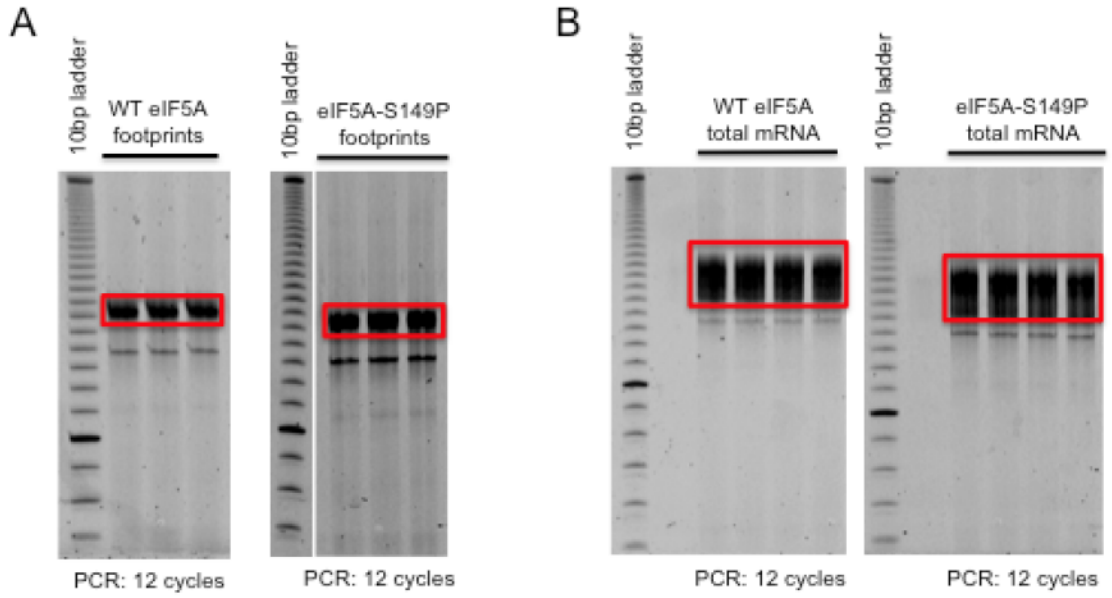

Figure 18. Isolation of PCR products for generation of cDNA library for deep sequencing.

(A) PCR products obtained following amplification of ribosome-protected mRNA fragment cDNAs generated from strains expressing wild-type (left panel) of mutant eIF5A (right panel) were separated on urea-PAGE gels and stained with SYBR Gold [Invitrogen]. The red boxes indicate the regions containing ~175 nucleotide cDNAs that were excised and purified. The faster migrating fragment below the red box represents the unextended reverse transcription primer.

(B) The cDNA products from the total mRNA samples of strains expressing wild-type (left panel) or mutant eIF5A (right panel) were amplified by PCR and separated by urea-PAGE. The cDNA species that were excised and eluted are enclosed by a red box.

strains expressing wild-type or mutant eIF5A. The total mRNA deep-sequencing libraries included slightly larger RNA segments for both wild-type and mutant eIF5A of 176-186

nucleotides (data not shown). Altogether, all samples were of high-quality and were subjected to multiplexed Illumina deep sequencing on a HiSeq2000 at the UC Riverside Sequencing facility.

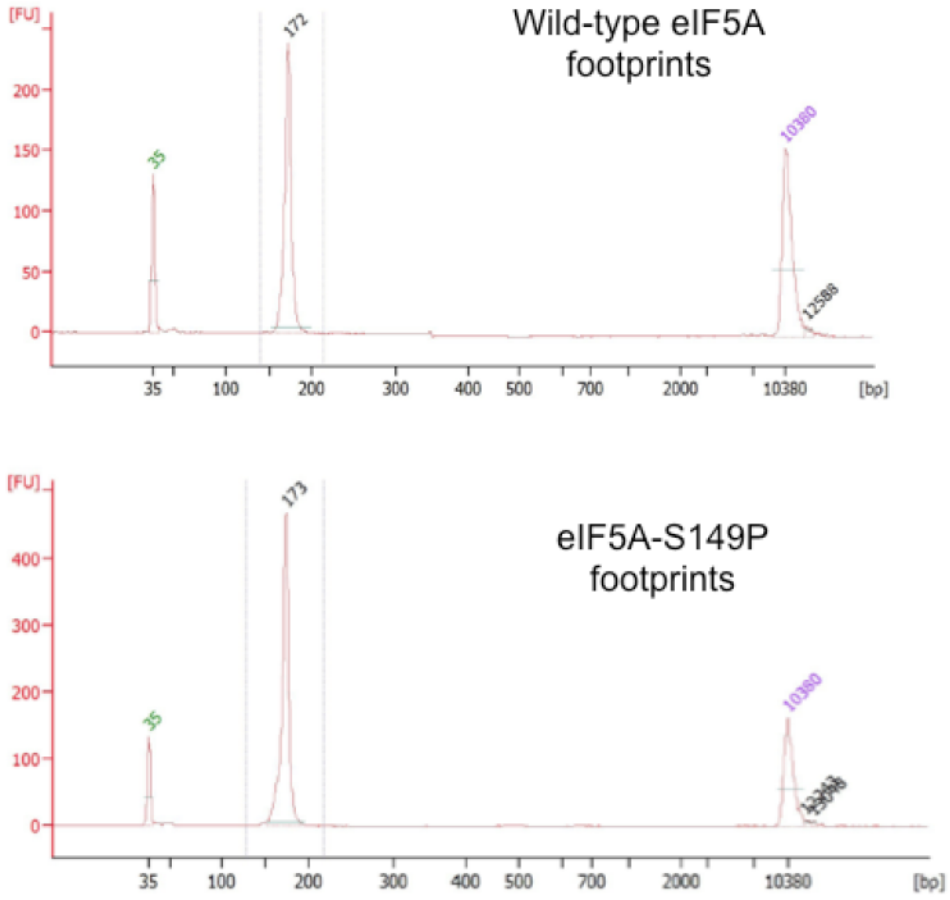

Figure 19. BioAnalyzer profiles of cDNA deep-sequencing libraries.

The cDNAs isolated as shown in Figure 18 were prepared for Agilent BioAnalyzer analysis on a high-sensitivity DNA chip according to the manufacturer's procedure (Agilent Technologies, 2013). BioAnalyzer profiles for cDNAs obtained from RNA footprints of wild-type eIF5A (top panel) or eIF5A-S149P samples (bottom panel) were generated. Arbitrary fluorescence unit [FU] measurements are plotted on the y-axis, and

the x-axis displays the size of the DNA fragments; the mobility of the short (35 nucleotides) and long (10,380 nucleotides) standards are indicated.

4.3 Ribosome profiling reveals widespread ribosomal pausing and drop-off around polyproline motifs

In collaboration with Nicholas Guydosh, Allen Buskirk, Christopher Woolstenhulme, and Rachel Green at Johns Hopkins Medical Institute, we proceeded to align the deep-sequencing results with the yeast transcriptome. If mutation of eIF5A causes ribosomal pausing, we hypothesized that distinct ribosome footprints would be more prevalent in the eIF5A-S149P mutant than in the wild-type strain. Due to length and content biases in the ribosome-protected mRNA sequences during the library preparation, and depth of coverage limitations, that made more sequences more enriched than others, we encountered difficulties in analyzing the isogenic wild-type strain (J697). These issues did not severely impact the generation of samples for the mutant strain (J699) as a significant number of mapped reads were between ~27-30 nucleotides (data not shown). Therefore, for comparative analysis, we used ribosome footprint data from the wild-type strain BY4741 that was obtained previously by Nicholas Guydosh. This is a possible shortcoming of the analysis as we would have preferred to use footprint data from an isogenic wild-type strain. The most prominent difference when comparing the recovery of ribosome-protected RNA fragments in the wild-type (BY4741) versus the eIF5A mutant strain was the enriched recovery of ribosomes on sequences encoding polyproline in the mutant strain.

Using algorithms he developed, Nicholas Guydosh analyzed the distribution of ribosome-protected mRNA fragments. Interestingly, whereas the strain expressing wild-type eIF5A (BY4741) exhibited a uniform translational efficiency (ribosome density before and after polyproline segments = ~1.0), the strain expressing the eIF5A-S149P mutant showed a step-wise decrease in ribosome density following polyproline sequences as the number of consecutive proline residues increased (Fig. 20A). Thus, the ability of ribosomes to translate polyproline stretches in the absence of eIF5A becomes more troublesome as the number of consecutive proline residues increases. Meta-analysis of all genes encoding six consecutive proline residues (in *S. cerevisiae*, this includes 21 genes) revealed a pronounced accumulation of ribosome occupancies within the polyproline stretch in the mutant strain, whereas the wild-type strain revealed a uniform distribution of averaged ribosome densities along the same collection of mRNA transcripts (Fig. 20B). Moreover, an mRNA encoding the yeast TIM50 protein, a component of the translocase of the inner mitochondrial membrane complex, showed nearly equivalent ribosome occupancies throughout the mRNA transcript in the wild-type strain BY4741. However, while ribosome densities were largely similar across the 5' end of the ORF in the mutant strain, a sudden drop-off of ribosome occupancies was clear following a seven consecutive polyproline motif (Fig. 20C). These signatures of ribosomal pausing (Fig. 20B) or drop-off (Fig. 20C) at polyproline sequences in the eIF5A mutant strain corroborate our published results (Gutierrez et al., 2013) and demonstrate that eIF5A plays a crucial role in promoting the translation of polyproline sequences for a significant number of mRNAs in the yeast genome.

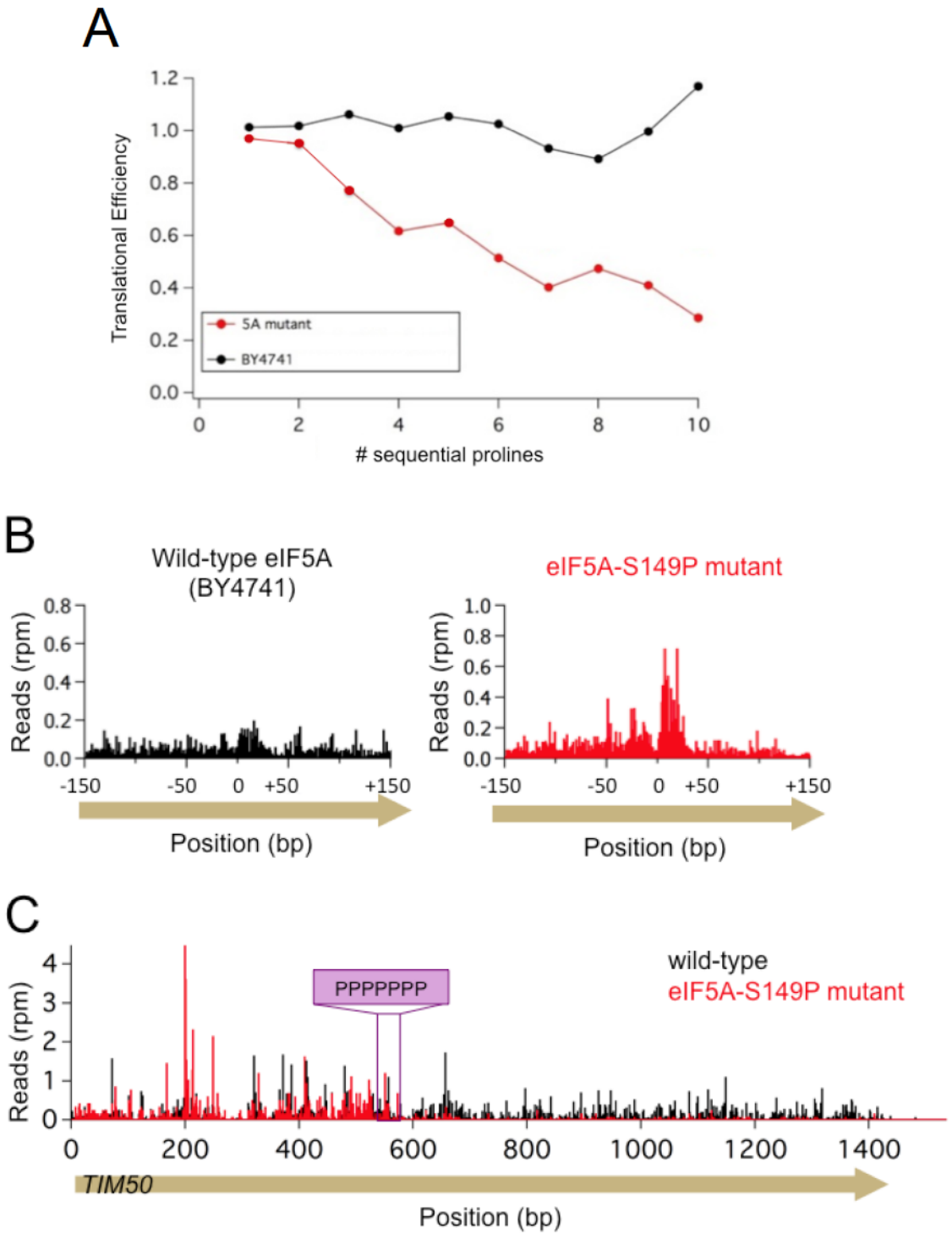

Figure 20. Genome-wide ribosome pausing and drop-off at polyproline sequences in the eIF5A mutant strain.

(A) Translational efficiency becomes rate-limiting as polyproline length increases in the eIF5A-S149P mutant. To calculate translational efficiency, sequencing reads from the ribosome-protected mRNA samples are normalized to the total mRNA samples. Using these normalized ratios, translational efficiency was determined by comparing the ribosome occupancies after a polyproline motif with the occupancies before the motif. BY4741 is a wild-type strain derived from the same S288C background as the eIF5A mutant.

(B) Ribosome occupancies, as mapped footprints in aggregate from wild-type (left panel) and eIF5A-S149P (right panel) strains, were analyzed at -150 to +150 nucleotides relative to the first nucleotide of the first proline codon, of a run of six consecutive prolines, set at 0. Reads are plotted as reads per million (rpm) mapped reads after Illumina deep sequencing.

(C) Ribosome occupancies along the entire 1430-nucleotide *TIM50* mRNA transcript for wild-type (black) and eIF5A-S149P mutant (red) strains.

*Data analyses in this figure were conducted by Nicholas Guydosh.

4.4 Conclusion

In this chapter, I present ribosome profiling results that support a genome-wide role for eIF5A in polyproline synthesis. Using a set of molecular biology techniques, ribosome footprint deep-sequencing libraries for both wild-type and mutant eIF5A-S149P strains were prepared. The sequence reads were then mapped to the yeast transcriptome to identify sites of high and low ribosome occupancy. Analysis of the mutant strain revealed prevalent ribosome pausing at polyproline sequences and loss of ribosome densities after

the polyproline motif in the *TIM50* mRNA. In addition, an increase in the polyproline length inversely correlated with the ability of ribosomes to translate through the polyproline segment. Altogether, this data supports the initial results using *in vivo* reporter and *in vitro* peptide synthesis assays that was presented in the previous chapter, and demonstrates that eIF5A plays a genome-wide role in promoting translation of polyproline motifs. Future ribosome profiling work will focus on repeating these experiments. It will be critical to concurrently analyze isogenic wild-type and eIF5A mutant strains. In addition, by analyzing more extensive libraries of ribosome-protected mRNA fragments, it may be possible to identify other peptide motifs that require eIF5A for their synthesis.

5. Identification and characterization of eIF5A mutants that require the hydroxyl group on hypusine

5.1 The significance and rationale for study

The hypusine modification on eIF5A is essential for cellular protein synthesis and cell growth, but its requirements for eIF5A function remains poorly understood. Hypusine, which is named for its hydroxyputrescine and lysine moieties (Shiba et al., 1971), is highly conserved in all eukaryotic eIF5A and some archaeal aIF5A proteins (Bartig et al., 1992; Bartig et al., 1990; Gordon et al., 1987a; Park et al., 1997). Interestingly, eIF5A is the only cellular protein known to contain hypusine (Park et al., 1981). Increasing levels of hypusine formation have been directly correlated with increased rates of protein synthesis in mammalian cells (Cooper et al., 1982; Cooper et al., 1983), and Hyp-eIF5A stimulated polyproline synthesis in *in vitro* reconstituted yeast translation assays (Gutierrez et al., 2013) (Fig. 12D). Hypusination on eIF5A occurs in two steps that require the enzymes DHS and DOHH. In the first step, DHS transfers an *N*-butylamine group from the polyamine spermidine to the ε-amino group of a specific lysine residue (K51 in yeast; K50 in humans) in eIF5A to form deoxyhypusine. Then, DOHH adds a hydroxyl group to deoxyhypusine to form hypusine on eIF5A. The hypusine modification is essential for eIF5A function as substitution of the conserved lysine residue by arginine blocks hypusination and abolishes the ability of yeast or human eIF5A to substitute for wild-type eIF5A in yeast (Magdolen et al., 1994; Schnier et al., 1991).

In this study, we aimed to probe the functional requirements of the hydroxyl group on hypusine. The *LIA1* gene encoding yeast DOHH is non-essential in budding and fission yeast (Park et al., 2006; Weir and Yaffe, 2004); whereas loss of DOHH was found to cause a recessive lethal phenotype in *C. elegans* (Sievert et al., 2014; Sugimoto, 2004), *Drosophila* (Patel et al., 2009), and mouse (Sievert et al., 2014). Here, I identified a

group of eIF5A mutants that require *LIA1* function for yeast growth. All of the mutations are located in the N-terminal domain of eIF5A and impair translation *in vivo* in the presence or absence of *LIA1*. Whereas it was previously postulated that hydroxylation was required to stabilize the hypusine modification and prevent the back conversion of deoxyhypusine to unmodified eIF5A, MS analyses of wild-type and mutant forms of eIF5A indicated that loss of *LIA1* did not lead to accumulation of unmodified forms of eIF5A. In contrast, *in vivo* reporter and *in vitro* reconstituted yeast translation assays revealed a requirement for the hydroxyl group for the eIF5A mutant proteins to stimulate Met-Pro-Pro-Pro-Lys (M-P-P-P-K) peptide synthesis. Taken together, these results provide evidence for a critical role of the hydroxyl group on hypusine in peptide bond formation. We propose that the hydroxyl group facilitates the positioning of the hypusine moiety within the PTC of the ribosome.

5.2 Isolation of randomly mutated *HYP2* alleles that confer a strong slow-growth phenotype in the absence of *LIA1*

In *Saccharomyces cerevisiae*, strains lacking the chromosomal *LIA1* gene have slight slow-growth phenotypes compared to wild-type yeast on rich medium (Park et al., 2006; Park, 2006). To understand the non-essential role of *LIA1* in yeast, we screened for *HYP2* (encoding eIF5A in yeast) mutants that require *LIA1* function. More specifically, I performed a genetic screen for mutations in *HYP2* that confer a normal or slow-growth phenotype on their own but cause exacerbated growth phenotypes when *LIA1* is repressed. To perform the screen, I combined galactose-inducible expression of *LIA1* with a plasmid shuffling strategy in strain J1058 (*MAT*a *trp1-Δ63 ura3-52 leu2-3 leu2-112 GAL2*$^{+}$ *gcn2Δ*

hyp2::HPHMX anb1::NAT GAL-LIA1::KANMX4 p[*HYP2, URA3*]) to identify mutant alleles in *HYP2* that are sensitive to loss of *LIA1* (Fig. 21A-B). In total, 979 yeast transformants containing a *HYP2* mutant plasmid were screened for growth on both galactose-containing medium, where *LIA1* expression is maintained, and on glucose-containing medium, where *LIA1* expression is repressed. Three *LIA1*-dependent transformants exhibited synthetic growth defects when *LIA1* expression was repressed, indicating that these strains contain mutations in *HYP2* that require *LIA1* function (Fig. 21C). The plasmids containing the eIF5A mutations were purified from individual transformants, re-tested to confirm the phenotype, and then sequenced. The three eIF5A mutants included one allele with a double mutation (eIF5A-C23Y,V60D) and two alleles with single mutations (eIF5A-N79I and eIF5A-S74F). Additionally, in a candidate-based mutational analysis of residues within the highly conserved hypusine loop, the eIF5A-H52A mutant was also found to exhibit a synthetic growth defect when *LIA1* expression was repressed in yeast.

Because *GAL-LIA1* expression is not completely repressed under glucose conditions, the plasmids expressing the eIF5A mutants were introduced into isogenic *LIA1*$^{+}$ (J1005) or *lia1*Δ (J1119) strains by plasmid shuffling, and the growth of individual colonies was assessed by streaking transformants on minimal medium containing all amino acids except leucine (Synthetic Complete - leucine, SC-Leu; note, the eIF5A mutant plasmids contain a *LEU2* marker) (Fig. 21D). Intriguingly, the strains harboring plasmids that express eIF5A-N79I and eIF5A-C23Y,V60D exhibited synthetic lethal phenotypes when *LIA1* was deleted, while the strains expressing eIF5A-H52A and eIF5A-S74F displayed synthetic growth defects when *LIA1* was deleted. When the two

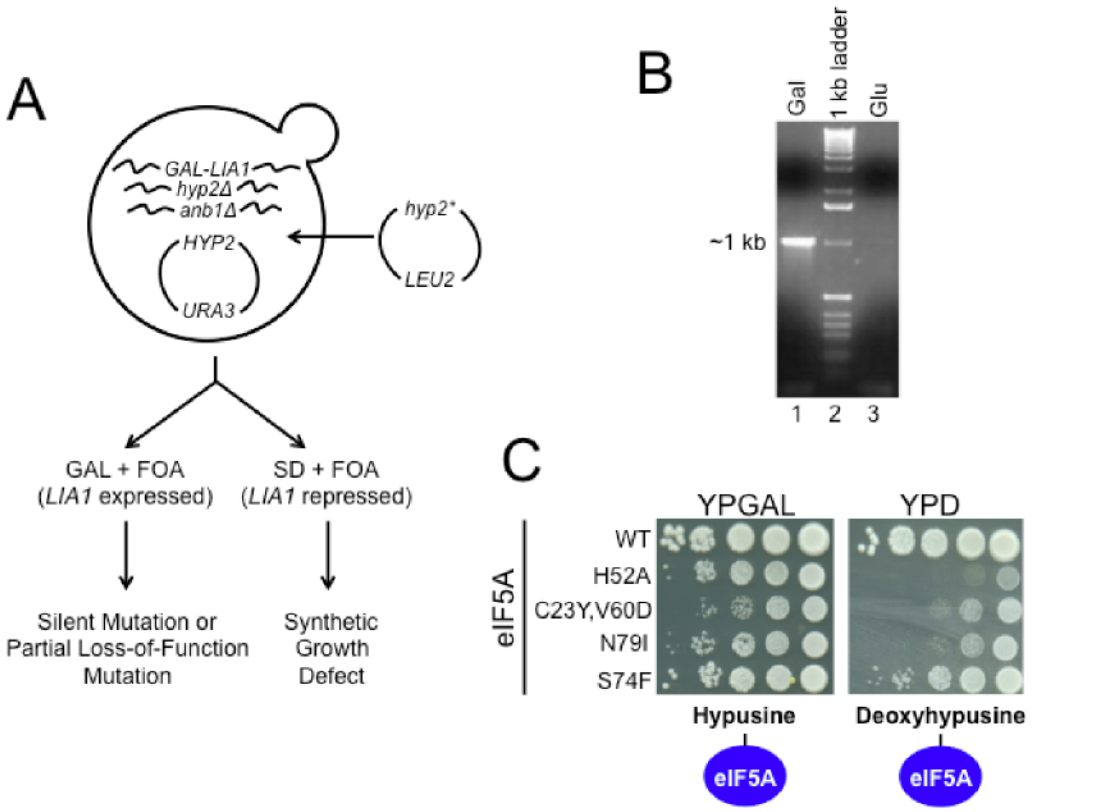
A
GAL-LIA1
hyp2Δ
anb1Δ
HYP2
URA3
hyp2*
LEU2
GAL + FOA
(LIA1 expressed)
SD + FOA
(LIA1 repressed)
Silent Mutation or
Partial Loss-of-Function
Mutation
Synthetic
Growth
Defect
B
Gal
1 kb ladder
Glu
~1 kb
1 2 3
C
YPGAL
YPD
eIF5A
WT
H52A
C23Y,V60D
N79I
S74F
Hypusine
Deoxyhypusine
eIF5A
eIF5A

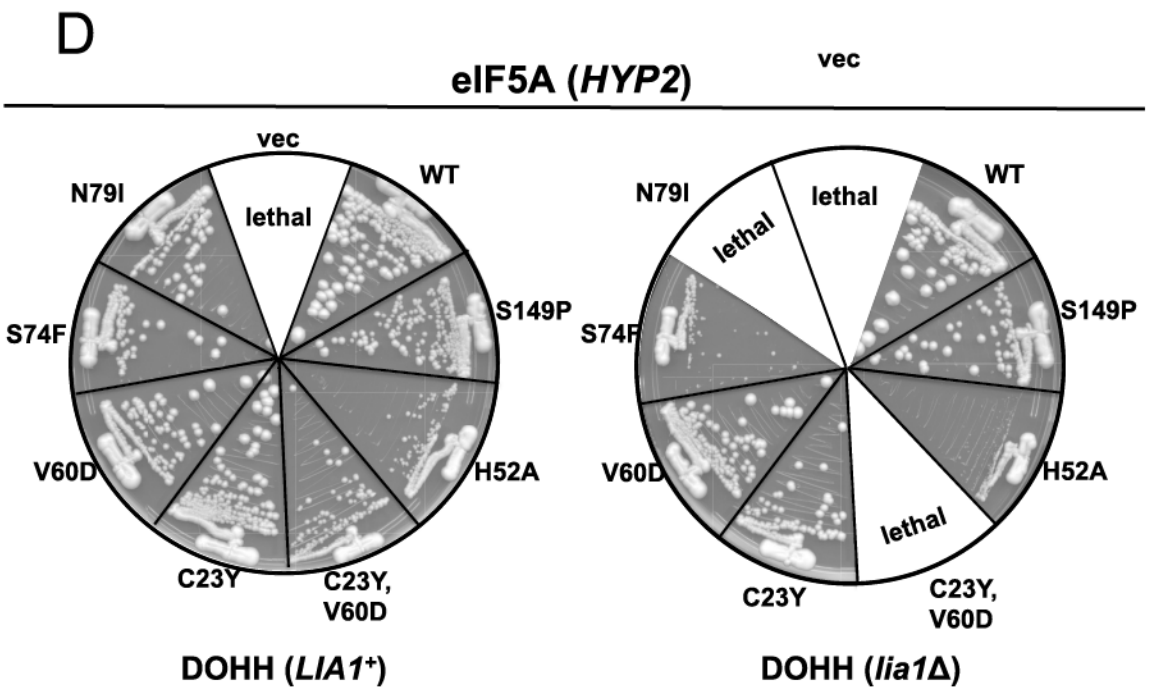
D
eIF5A (HYP2)
vec
vec
WT
S149P
H52A
C23Y,
V60D
C23Y
V60D
S74F
N79I
lethal
DOHH (LIA1+)
vec
WT
S149P
H52A
C23Y,
V60D
C23Y
V60D
S74F
N79I
lethal
lethal
lethal
DOHH (lia1Δ)

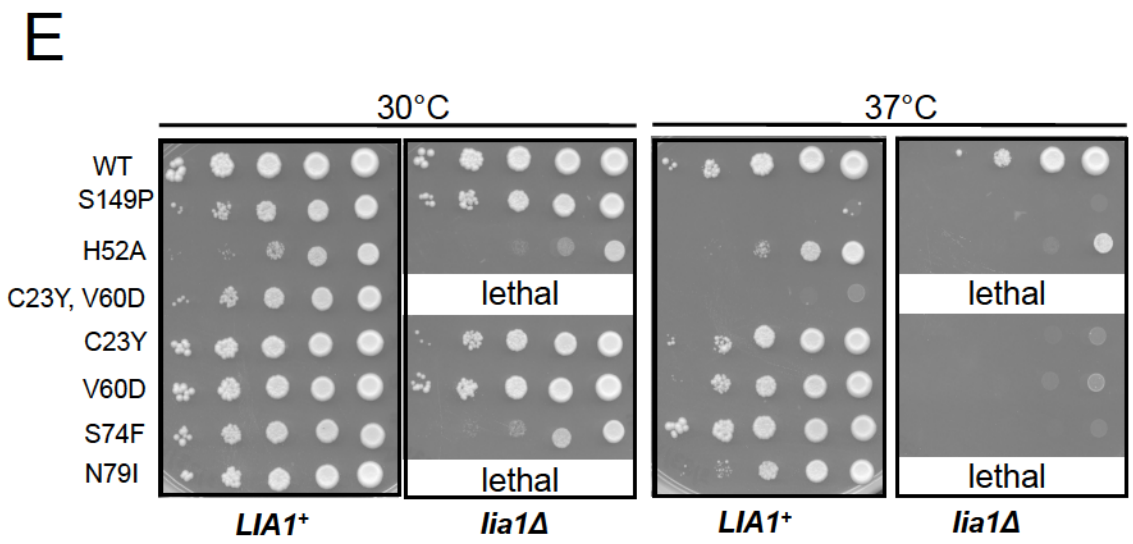

Figure 21. Genetic screen to identify *LIA1*-dependent mutants of eIF5A in yeast.

(A) Schematic of yeast genetic screen using strain J1058. Galactose-inducible expression of *LIA1* is combined with a plasmid shuffling strategy on plates containing 5-fluoroorotic acid (5-FOA) to swap the wild-type [*HYP2, URA3*] plasmid for a mutant [*hyp2**, *LEU2*] construct. The library of [*hyp2**, *LEU2*] mutant plasmids was generated by error-prone PCR using a low-fidelity DNA polymerase. Yeast transformants were screened for normal or slow-growth on galactose medium where *LIA1* is expressed and for slower or no growth on glucose medium where *LIA1* expression is repressed.

(B) RT-PCR analysis of *LIA1* expression in strain J1058. Total RNA was prepared for cells grown in galactose (lane 1) or glucose (lane 3) medium, and RT-PCR was performed using primers designed to amplify a ~975 bp product for *LIA1*.

(C) Transformants were isolated, grown to saturation in Yeast Peptone Galactose (YPGAL) medium, and 4-µl volumes of serial dilutions (OD_{600} = 1.0, 0.1, 0.01, 0.001, and 0.0001) were spotted on YPGAL or YPD medium and incubated for 2 days at 30°C.

(D) Empty vector or *LEU2* plasmids expressing wild-type or the indicated mutant versions of eIF5A were introduced into isogenic *LIA1*$^+$ (J1005) or *lia1*Δ (J1119) strains. The resulting strains, carrying two eIF5A plasmids, were replica-plated to 5-FOA medium to select for cells that have lost the *URA3* plasmid containing the wild-type eIF5A allele. Finally, the strains containing only the eIF5A, *LEU2* plasmid were streaked on SC-Leu medium and incubated for 3 days at 30°C.

(E) The strains from Figure 21D containing the eIF5A mutant plasmids were grown to saturation in SC (-Leu) medium, and 4-µl volumes of serial dilutions (OD_{600} = 1.0, 0.1, 0.01, 0.001, and 0.0001) were spotted on SC (-Leu) medium and incubated for 3 days at 30°C or 37°C.

---

mutations in the eIF5A-C23Y,V60D double mutant were separated and tested independently, the eIF5A-C23Y and eIF5A-V60D single mutants exhibited wild-type growth phenotypes in the absence or presence of *LIA1*. Thus, the synthetic lethal phenotype is dependent on the simultaneous mutation of Cys23 and Val60 together with the loss of the hydroxyl group on hypusine. In an *LIA1*$^+$ background, all mutants, except the strain expressing eIF5A-S74F, have mild *ts*$^-$ phenotypes when grown at 37°C (Fig 21E). In contrast, all of the *LIA1*-dependent mutants had lethal or severe *ts*$^-$ phenotypes at 37°C in the *lia1*Δ background. Notably, the strains expressing eIF5A-H52A and eIF5A-C23Y,V60D are constitutively slow-growth in a wild-type (*LIA1*$^+$) background, indicating that these mutations impair the function of the Hyp form of eIF5A. Overall, the screening strategy identified eIF5A mutations that impose an *LIA1* requirement for eIF5A

function in yeast, suggesting that the hydroxyl group on hypusine serves a critical function for eIF5A.

5.3 *LIA1*-dependent mutations in *HYP2* are positioned in the N-terminal domain of eIF5A

Similar to bacterial EF-P, eIF5A was predicted to bind between the P and E sites of the 80S ribosome and adjacent to the P-site tRNA (Blaha et al., 2009; Gutierrez et al., 2013). In directed hydroxyl radical probing experiments, the hypusine loop was found to be positioned near the CCA acceptor end of the P-site tRNA. However, unlike eIF5A, EF-P has a third C-terminal domain that overlaps the 30S subunit. Thus, it is thought that eIF5A primarily interacts with the 60S subunit. Incidentally, the residues 20-90 of the eIF5A N-terminal domain represent the required region for binding DOHH and for effective hydroxylation of the deoxyhypusine-containing substrate (Kang et al., 2007). The *LIA1*-dependent eIF5A mutants identified in the screen are located in the N-terminal domain of eIF5A (Fig. 22). Specifically, residues C23 and V60, identified in the eIF5A-C23Y,V60D double mutant, are located on the β1 and β4 strands respectively. Residues S74 and N79 are positioned on the β5 and β6 strands, respectively, and H52, a residue present in eukaryotic eIF5A and archaeal aIF5A but absent in bacterial EF-P, is adjacent to K51, the site of hypusine modification. Examination of the approximate positions of these residues on the EF-P–70S ribosome co-complex (Blaha et al., 2009), all residues except C23 are surface-exposed and interact with the ribosome (V60, S74, N79) or the P-site tRNA (H52). Notably, I did not identify any mutations that exhibited an *LIA1* requirement in the C-terminal domain of eIF5A; however, the screen was clearly not

saturated, since I did not identify the H52A mutation in the screen. Interestingly, the eIF5A-S149P mutation, located in the C-terminal domain, confers a *ts*⁻ phenotype. This mutation impairs yeast cell growth (Fig. 8A & 21D-E), eIF5A expression (Fig. 8B), and translation elongation at the non-permissive temperature (Fig. 8C) (Saini et al., 2009); however, these phenotypes are not exacerbated by loss of *LIA1*.

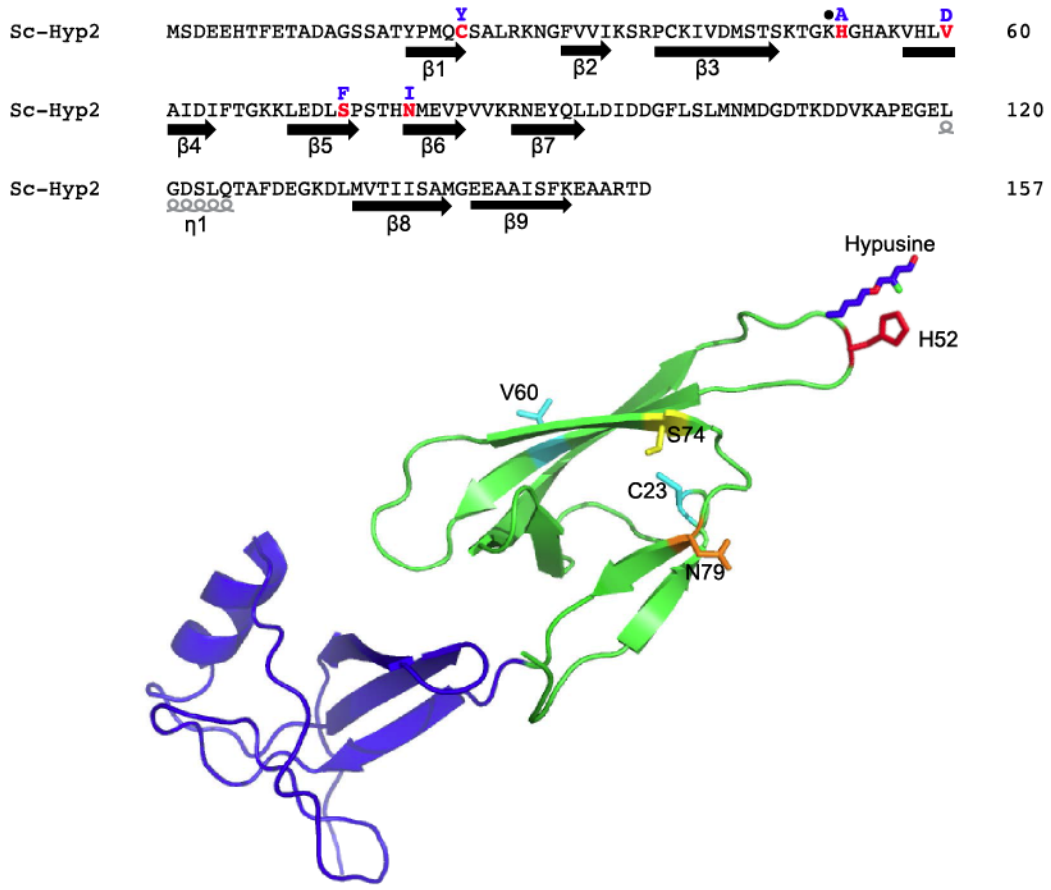

Figure 22. eIF5A primary sequence and location of mutations in *LIA1*-dependent eIF5A mutants.

(Top) The primary sequence of yeast (*Saccharomyces cerevisiae*, Sc) Hyp2. Sites of point mutations are colored red and substituted residues are in blue. Secondary structure elements are shown below of the sequence (arrow = β-strand, loops = α-helix).

(Bottom) Ribbons representation of *Saccharomyces cerevisiae* eIF5A (PDB: 3ER0) generated using PyMOL software (PyMOL Molecular Graphics System, Version 1.5.0.4 Schrödinger, LLC). The eIF5A N-terminal domain is colored in green and the C-terminal domain is shown in blue. The sites of *LIA1*-dependent mutations are depicted as sticks and highlighted: C23,V60 (cyan), H52 (red), S74 (yellow), and N79 (orange). Hypusine at position 51 is modeled on the structure and depicted in stick mode.

5.4 *LIA1*-dependent eIF5A mutants exhibit altered polysome profiles

In previous studies, polysome profile analyses and eIF5A depletion experiments were combined to assess eIF5A function. While one report observed a loss of larger polysomes and an accumulation of 80S monosomes, indicating a translation initiation defect (Henderson and Hershey, 2011), other reports revealed polysome retention in the absence of CHX upon depletion of eIF5A (Saini et al., 2009) or when shifting eIF5A *ts*$^{-}$ mutants to a restrictive temperature (Zanelli et al., 2006), revealing a role in translation elongation. To assess the impact of the *LIA1*-dependent eIF5A mutants on general protein synthesis, I performed polysome profile analyses of yeast strains expressing eIF5A-H52A, eIF5A-S74F, eIF5A-N79I, or eIF5A-C23Y,V60D in an *LIA1*$^{+}$ background and eIF5A-H52A, or eIF5A-S74F in an *lia1*Δ background with the expectation that loss of *LIA1* would exacerbate the translation defects associated with the mutations.

In order to freeze translating ribosomes in growing yeast cultures, the eukaryotic translation elongation inhibitor CHX was added just prior to harvesting. CHX is thought to inhibit the translocation of the mRNA and tRNA on elongating ribosomes by occupying the E site (Schneider-Poetsch et al., 2010). To determine whether any *LIA1*-

dependent eIF5A mutations conferred translation elongation defects, yeast cultures were also harvested in the absence of the CHX treatment. If any mutant strains exhibited polysome retention similar to wild-type strains in the presence of CHX, then those mutants were determined to have defects in translation elongation. Consistent with the fact that removal of *LIA1* did not result in any severe growth defects (Fig. 21D-E), loss of *LIA1* resulted in polysome run-off in the absence of CHX and an accumulation of 80S monosomes similar to wild-type strains (Fig. 23A). On the other hand, the strain expressing eIF5A-H52A exhibited polysome retention in the absence of CHX (P/M = 0.80 versus 0.18 for the wild-type control), indicative of a defect in translation elongation (Fig. 23B). However, loss of *LIA1* in the strain expressing eIF5A-H52A did not further increase the P/M ratio (P/M = 0.71), suggesting that the synthetic growth defect is not due to a more pronounced elongation defect. We are uncertain why loss of *LIA1* in the strain expressing eIF5A-H52A does not result in a more deleterious translation defect in polysome profiles. It may be that loss of *LIA1* severely impairs translation of a subset of mRNAs encoding proteins that are critical for cell growth and this severely impaired translation cannot be detected over the general background translational inhibition observed in the polysome profiles. Alternatively, it may be possible that translational stalling in the *lia1*Δ strain expressing eIF5A-H52A could subject this subclass of mRNAs to quality control mechanisms leading to their degradation.

While the polysome profile of the strain expressing eIF5A-S74F (P/M (-CHX) = 0.24; P/M (+CHX) = 2.16) was similar to the wild-type control, combining loss of *LIA1* with the eIF5A-S74F mutation resulted in a severe loss of polysomes in the presence of CHX (P/M = 0.52) (Fig. 23C). Similarly, the strain expressing eIF5A-N79I, though

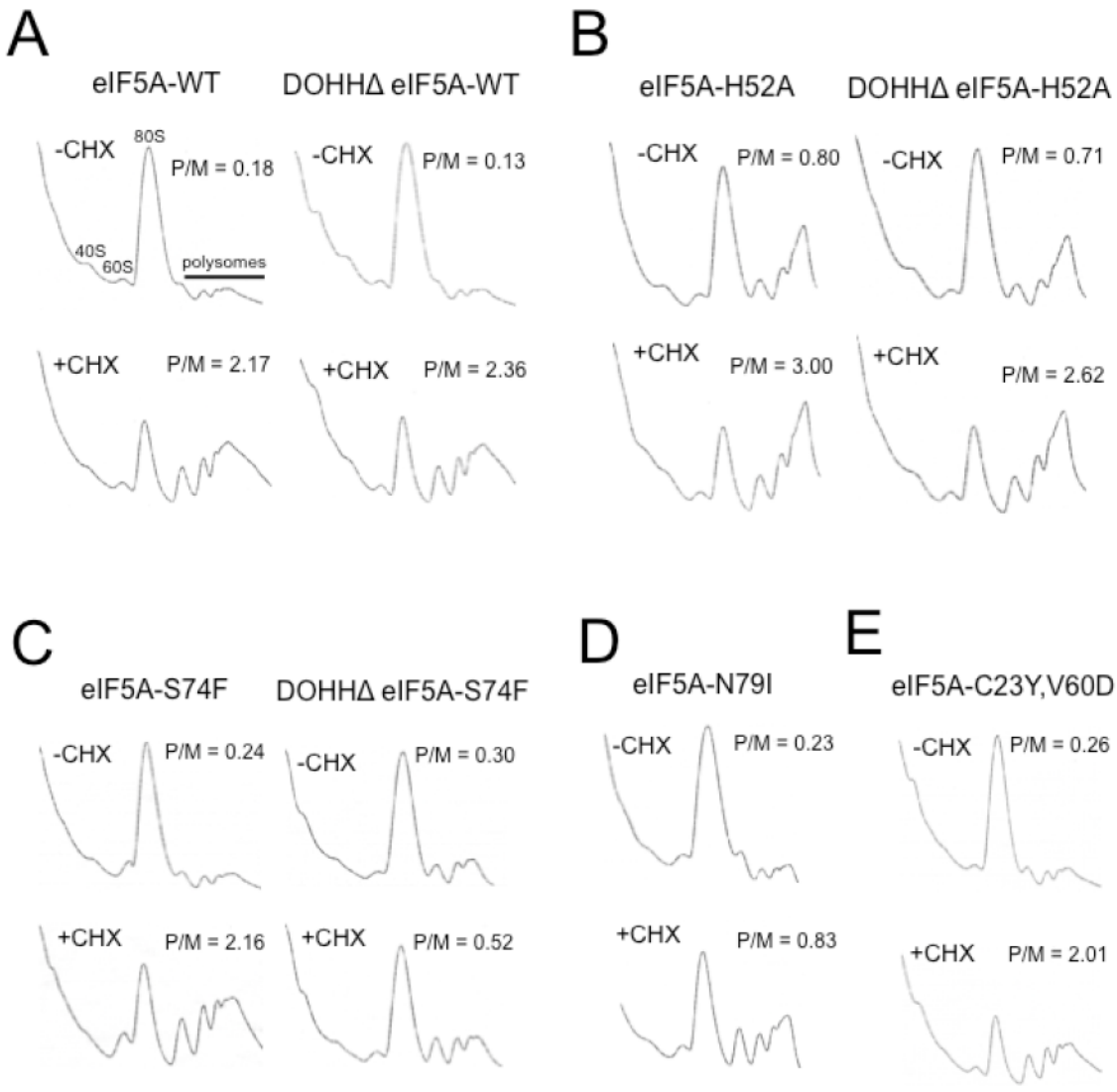

Figure 23. *LIA1*-dependent eIF5A mutants exhibit translation elongation defects and a loss of polysomes.

Polysome profiles were analyzed from wild-type and mutant strains grown at 30°C to mid-log phase, treated with 50 µg/ml CHX (+CHX) or left untreated (-CHX), and WCEs were separated on sucrose gradients and fractionated while monitoring absorbance at OD_{254} to visualize polysomes and the indicated ribosomal species. P/M ratios were calculated by comparing the areas under the polysome and 80S peaks.

showing a minor slow-growth defect in an *LIA1*$^{+}$ background (Fig. 21C-D), exhibited loss of polysomes in the presence of CHX (Fig. 23D). Traditionally, it is thought that the absence of polysomes in the presence of CHX is indicative of a translation initiation defect (Foiani et al., 1991; Hartwell and McLaughlin, 1969). While it is possible that some of the eIF5A mutations are directly impairing translation initiation, an alternative explanation for the apparent initiation defect is that severe impairment of translation elongation in the mutants is triggering surveillance pathways and subsequent mRNA turnover and loss of polysomes. The eIF5A-C23Y,V60D double mutant did not show any significant defects in translation in the *LIA1*$^{+}$ background (Fig. 23E), and it is not known if the synthetic lethal phenotype for this mutant in the *lia1*Δ background (Fig. 21D-E) is due to a severe translation defect. As the polysome analyses did not provide clear insights into the *LIA1*-dependence of the eIF5A mutations, it is possible that the residues mutated in the eIF5A mutants and the hydroxyl group on hypusine serve distinct functions to maintain cell viability. We hypothesized that loss of the hydroxyl group on hypusine could impair the function of the eIF5A mutants in three possible ways: 1) decrease eIF5A protein levels, 2) impair stability of the hypusine modification, or 3) impair eIF5A function to promote translation elongation.

5.5 Loss of *LIA1* does not result in decreased levels of the eIF5A mutant proteins

The first hypothesis to consider was that the synthetic growth defects in the *hyp2 lia1*Δ double mutants were due to lower eIF5A protein levels. To test this hypothesis, immunoblot analyses were used to monitor the levels of C-terminally FLAG-tagged

variants of the *LIA1*-dependent eIF5A mutants in isogenic *LIA1*$^{+}$ (J1005) or *lia1*Δ (J1119) backgrounds (Fig. 24). Because the eIF5A-C23Y,V60D and -N79I mutations are lethal in the *lia1*Δ strain, untagged wild-type eIF5A was co-expressed in the strains to maintain cell viability. Consistent with previous reports for the human eIF5A variant (Cano et al., 2008), protein levels for eIF5A-H52A in the *LIA1*$^{+}$ background are similar to wild-type eIF5A. Likewise, the S74F, N79I and double C23Y,V60D mutations did not reduce eIF5A protein levels in the *LIA1*$^{+}$ strain. Furthermore, when these eIF5A mutants were expressed in strains lacking *LIA1*, no reduction in eIF5A protein levels was observed. These results indicate that *LIA1* function is not required to maintain the stability of the eIF5A proteins, and they suggest that loss of *LIA1* and hence, hydroxylation of deoxyhypusine, exacerbates the growth defect of these eIF5A mutants in a manner that is independent of eIF5A protein levels.

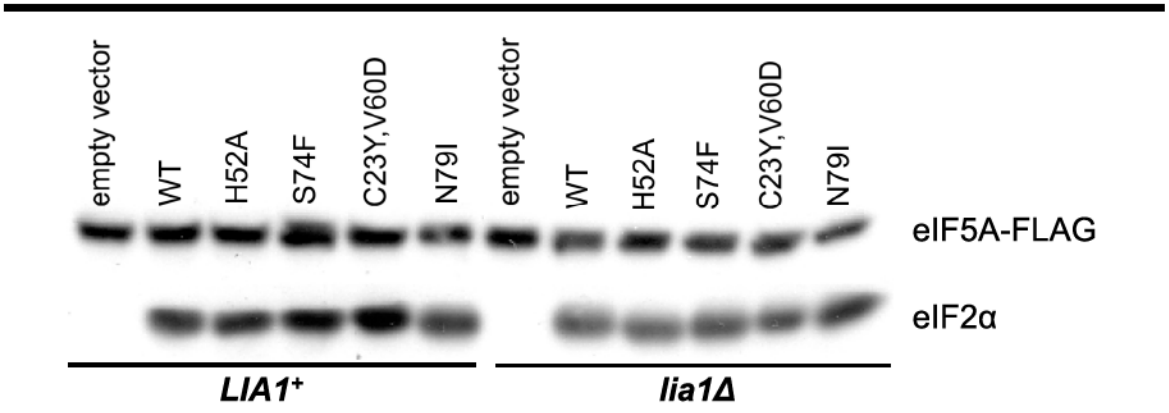

Figure 24. *LIA1*-dependent mutations in *HYP2* do not affect eIF5A protein levels. Plasmids expressing the indicated mutant FLAG-tagged *HYP2* alleles were introduced into isogenic (J1005) or *lia1*Δ (J1119) strains expressing wild-type eIF5A. Cells were grown to OD_{600} 1.0 at 30°C and then broken with glass beads in the presence of 10% TCA. Cells were treated with TCA to inactivate all cellular enzymes and prevent the

possible degradation of proteins in the extracts by cellular proteases. WCEs were separated by SDS-PAGE and subjected to immunoblot analysis using anti-FLAG or polyclonal anti-yeast eIF2α antiserum.

5.6 *LIA1*-dependent eIF5A mutations do not promote the reversibility of the deoxyhypusine modification

In previous reports, the DHS-catalyzed formation of deoxyhypusine was found to be reversible (Park et al., 2003). Assays containing [^{3}H]dHyp-eIF5A, human deoxyhypusine synthase, NAD, and 1,3-diaminopropane, generated [^{3}H]spermidine, a precursor for deoxyhypusine biosynthesis. Intriguingly, when [^{3}H]Hyp-eIF5A replaced [^{3}H]dHyp-eIF5A in this assay, no reversal to [^{3}H]spermidine was observed. Moreover, Park et. al determined that the DHS forward reaction was largely favorable compared to the reverse reaction in formation of a DHS-imine intermediate (Park et al., 2003). Thus, by forming a stable product such as Hyp-eIF5A, hydroxylation could function to deplete the dHyp intermediate and drive the equilibrium of the DHS reaction forward.

In an effort to test whether the *LIA1*-dependent eIF5A mutations promote the reverse DHS reaction and result in the accumulation of unmodified forms of eIF5A, we performed ESI QTOF MS analysis in collaboration with Peter Backlund to assess the modification status of intact *LIA1*-dependent eIF5A mutant proteins expressed in yeast. We analyzed intact eIF5A protein to avoid biases associated with protease digestion used to generate peptide fragments. If loss of *LIA1* combined with specific mutations in eIF5A resulted in the loss of dHyp-eIF5A and the accumulation of unmodified forms of eIF5A,

then hydroxylation could function to stabilize the modification and the synthetic growth defects could be attributed to the loss of the functional deoxyhypusine form of eIF5A.

MS analyses were performed on intact C-terminal FLAG-tagged eIF5A proteins purified from *LIA1*$^+$ or *lia1*Δ yeast strains. Whereas MS analysis of intact wild-type eIF5A purified from the *LIA1*$^+$ strain confirmed the presence of hypusine on eIF5A (MW = 18187 Da), eIF5A purified from the *lia1*Δ strain accumulated in the dHyp form (MW = 18171 Da) (Fig. 25A). Importantly, in this analysis, no unmodified eIF5A (MW = 18100 Da) was observed. It is noteworthy that eIF5A expressed in yeast is differentially phosphorylated on Ser2. While this phosphorylation does not appear to be important for eIF5A function (Kang et al., 1993; Klier et al., 1993), both the phosphorylated and unphosphorylated (80 Da less) forms of eIF5A were detected in these experiments (Fig. 25A) and the phosphorylation of eIF5A did not appear to be influenced by the presence or absence of LIA1. MS analysis of purified eIF5A-H52A revealed two major peaks consisting of Hyp (MW = 18121 Da) and dHyp forms of eIF5A-H52A (MW = 18105 Da) in the *LIA1*$^+$ yeast background (Fig. 25B). The presence of both Hyp- and dHyp-eIF5A-H52A in *LIA1*$^+$ strains is consistent with the notion that residues in the hypusine loop contribute to LIA1 (DOHH) recognition of dHyp-eIF5A (Cano et al., 2008; Kang et al., 2007). Furthermore, it is noteworthy that overexpression of *LIA1* partially suppressed the constitutive slow-growth phenotype of the eIF5A-H52A mutant strain, suggesting that eIF5A-H52A is poorly recognized by the DOHH enzyme (Fig. 25C). These results are consistent with the results from previous studies of human eIF5A expressed in yeast where mutation of His51, adjacent to the Lys50 site of hypusine modification in human eIF5A, impaired hydroxylation of deoxyhypusine (Cano et al., 2008). Analysis of eIF5A-

H52A purified from the *lia1*Δ strain revealed the predominantly dHyp form of the protein with no accumulation of unmodified eIF5A-H52A (MW = 18034 Da) (Fig. 25B). Finally, we also examined the eIF5A-S74F mutant. Like wild-type eIF5A, purified eIF5A-S74F was mostly Hyp (MW = 18247 Da) when purified from *LIA1*$^{+}$ strain and dHyp (MW = 18131 Da) when obtained from the *lia1*Δ strain (Fig. 25D). Most, if not all, of the

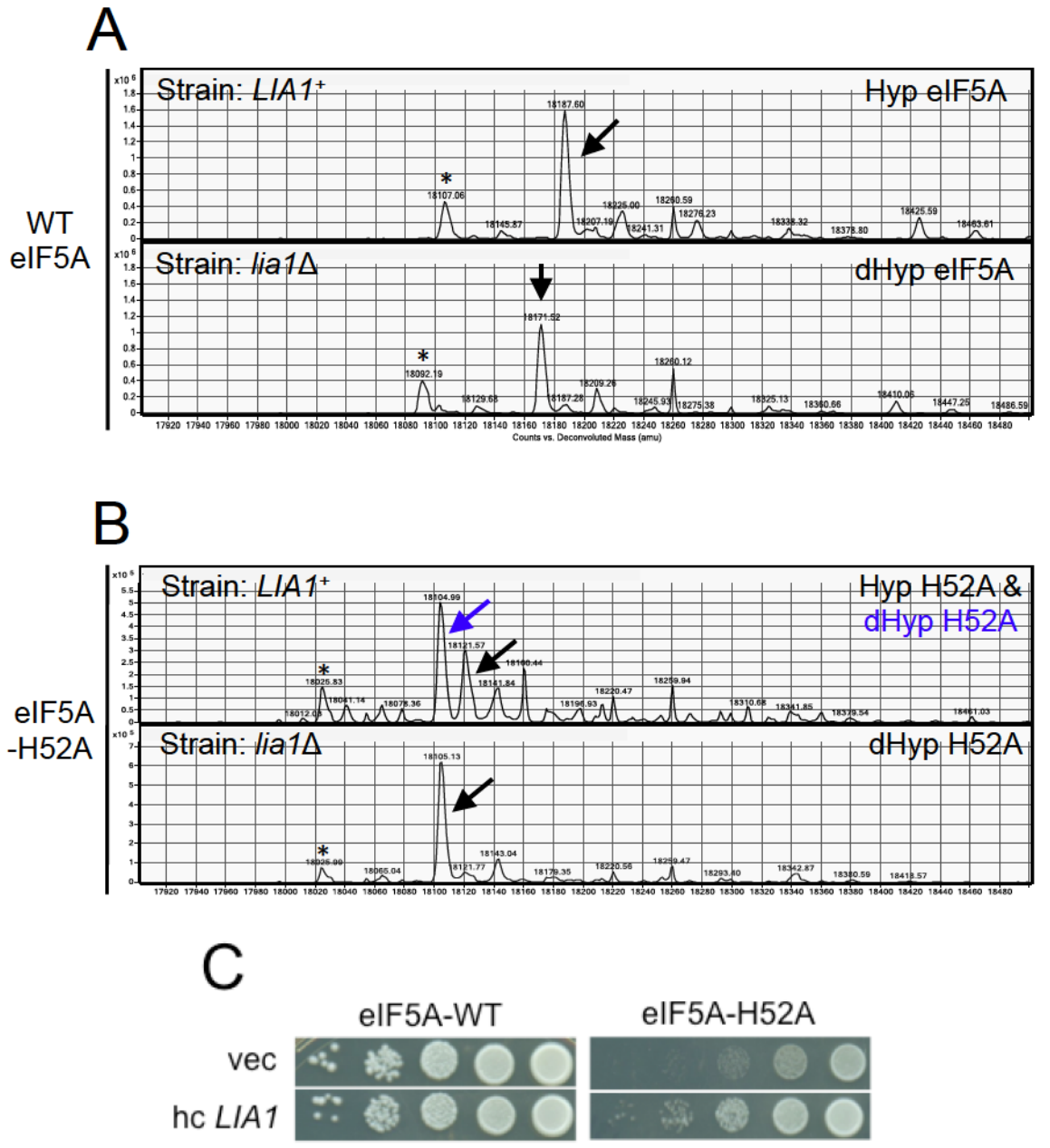

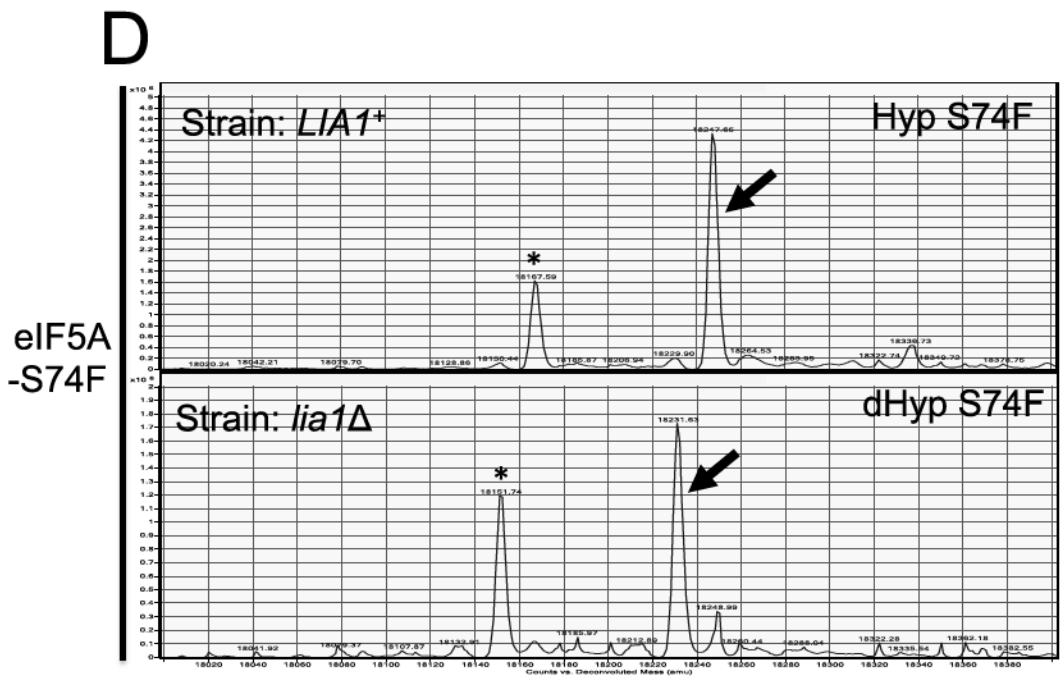

Figure 25. MS analyses of *LIA1*-dependent eIF5A mutants purified from yeast.

ESI-QTOF MS analysis of C-terminal FLAG-tagged eIF5A wild-type (A), eIF5A-H52A (B), and eIF5A-S74F (D) purified from *LIA1*$^{+}$ (top panels) or *lia1*Δ (bottom panels) strains. Peaks corresponding to Hyp or dHyp forms of eIF5A are marked by arrows; and peaks marked with an asterisk (*) represent unphosphorylated forms of eIF5A.

(C) A High-copy number (hc) *LIA1* plasmid or empty vector (vec) was introduced into strains expressing wild-type eIF5A or eIF5A-H52A. The strains were grown to saturation in YPD medium, and 4-µl volumes of serial dilutions (OD_{600} = 1.0, 0.1, 0.01, 0.001, and 0.0001) were spotted on YPD medium and incubated for 2 days at 30°C.

---

additional peaks observed in the MS analyses cannot be attributed to eIF5A and likely represent proteins that were co-purified with FLAG-tagged eIF5A. As accumulation of unmodified forms of eIF5A was not observed in yeast, these results indicate that removal

of *LIA1* and thus, the absence of the hydroxyl group on hypusine, does not drive the reversibility of the DHS reaction for the eIF5A-H52A and eIF5A-S74F mutants as an accumulation of unmodified eIF5A was not observed in yeast. These findings are inconsistent with the previously held notion that hydroxylation of deoxyhypusine prevents the back reaction of deoxyhypusine to unmodified eIF5A. While we cannot rule out the possibility that the reversible back reaction may be specific to eIF5A in higher eukaryotes (Sievert et al., 2014), the results of the MS analyses indicate that hydroxylation is not required for stable modification of eIF5A in yeast, and instead suggest that the primary requirement for hydroxylation of deoxyhypusine on the eIF5A mutants is to promote eIF5A function during protein synthesis.

5.7 Impaired stimulation of polyproline synthesis by deoxyhypusine forms of eIF5A mutants

Based on biochemical and genetic studies, eIF5A and its bacterial homolog EF-P are factors that promote translation of mRNAs encoding consecutive proline residues (Doerfel et al., 2013; Gutierrez et al., 2013; Ude et al., 2013). As stimulation of M-P-P-P-K peptide synthesis by eIF5A depends on the hypusine modification (Gutierrez et al., 2013) (Fig. 12D), we rationalized that the hydroxyl group on hypusine may facilitate eIF5A function as well. To determine the functional requirements of the hydroxyl group on eIF5A for stimulation of polyproline synthesis, I utilized the *in vivo* and *in vitro* assays previously described (Gutierrez et al., 2013). First, using the dual luciferase assays described in Chapter 3 and by Letzring et al. (Letzring et al., 2010), I measured the ratio of firefly to *Renilla* luciferase activity for reporters containing no insert and 10 codon

repeats for AlaGCU or ProCCA in strains containing (J1005) or lacking (J1119) *LIA1* (Fig 26A). No major differences in firefly to *Renilla* luciferase ratios were observed between wild-type and mutant strains for the AlaGCU or the ProCCA reporters. Similarly, the *LIA1*$^{+}$ strains expressing eIF5A-H52A or eIF5A-S74F exhibited no significant changes in reporter activity for constructs containing the same AlaGCU or ProCCA repeats (Fig 26B, left panel). Conversely, the firefly to *Renilla* ratio for the ProCCA reporter was significantly reduced in the *lia1*Δ strain expressing eIF5A-H52A or eIF5A-S74F (~45% for H52A versus WT; ~30% for S74F versus WT). These results reveal that, like the *ts*$^{-}$ eIF5A-S149P mutant (Fig. 6B), the deoxyhypusine forms of eIF5A-H52A and eIF5A-S74F are impaired for polyproline synthesis *in vivo*.

As described above, eIF5A strongly stimulated the synthesis of M-P-P-K and M-P-P-P-K in *in vitro* reconstituted yeast translation assays (Gutierrez et al., 2013) (Fig. 12B-C). Using similar *in vitro* assays (see schematic in Fig. 12A), I examined M-P-P-P-K peptide synthesis using reconstituted yeast translation assays and purified Hyp or dHyp forms of eIF5A, eIF5A-H52A, or eIF5A-S74F from yeast (the modification of these proteins was assessed by MS in Fig. 25). I reasoned that if the deoxyhypusine forms of the eIF5A mutants are defective relative to the Hyp forms of these factors in M-P-P-P-K synthesis, then the hydroxyl group on hypusine is contributing to eIF5A function. As previously described, I limited the analysis to overall yield (Y_{max} values) and reaction endpoints as opposed to observed rates (Gutierrez et al., 2013) (see Chapter 3). Consistent with previous results (Fig. 12D), Hyp-eIF5A strongly stimulated M-P-P-P-K peptide synthesis (Y_{max} = 0.06 ±0.01 in the absence of eIF5A and 0.49 ±0.04 in the presence of Hyp-eIF5A) (Fig. 26C). Likewise, the dHyp form of wild-type eIF5A

strongly stimulated M-P-P-P-K peptide synthesis (Y_{max} = 0.61 ±0.17). In contrast, whereas the Hyp forms of eIF5A-H52A (Y_{max} = 0.46 ±0.02) and eIF5A-S74F (Y_{max} = >0.50) strongly stimulated M-P-P-P-K synthesis, the dHyp forms of these mutant proteins were partially (dHyp-eIF5A-H52A, Y_{max} = 0.22 ±0.02) or substantially (dHyp-eIF5A-S74F, Y_{max} = not determined) impaired for stimulating M-P-P-P-K synthesis (Fig. 26C).

Because the eIF5A proteins purified from yeast sometimes contained mixtures of differentially modified forms (±Hyp, dHyp, phosphorylation), I chose to repeat the analysis using preparations of unmodified, dHyp or Hyp forms of eIF5A. Recombinant eIF5A was purified from *E. coli* harboring a plasmid that expresses the wild-type or mutant eIF5A alone (pC4181) or co-expresses *DYS1* (pC4182) or both *DYS1* and *LIA1* (pC4183) (Fig. 26D). ESI QTOF MS analyses confirmed the presence of unmodified, deoxyhypusine- or hypusine-containing forms of eIF5A (Fig. 26E). Unlike the MS analyses for the eIF5A proteins purified from yeast (Fig. 25A-B & D), peaks representing unmodified eIF5A were present in *E. coli* co-expressing eIF5A and DHS. This presence of unmodified eIF5A in cells co-expressing eIF5A and DHS is consistent with previous reports on eIF5A and DHS co-expressed in bacteria (Park et al., 2011) and with the reversibility of the DHS reaction *in vitro* (Park et al., 2003). Despite the inability to obtain homogenous preparations of deoxyhypusine forms of eIF5A produced in *E. coli*, the unmodified and hypusine derivatives were obtained in good yield and devoid of the other forms of eIF5A. Similar to the eIF5A proteins purified from yeast, hypusine and deoxyhypusine forms of eIF5A stimulated M-P-P-P-K peptide synthesis to similar extents (Y_{max} = 0.49 ±0.06 and Y_{max} = 0.50 ±0.10, respectively) (Fig. 26F). Hyp-eIF5A-

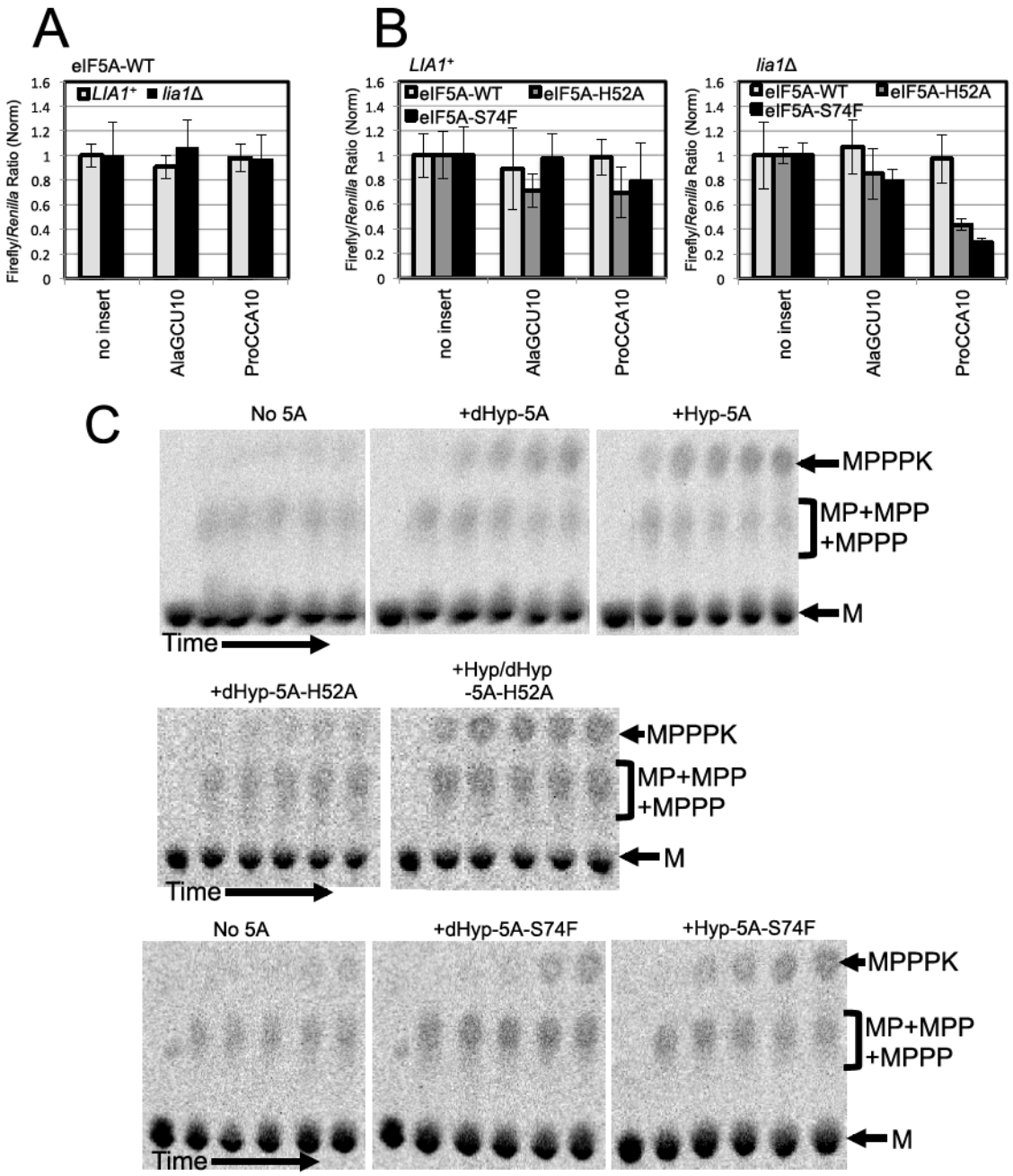
A
eIF5A-WT
LIA1+ lia1Δ
Firefly/Renilla Ratio (Norm)
1.6
1.4
1.2
1
0.8
0.6
0.4
0.2
0
no insert
AlaGCU10
ProCCA10
B
LIA1+
eIF5A-WT
eIF5A-H52A
eIF5A-S74F
lia1Δ
C
No 5A
+dHyp-5A
+Hyp-5A
MPPPK
MP+MPP
+MPPP
M
Time
+dHyp-5A-H52A
+Hyp/dHyp
-5A-H52A
No 5A
+dHyp-5A-S74F
+Hyp-5A-S74F

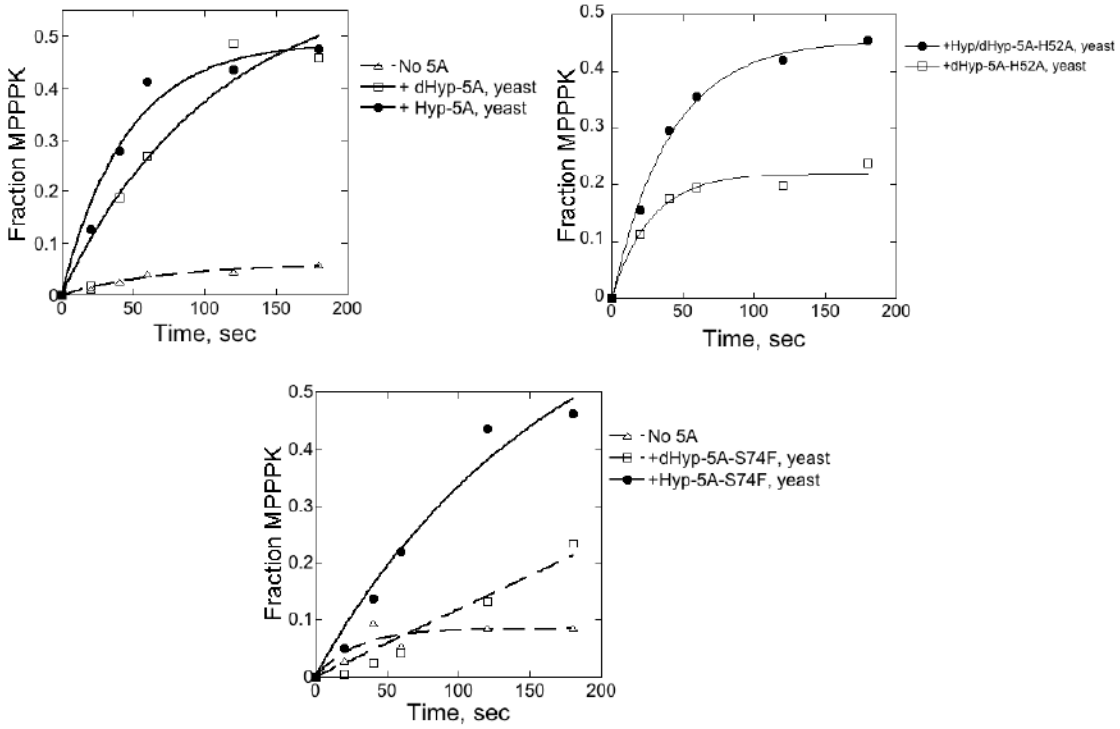
Fraction MPPPK
Time, sec
- No 5A
+ dHyp-5A, yeast
+ Hyp-5A, yeast
+Hyp/dHyp-5A-H52A, yeast
+dHyp-5A-H52A, yeast
- No 5A
+dHyp-5A-S74F, yeast
+Hyp-5A-S74F, yeast

D

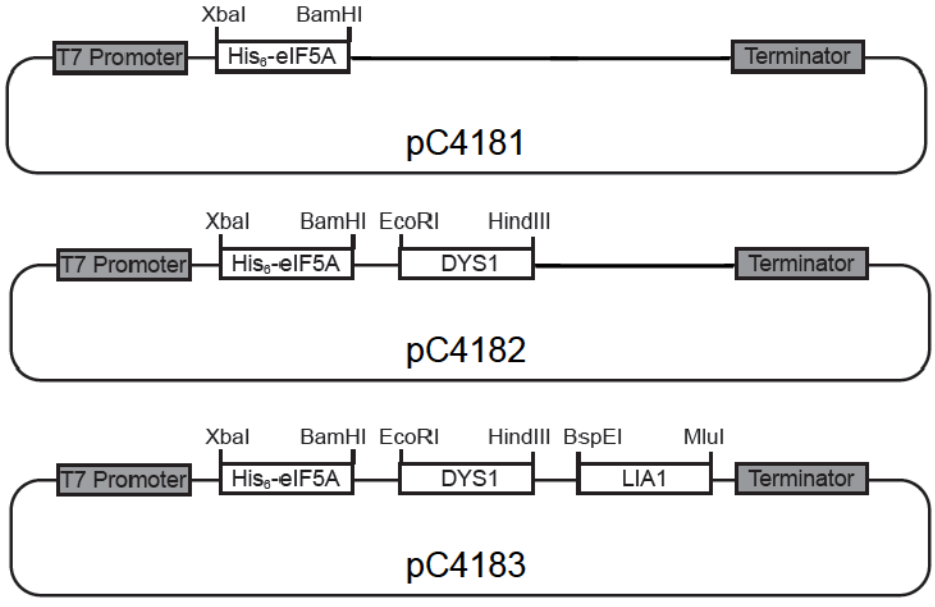
XbaI
BamHI
T7 Promoter
His6-eIF5A
Terminator
pC4181
EcoRI
HindIII
DYS1
pC4182
BspEI
MluI
LIA1
pC4183

E

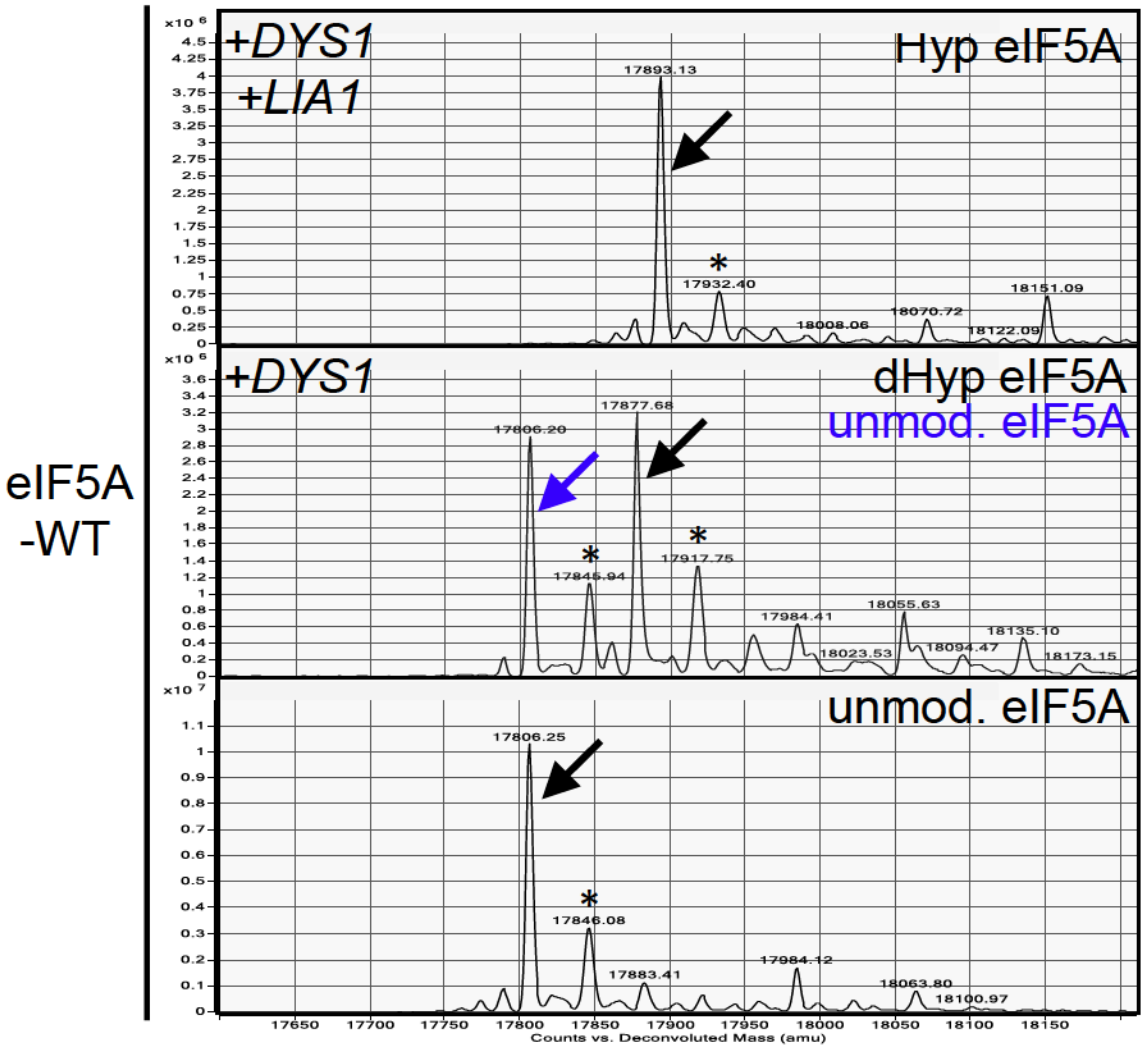
eIF5A
-WT
+DYS1
+LIA1
Hyp eIF5A
17893.13
17932.40
18008.06
18070.72
18122.09
18151.09
+DYS1
dHyp eIF5A
unmod. eIF5A
17806.20
17877.68
17845.94
17917.75
17984.41
18023.53
18055.63
18094.47
18135.10
18173.15
unmod. eIF5A
17806.25
17846.08
17883.41
17984.12
18063.80
18100.97
17650
17700
17750
17800
17850
17900
17950
18000
18050
18100
18150
Counts vs. Deconvoluted Mass (amu)

eIF5A
-H52A

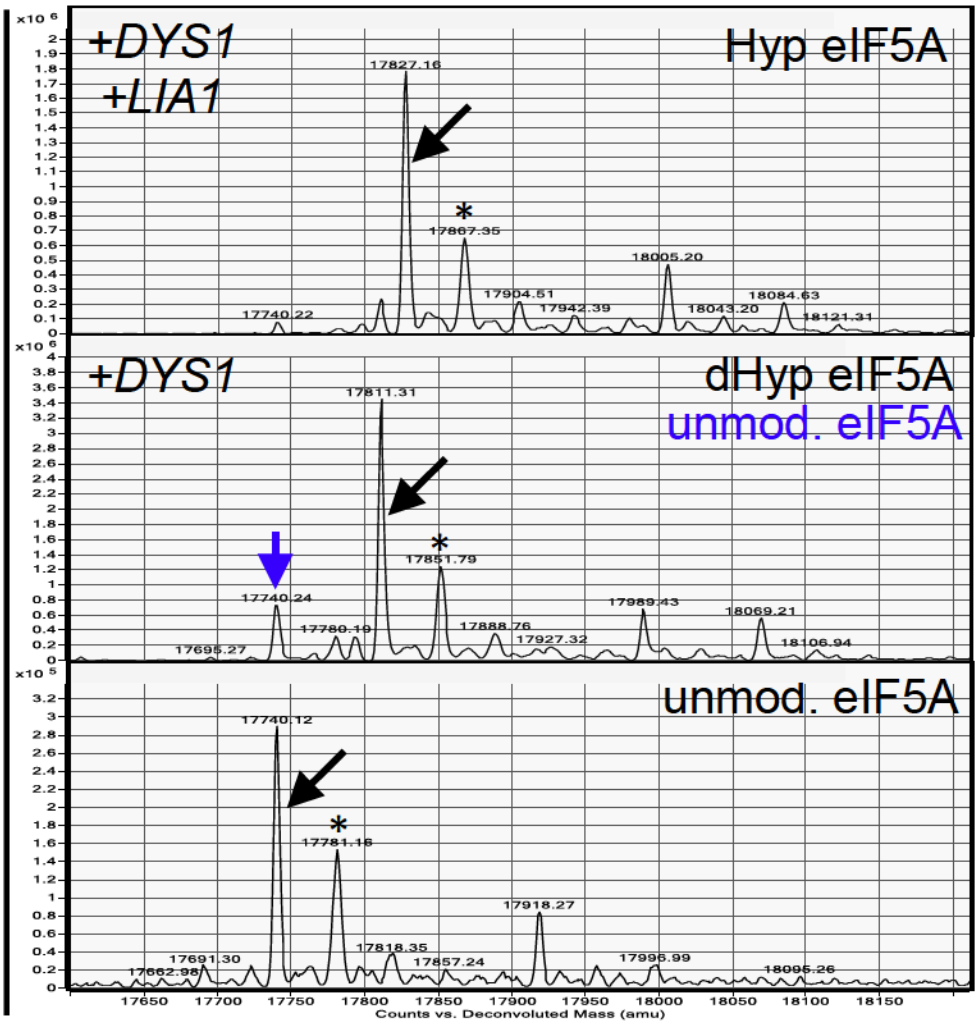
+DYS1
+LIA1
Hyp eIF5A
17827.16
17867.35
17740.22
17904.51
17942.39
18005.20
18043.20
18084.63
18121.31
+DYS1
dHyp eIF5A
unmod. eIF5A
17811.31
17851.79
17740.24
17695.27
17780.19
17888.76
17927.32
17989.43
18069.21
18106.94
unmod. eIF5A
17740.12
17781.18
17691.30
17662.98
17818.35
17857.24
17918.27
17996.99
18095.26
17650
17700
17750
17800
17850
17900
17950
18000
18050
18100
18150
Counts vs. Deconvoluted Mass (amu)

eIF5A
-S74F

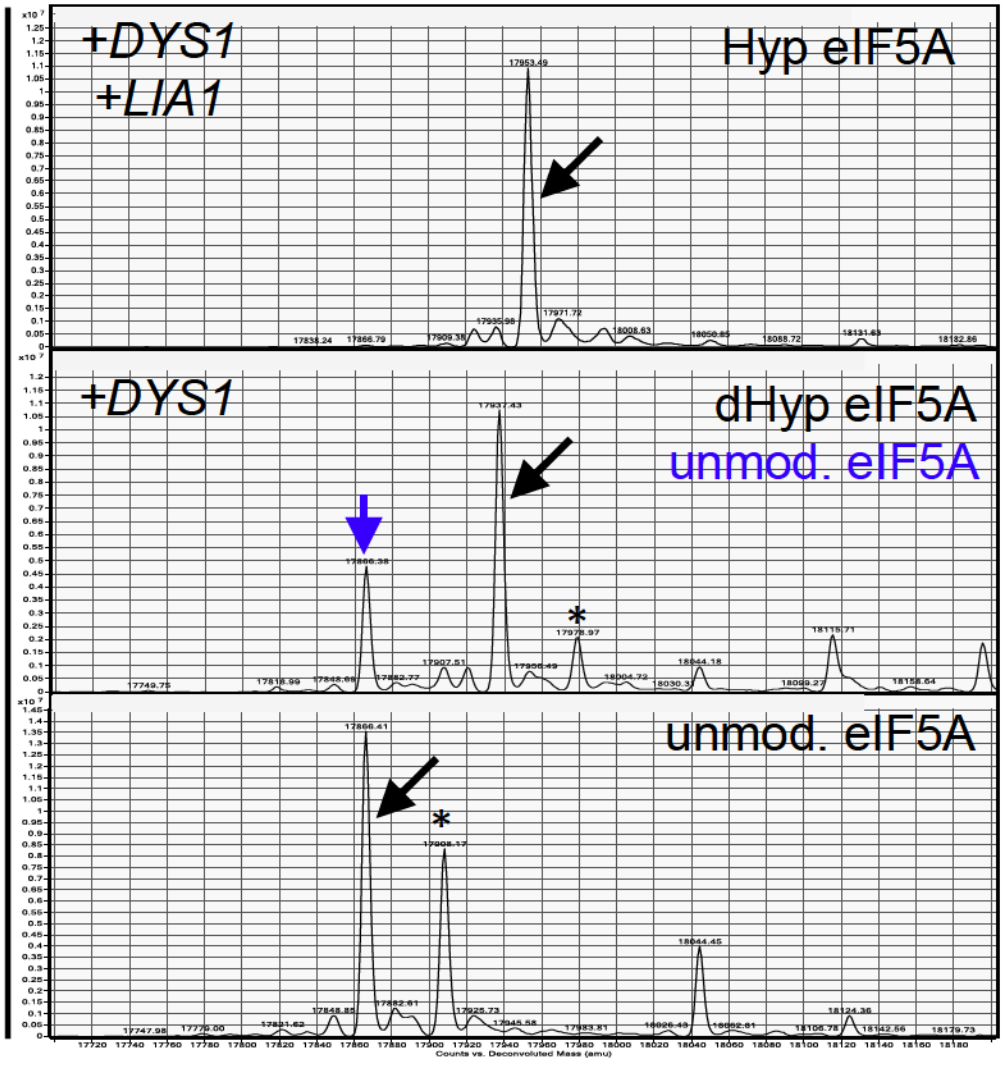
+DYS1
+LIA1
Hyp eIF5A
17953.49
17971.72
+DYS1
dHyp eIF5A
unmod. eIF5A
17866.38
17937.43
17978.97
unmod. eIF5A
17866.41
17908.17
Counts vs. Deconvoluted Mass (amu)

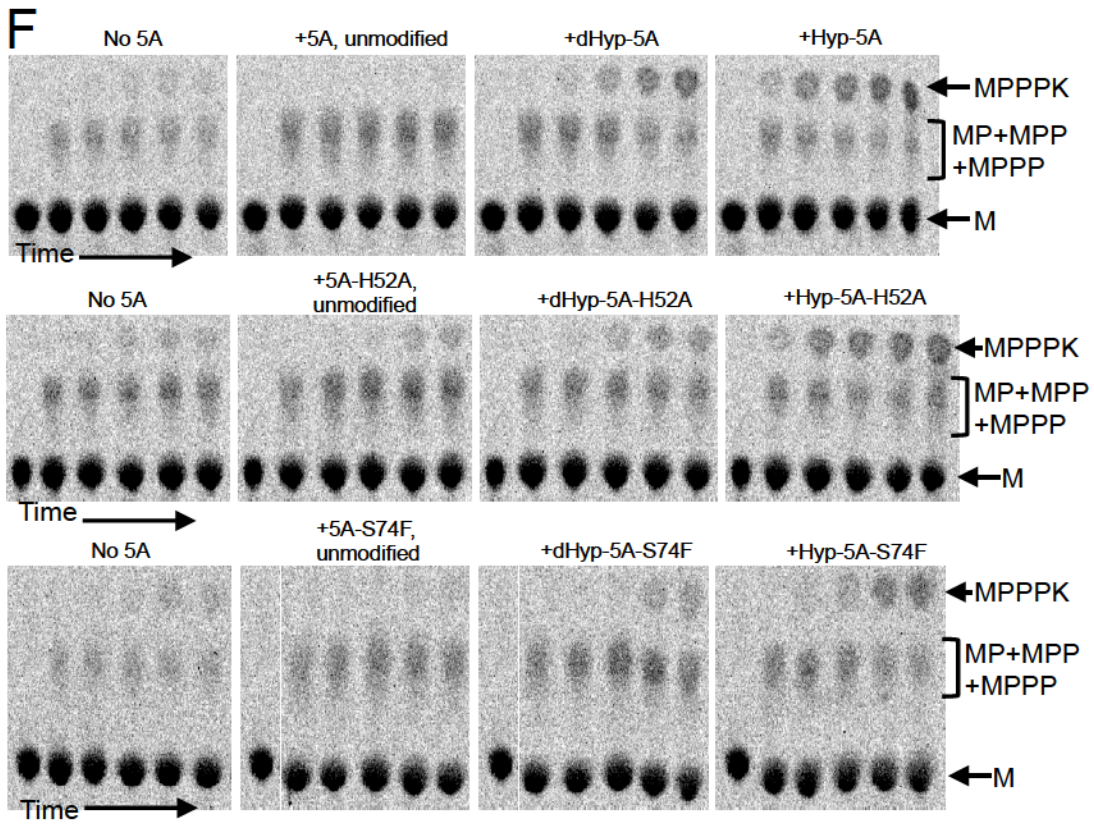
F
No 5A
+5A, unmodified
+dHyp-5A
+Hyp-5A
MPPPK
MP+MPP
+MPPP
M
Time
No 5A
+5A-H52A, unmodified
+dHyp-5A-H52A
+Hyp-5A-H52A
MPPPK
MP+MPP
+MPPP
M
Time
No 5A
+5A-S74F, unmodified
+dHyp-5A-S74F
+Hyp-5A-S74F
MPPPK
MP+MPP
+MPPP
M
Time

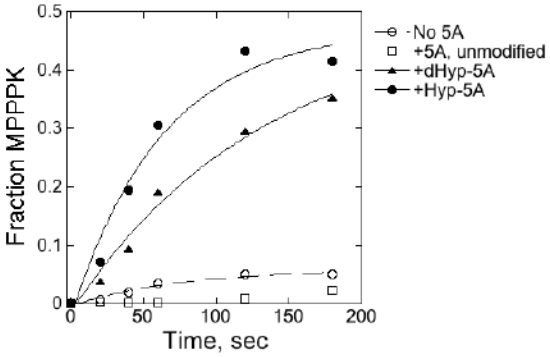
Fraction MPPPK
Time, sec
No 5A
+5A, unmodified
+dHyp-5A
+Hyp-5A

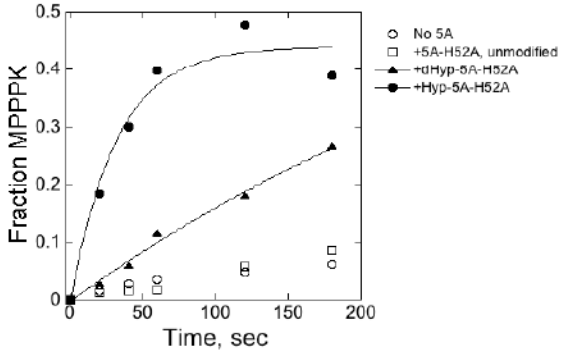
Fraction MPPPK
Time, sec
No 5A
+5A-H52A, unmodified
+dHyp-5A-H52A
+Hyp-5A-H52A

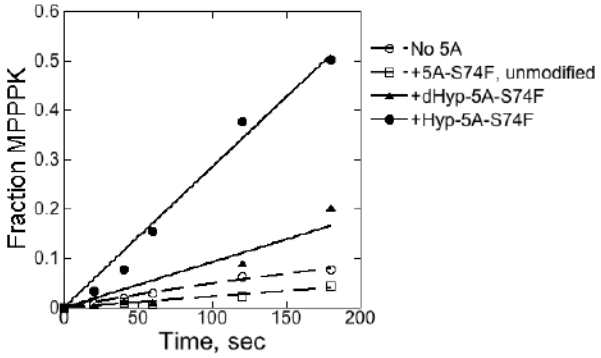
Fraction MPPPK
Time, sec
No 5A
+5A-S74F, unmodified
+dHyp-5A-S74F
+Hyp-5A-S74F

Figure 26. Stimulation of polyproline synthesis by eIF5A both *in vivo* and *in vitro* requires the hydroxyl group on hypusine.

(A,B) Dual luciferase reporter constructs containing 10 repeats of the AlaGCU or ProCCA codon were introduced into isogenic *LIA1*$^+$ (J1005) or *lia1*Δ (J1119) yeast strains expressing the indicated form of eIF5A. Yeast were grown to OD_{600} = 1.0 at 30°C, and *Renilla* and firefly luciferase activities were quantitated. Results were quantitated and normalized to the no insert control as described in Fig. 6. Error bars were calculated as propagated standard deviations for three independent transformants.

(C,F) Electrophoretic TLC analyses of peptide products from elongation assays programmed to synthesize M-P-P-P-K. The identities of spots corresponding to M-P, M-P-P, M-P-P-P, M-P-P-P-K and free methionine are indicated. The fraction of M-P-P-P-K synthesis in elongation assays lacking or containing wild-type or mutant eIF5A purified from yeast (C) or *E. coli* (F) was quantitated, plotted, and fit to a single exponential equation. Whether prepared from yeast or *E. coli*, 100 nM wild-type eIF5A, 100 nM eIF5A-H52A or 1 μM eIF5A-S74F was used in the peptide synthesis assays.

(D) Schematic of plasmids pC4181, pC4182 and pC4183, derived from pST39 (Tan, 2001), for co-expression of eIF5A, DYS1 and LIA1 in *E. coli*. Mutations in eIF5A were introduced by site-directed mutagenesis.

(E) ESI QTOF MS analysis of recombinant N-terminal His_6-tagged eIF5A, eIF5A-H52A, and eIF5A-S74F produced in *E. coli* (bottom panels) or produced in cells co-expressing DYS1 (middle panels) or DYS1 and LIA1 (top panels). Peaks corresponding to Hyp, dHyp, and unmodified (unmod.) forms of eIF5A are marked by arrows; and peaks representing acetylated forms of eIF5A are marked with an asterisk (*).

H52A and Hyp-eIF5A-S74F stimulated M-P-P-P-K synthesis (Y_{max} = 0.45 ±0.05 and Y_{max} = >0.50, respectively), while unmodified eIF5A, eIF5A-H52A and eIF5A-S74F were defective in stimulating polyproline peptide synthesis. Intriguingly, dHyp-eIF5A-H52A and dHyp-eIF5A-S74F were impaired in M-P-P-P-K peptide synthesis. This inability of the deoxyhypusine forms of eIF5A-H52A and eIF5A-S74F to robustly stimulate M-P-P-P-K synthesis is consistent with the *in vivo* reporter analyses (Fig. 26A) and indicate that the hydroxyl group on hypusine plays a crucial role for the function of eIF5A-H52A and eIF5A-S74F in polyproline synthesis.

5.8 Conclusion

The function of the hypusine modification on eIF5A, including its hydroxyl group, is poorly understood. While the *LIA1* gene encoding DOHH is non-essential in yeast, I isolated a distinct class of eIF5A mutants that require full hypusine maturation for yeast cell growth. All of the mutations lie on the surface of the N-terminal domain of eIF5A with the eIF5A-H52A mutation located on the hypusine loop adjacent to the site of the modification and the S74F, N79I and C23Y,V60D mutations positioned on the "body" of eIF5A. In polysome analyses, the eIF5A-H52A and eIF5A-S74F mutants exhibited defects in translation, and further biochemical analyses of the mutants revealed that the hydroxyl group on hypusine promoted eIF5A function in polyproline synthesis. Thus, based on the proposed binding of eIF5A near the PTC of the ribosome, we propose that the hydroxyl group is an essential component of the hypusine modification and serves to position hypusine such that it can enhance the synthesis of poor substrates like polyproline.

6. Discussion

Based on its ability to stimulate Met-Pmn synthesis, eIF5A was long thought to be an initiation factor that promoted formation of the first peptide bond (Benne and Hershey, 1978; Glick and Ganoza, 1975; Kemper et al., 1976; Schreier et al., 1977). Later, it was shown, using elegant polysome profile analyses and *in vitro* translation experiments, that eIF5A promotes translation elongation (Gregio et al., 2009; Saini et al., 2009). As detailed in this dissertation, our work on eIF5A, concurrent with studies on bacterial EF-P, have provided new insights into the function of the two factors, and solidified a role for these factors in translation elongation and, in particular, in the production of polyproline-containing proteins. These data also demonstrate a requirement for the conserved hydroxyl group on hypusine for eIF5A function in protein synthesis. In this Discussion Chapter, I will review the newfound translation functions and recent developments of eIF5A/EF-P and their hypusine/β-lysyl-lysine modifications and discuss the broader implications of our work within the field.

6.1 eIF5A and EF-P promote production of polyproline proteins

At the time that I joined the Dever lab in early 2011, we hypothesized that eIF5A functions to promote peptide bond synthesis of particular amino acids. Based on previous reports (Glick et al., 1979; Glick and Ganoza, 1975), we originally proposed that eIF5A functioned in a similar manner to bacterial EF-P. We initially focused our attention on the possible dependency for eIF5A in polyglycine and/or polyalanine synthesis using *in vivo* dual luciferase assays. We chose to initially test polyglycine and polyalanine because, according to Glick and colleagues, EF-P stimulatory activity was most pronounced for dipeptide synthesis between fMet-tRNA and the A-site substrates C-A-Gly, C-A-Ala and

puromycin (Glick et al., 1979). However, I did not observe any significant dependency for eIF5A in polyalanine or polyglycine synthesis in the reporter assays (Fig. 6B). (Note that the *in vitro* assays employed by Glick et al. were limited to the C-A acceptor ends of the aminoacyl-tRNA). With the work conducted by Ude and colleagues (Ude et al., 2013) and Doerfel and co-workers (Doerfel et al., 2013), who showed that EF-P enhanced the synthesis of proteins containing runs of consecutive proline codons, I used the dual luciferase assay system to reveal the eIF5A requirement for polyproline peptide synthesis. Here, I describe the experiments conducted on EF-P and polyproline synthesis that set the stage for our work with eIF5A.

Coming from a genetics perspective, Ude et al. found that production of CadC, a transcriptional regulator of the *cadBA* operon in *E. coli*, was impaired in cells lacking EF-P or its β-lysyl-lysine modifying enzymes YjeA/PoxA or YjeK (Ude et al., 2013). The sensitivity of *cadC* mRNA translation to defects in EF-P function was mapped to a cluster of proline codons within the *cadC* open reading frame. Mutating these proline codons substantially restored *cadC* expression in cells lacking EF-P. Moreover, expression of reporter constructs containing three or more consecutive proline codons was diminished in cells lacking EF-P, and this effect was specific for proline as runs of five consecutive codons for each of the other 19 amino acids did not confer sensitivity to loss of EF-P function. Coming from a molecular perspective and based in part on previous findings that Gly and Pro are poor substrates for peptide bond formation (Pavlov et al., 2009; Tanner et al., 2009), Doerfel and co-workers used *in vitro* translation elongation assays to examine EF-P stimulation of peptide bond formation (Doerfel et al., 2013). Whereas EF-P did not stimulate M-P-F synthesis, M-P-G and M-P-P synthesis

was simulated 8- and 16-fold, respectively, by addition of EF-P. Synthesis of peptides containing longer stretches of proline residues showed practically an absolute dependence on EF-P. This requirement for EF-P was also observed when translating derivatives of the PrmC protein with the sequence P-P-P or P-P-G inserted after the 19th codon or when translating native *E. coli* proteins containing polyproline sequences. Consistent with these studies, polyproline sequences were found to cause ribosomal stalling in bacteria in a manner that could be alleviated by addition of EF-P *in vitro* (Woolstenhulme et al., 2013). Taken together, this work established a role for EF-P in the specialized translation of polyproline sequences, and demonstrated that EF-P function is not limited to first peptide bond synthesis.

Recently, three studies have further examined the sequence motifs that impose a requirement for EF-P. Two studies employed stable isotope labeling by amino acids in cell culture (SILAC) to differentially label proteins expressed in bacteria that express or lack EF-P (Hersch et al., 2013; Peil et al., 2013), and Peil et al. also examined cells lacking the modifying enzymes yjeK, yjeA or yfcM (Peil et al., 2013). Bioinformatic analysis of the data revealed down-regulation of proteins containing polyproline sequences especially the motifs P-P-P and P-P-G. Systematic analyses of reporter expression containing various X-P-P or P-P-Y motifs revealed strong EF-P dependence when X was Pro, Asp or Ala and Y was Pro, Gly, Trp, Asp, or Asn (Peil et al., 2013). Interestingly, Hersch et al. reported that loss of EF-P impaired expression of several non-proline containing motifs when inserted at the fourth codon position of a GFP reporter (Hersch et al., 2013). However, when Peil et al. inserted these motifs into a *lacZ* reporter they did not observe EF-P dependence either *in vivo* or *in vitro* (Peil et al., 2013). Thus, it

remains to be determined whether EF-P contributes to the translation of non-proline containing motifs.

A third report utilized genome-wide ribosome profiling to examine EF-P–dependent ribosomal pausing on P-P-X motifs (Elgamal et al., 2014). X, in this case, represents any of the 20 amino acids. Though a surprisingly low number of P-P-X motifs (2.8% of all P-P-X motifs in the *E. coli* proteome) exhibited significant ribosome pausing (45-fold increase in ribosomal pausing at P-P-X motifs in cells lacking EF-P), Elgamal et al. found that pausing was largely dependent on sequences as far as three codons upstream of the second proline of the P-P-X motif (Elgamal et al., 2014). This suggests that interactions of the nascent chain with constituents in the ribosome exit tunnel can influence the strength of the ribosomal pause in the absence of EF-P. Curiously, no reliable correlation was observed when the ribosomal occupancies from cells lacking EF-P were compared with representative total protein levels from previous proteomic SILAC data (Peil et al., 2013). Thus, it remains to be seen if other factors compensate for ribosomal pausing on P-P-X motifs or if the paused proteins are subject to quality control. Coincidentally, this also raises the question of whether pausing of ribosomes translating polyproline sequences in the absence of EF-P (or eIF5A) targets the mRNAs to mRNA surveillance mechanisms. Finally, while these recent studies indicated that polyproline sequences confer the greatest dependency on EF-P, the chemical nature of the other amino acids that when juxtaposed with diproline impose EF-P dependency may provide new mechanistic insights into the interplay between the ribosome exit channel, the A-site substrate and the PTC of the ribosome.

Consistent with the reports on EF-P, we reported that eIF5A likewise plays a critical role in the translation of polyproline motifs (Gutierrez et al., 2013). A set of dual luciferase reporter constructs in which the two luciferase ORFs were separated by ten consecutive codons for each of the twenty amino acids were introduced into wild-type and eIF5A mutant strains of yeast. Interestingly, expression from the reporter containing the run of proline codons was specifically impaired in the eIF5A mutant (Fig. 6). This 3-5–fold impact of the eIF5A mutation on polyproline reporter expression was observed when the polyproline insert was reduced from 10 to 8 or 6 codons, and was still apparent, albeit with weaker impact, when only 3 or 4 proline codons were inserted in the reporter (Fig. 10). Similar to this *in vivo* requirement for eIF5A stimulation of polyproline synthesis, polyproline peptide synthesis in a reconstituted yeast *in vitro* translation system was also dependent on eIF5A (Fig. 12). Addition of eIF5A modestly (<2-fold) stimulated M-P-K or M-F-F tripeptide synthesis, suggesting a basic enhancement of peptidyl transferase activity that is not specific for proline. In contrast, synthesis of a peptide containing two consecutive Pro residues was stimulated ~4-fold by addition of eIF5A, and the *in vitro* synthesis of a peptide containing three consecutive Pro residues showed absolute dependence on eIF5A. These data also suggest that the amino acid proline rather than the tRNA impose a requirement for eIF5A (Fig. 9C). Future *in vitro* studies using misacylated $tRNA^{Pro}$ or an Pro mis-acylated on a non-cognate tRNA may define the precise tRNA and/or amino acid requirements for eIF5A in polyproline synthesis.

Further analyses of ribosomes translating polyproline sequences have provided insight into the requirement for EF-P or eIF5A. In the *in vitro* bacterial system, ribosomes translating the sequence P-P-G in the absence of EF-P stalled with diproline bound to the

P-site tRNA and Gly-tRNA in the A site (Doerfel et al., 2013). Likewise, toe-printing studies of bacterial ribosomes stalled *in vivo* or *in vitro* on polyproline sequences indicated that proline is bound to the P-site tRNA and Pro-tRNA is in the A site (Woolstenhulme et al., 2013). Interestingly, Woolstenhulme et al. also found that both the length and amino acid sequence preceding the polyproline stretch affects the efficiency of stalling, consistent with the notion mentioned above, that the conformation of the peptide in the active site and exit tunnel of the ribosome can impose a requirement for EF-P (Elgamal et al., 2014). In experiments performed in collaboration with Chris Woolstenhulme and Allen Buskirk, toe-printing studies of eukaryotic ribosomes translating polyproline sequences in the absence of eIF5A likewise revealed stalling with the second Pro codon in the P site (diproline bound to the P-site tRNA) and a Pro codon in the A site (Gutierrez et al., 2013). Thus EF-P and eIF5A appear to rescue similarly stalled complexes, suggesting that both proteins are required to promote synthesis of proline-proline peptide bonds needed to convert di-proline to tri-proline and higher-order polyproline sequences.

While no structures of eIF5A bound to the ribosome are available, the results of directed hydroxyl radical probing experiments indicate that eIF5A binds to a comparable site on the eukaryotic ribosome as EF-P binds to the bacterial ribosome. Hydroxyl radicals generated by iron linked to the hypusine loop of eIF5A resulted in cleavages to the acceptor stem of the P-site tRNA and to rRNA at the top of the E and P sites including the PTC of the ribosome (Gutierrez et al., 2013). In addition, hydroxyl radicals generated by iron tethered to the "body" of eIF5A yielded cleavages on the side of the P-site tRNA that faces the E site. Consistent with the smaller size of eIF5A compared to

EF-P, and the lack of domain III in eIF5A, there was no evidence that eIF5A contacts the small ribosomal subunit. Thus, when bound to the ribosome, eIF5A is predicted to lie adjacent to the P-site tRNA in a position that partially overlaps the E site with the N-terminal domain of eIF5A lying close to the acceptor stem of the P-site tRNA. Due to its close proximity to the acceptor stem of the P-site tRNA, the hypusine modification is predicted to extend near the PTC of the ribosome.

Examination of the yeast proteome revealed that 549 out of 5886 proteins contain at least one triproline motif. The number of hits increases to 749 if P-P-G motifs are included as well, and the number of hits increases to nearly 2000 if all poor P-P-X motifs, as defined for EF-P by Peil et al. (Peil et al., 2013), are included in the search. In humans, proline accounts for ~6% of the total encoded residues (Morgan and Rubenstein, 2013). Among ~18,000 human proteins, there are roughly 10,000 motifs consisting of 3 or more consecutive proline residues (Morgan and Rubenstein, 2013). In the analysis of protein expression in yeast, we reported that levels of the polyproline-containing proteins Ldb17 (Fig. 11A), Eap1, and Vrp1 were reduced in eIF5A mutant strains (Gutierrez et al., 2013). Moreover, the expression of Ldb17 was restored when the polyproline sequence in this protein was mutated to polyalanine (Fig. 11B). In addition, the preliminary analysis of ribosome profiling of the *ts*$^{-}$ eIF5A-S149P mutant has shown ribosome pausing at polyproline sequences and a dramatic loss of ribosome occupancy after the polyproline segment in the *TIM50* mRNA (Fig. 20). At present, it is still unclear whether the polysome retention observed in polysome profile analyses upon inactivation of eIF5A in yeast (Fig. 8) reflects impaired translation elongation on the majority of cellular mRNAs or is due to impaired translation of just the mRNAs containing polyproline motifs.

Additional ribosome profiling studies to obtain greater and more in-depth coverage of mRNAs combined with more specific bioinformatics analyses will enable the identification of the entire collection of amino acid motifs that require eIF5A for their translation. However, based on ribosome profiling data from *E.* coli cells lacking EF-P (Elgamal et al., 2014) and our ribosome profiling results, the most convincing amino acid sequence motifs that strongly require eIF5A are those containing polyproline. The prevalence of polyproline motifs in yeast (95 out of 5886 proteins with motifs containing 4 or more consecutive prolines) is consistent with eIF5A being essential in yeast; whereas, the *efp* gene can be deleted in *E. coli* in which only 9 out of ~4000 proteins contain motifs of four or more proline residues (Doerfel et al., 2013). Interestingly, while polyproline sequences are found in a variety of proteins in yeast, it is notable that several proteins involved in the actin cytoskeleton contain polyproline motifs. Of particular interest, the protein BNI1, which functions in polarized cell growth, contains a polyproline sequence. Production of BNI1 is impaired in an eIF5A mutant strain (Li et al., 2014) and, interestingly, overexpression of BNI1 partially suppresses the slow-growth phenotype of an eIF5A mutant yeast strain (Zanelli and Valentini, 2005). Based on this finding it seems reasonable to propose that the impacts of eIF5A mutants on the yeast cell cycle, cytoskeleton, and PKC pathways (Chatterjee et al., 2006; Frigieri et al., 2008; Galvao et al., 2013; Valentini et al., 2002), as well as the association of eIF5A with oncogenesis and, paradoxically, tumor suppression in mammals (Scuoppo et al., 2012; Silvera et al., 2010; Zender et al., 2008), may reflect impaired expression of specific proteins containing polyproline sequences.

6.2 The requirement of the hypusine/β-lysyl-lysine modification for eIF5A/EF-P function in protein synthesis

In addition to amino acid sequence and structural similarities, both eIF5A and EF-P are post-translationally modified. As described earlier, the ε-amino group of a conserved Lys residue in eIF5A from some archaea and all eukaryotes is modified by DHS and DOHH to generate hypusine. Similarly, the *E. coli* gene products YjeA, YjeK and YfcM attach a β-lysine residue to the ε-amino group of a specific Lys residue in EF-P from some bacteria and then hydroxylate the side chain of the original Lys residue (Navarre et al., 2010; Peil et al., 2012; Roy et al., 2011; Yanagisawa et al., 2010). Interestingly, the Lys residue that is the site of the modification (Lys34 in *E.*coli EF-P) is substituted by Arg in some bacteria (e.g. *T. thermophilus*), and it is not known whether this Arg residue is post-translationally modified. Both the hypusine modification of eIF5A and the β-lysyl-lysine modification of EF-P are required for these factors to stimulate polyproline synthesis (Doerfel et al., 2013; Ude et al., 2013) (Fig. 12D). Similar to *E. coli* strains lacking EF-P, loss of β-lysinylation in *E. coli* impairs translation of the polyproline motif in *cadC*; likewise, loss of β-lysinylation in *Salmonella enterica* alters the expression of a variety of cellular proteins, impairs virulence in mice, and alters resistance to antibiotics (Navarre et al., 2010), presumably due to impaired translation of polyproline sequences. Moreover, mouse models have shown that homozygous knockouts of eIF5A, DHS, or DOHH result in embryonic lethality supporting a critical function of eIF5A and the hypusine modification in mammalian development (Nishimura et al., 2012; Sievert et al., 2014).

Recent studies have further illuminated the biosynthesis of the β-lysyl-lysine modification on EF-P. The initial studies on the EF-P modification did not determine

whether YjeK acted before or after YjeA/PoxA added an extra molecule of lysine to the Lys34 side chain in *E. coli* EF-P. However, further biochemical analysis of the β-lysinylation reaction revealed that β-lysine was a much-preferred substrate for YjeA/PoxA than was α-lysine (K_m decreased 40-fold and k_{cat} increased 2-fold with β-lysine) (Roy et al., 2011). Thus, the EF-P modification pathway is predicted to proceed first with conversion of α-lysine to β-lysine by YjeK and then with addition of the β-lysine to EF-P by YjeA/PoxA to form β-lysyl-lysine (Fig. 27). Analysis of Met-Pmn synthesis *in vitro* using recombinant forms of unmodified and α- versus β-lysinylated EF-P demonstrated the critical importance of the β-lysyl-lysine modification for EF-P function (Bullwinkle et al., 2013; Park et al., 2012).

Whereas β-lysinylation is predicted to increase the mass of EF-P by 128 Da, analysis of native EF-P indicated that the modification increased EF-P mass by 144 Da (Aoki et al., 2008; Peil et al., 2012). This discrepancy was resolved when Peil et al. demonstrated that YfcM (EpmC) hydroxylates the original lysine side chain of the modified residue in EF-P (Peil et al., 2012). Moreover, MS analysis of purified *E. coli* EF-P established that β-lysine is attached to the ε-amino group of Lys34 (Peil et al., 2012). Thus, similar to the conversion of deoxyhypusine to hypusine by DOHH, YfcM adds a hydroxyl group (+16 Da) to complete the post-translational biosynthesis of the β-lysyl-lysine modification on EF-P (Fig. 27). However, in contrast to eIF5A, where the hydroxyl group is added to the spermidine-derived portion of the modification, the hydroxylation of EF-P is directed to the γ or δ carbons of the Lys34 sidechain (and not to the added β-lysine) (Peil et al., 2012). Interestingly, similar to the minimal effect of *LIA1*

deletion in yeast, loss of *yfcM* in *E. coli* did not affect bacterial growth or antibiotic sensitivity (Bullwinkle et al., 2013).

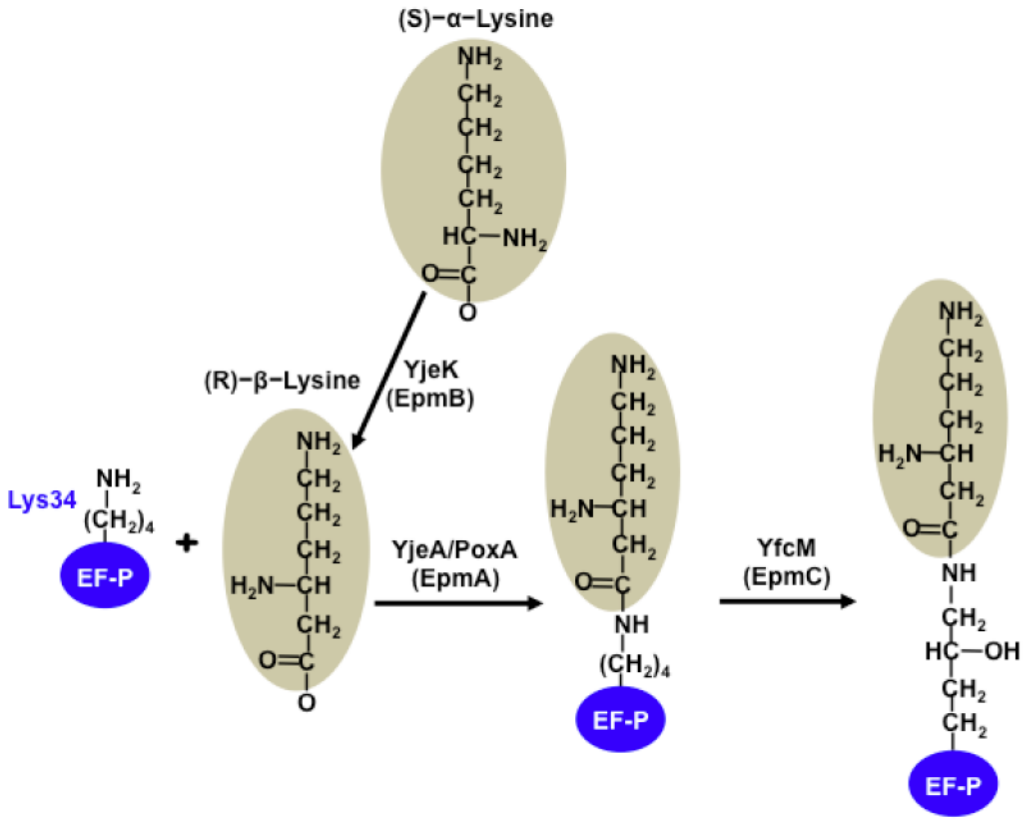

Figure 27. Post-translational modification pathway for EF-P.

In bacteria, β-lysinylation of EF-P occurs in three steps catalyzed by YjeK (EpmB), YjeA/PoxA (EpmA) and YfcM (EpmC). First, YjeK, a lysine aminomutase, converts lysine to β-lysine. Next, YjeA/PoxA catalyzes the addition of β-lysine onto a specific lysine residue in EF-P (Lys34 of *E. coli* EF-P). In a final step, YfcM hydroxylates the lysine residue.

Yeast lacking LIA1 grow slightly slower than wild-type strains. In addition, recent studies have linked loss of *LIA1* to a defect in synthesis of the polyproline-

containing BNI1 protein, resulting in an impaired ability of yeast to shmoo and mate (Li et al., 2014). In contrast to loss of *LIA1* in yeast, loss of DOHH is recessively lethal in *C. elegans* (Sievert et al., 2014; Sugimoto, 2004), *Drosophila* (Patel et al., 2009), and mouse (Sievert et al., 2014). Thus, the hydroxyl group may be more critical for eIF5A function in higher eukaryotes and multi-cellular organisms. In my studies of the hypusine modification on eIF5A, I focused on the role of the hydroxyl group on hypusine and identified a collection of eIF5A mutants that require hydroxylation of deoxyhypusine for yeast cell growth (Fig. 21). The *LIA1*-dependent mutations in *HYP2* were localized to the N-terminal domain of the eIF5A protein (Fig. 22). Following discovery of these *LIA1*-dependent eIF5A mutants, we investigated whether the synthetic growth defects in these mutants could be explained by negative impacts on eIF5A protein levels, the stability of the hypusine modification, or eIF5A function. Western analyses revealed that the mutations did not diminish protein levels (Fig. 24), and MS analyses demonstrated that the mutations did not result in the accumulation of unmodified forms of eIF5A (Fig. 25). This latter result is inconsistent with cell-free experiments that suggested that the hydroxylation of deoxyhypusine to hypusine blocks the reversible back reaction of deoxyhypusine to unmodified eIF5A (Park et al., 2003). Also at odds with this result, recent evidence from Sievert et al. have shown that mouse 3T3 cells lacking DOHH accumulate unmodified eIF5A (Sievert et al., 2014). It is unclear whether differences between yeast and mammalian DHS underlie the differential requirement for the hydroxyl group to prevent the back reaction of deoxyhypusine to unmodified eIF5A. Preventing the back reaction and the accumulation of unmodified eIF5A by

hydroxylating deoxyhypusine to make hypusine may be necessary to ensure adequate pools of Hyp-eIF5A for early mammalian development.

These data demonstrate that the hydroxyl group on hypusine has a primary function in protein synthesis and in translation of polyproline motifs. Although loss of *LIA1* results in a minor slow-growth and shmooing defect in yeast (Li et al., 2014), our studies suggest that *lia1*Δ is hypomorphic and displays exacerbated growth defects when combined with an eIF5A mutant. My data, using *in vivo* reporter and *in vitro* translation assays, revealed that the dHyp forms of eIF5A-H52A and eIF5A-S74F are defective in stimulating polyproline synthesis (Fig. 26). Thus, the synthetic growth defects associated with these eIF5A mutants in the *lia1*Δ background can be attributed to an impairment of the eIF5A mutants in the translation of polyproline sequences. As shown above, the MS analysis of eIF5A-H52A purified from yeast confirmed the presence of Hyp-eIF5A-H52A and dHyp-eIF5A-H52A in *LIA1*$^{+}$ strains. This is consistent with previous reports that corresponding mutations in the hypusine loop of human eIF5A impair DOHH recognition (Cano et al., 2008; Kang et al., 2007). Notably, in addition to the apparent elongation defect (Fig. 23B) and reduced stimulation of polyproline synthesis by dHyp-eIF5A-H52A (Fig. 26C&F), eIF5A-H52A is impaired in hypusine formation. Curiously, whereas 50-100 nM eIF5A was sufficient to stimulate M-P-P-P-K synthesis in the *in vitro* assays, 1 μM eIF5A-S74F was added to the same assays in order to observe moderate M-P-P-P-K synthesis. In addition to the hypusine hydroxyl group requirement for M-P-P-P-K peptide synthesis, the eIF5A-S74F mutant may be impaired in productive binding to the ribosome reflected by the 10-fold higher $k_{1/2}$ value for eIF5A-S74F versus wild-type eIF5A in my assays (data not shown). While additional structural and binding

experiments with 80S initiation complexes may be necessary to gain insights into the dynamics of eIF5A-H52A and eIF5A-S74F binding to the ribosome and to define the critical interactions of eIF5A residues with the 80S ribosome and P-site tRNA, we propose that the primary function of the hydroxyl group is to position the hypusine residue in the PTC to promote peptide bond formation for poor substrates like proline.

6.3 eIF5A is the keymaster that presents hypusine to the ribosome active site

Previous studies revealed that peptidyl-prolyl-tRNA in the ribosomal P site reacts poorly with puromycin (Muto and Ito, 2008) and that proline is an inefficient A-site substrate for peptide bond formation (Pavlov et al., 2009). These data, as well as the recent studies with EF-P (Doerfel et al., 2013; Ude et al., 2013; Woolstenhulme et al., 2013), demonstrated that combining peptidyl-diprolyl-tRNA in the P site with a poor substrate like prolyl-tRNA in the A site dramatically impairs protein synthesis and establishes a dependency for eIF5A/EF-P and their hypusine/β-lysyl-lysine modifications (Fig. 28). At present, it is not clear why polyproline is such a poor substrate for protein synthesis; however, it may reflect the imino acid nature of proline, the geometrical or steric constraints of a cyclic side chain, or the unique ability of proline to readily sample both *cis* and *trans* conformations of peptide bonds (Ramachandran and Mitra, 1976). Perhaps insertion of the extended hypusine (or β-lysyl-lysine) side chain into the PTC stabilizes the proper conformation of the PTC or restricts the conformation of proline in the P site enabling a favorable geometry for peptide bond formation with the A-site amino acid. While the data reported in this thesis and the recent studies on EF-P establish that translation of homopolyproline motifs requires eIF5A/EFP, additional studies, including

more extensive ribosome profiling of wild-type and eIF5A mutant strains, will be needed to define the spectrum of amino acids and motifs that rely on eIF5A or its hypusine modification for their efficient translation. In addition, structural (X-ray crystallography and cryo-electron microscopy (EM)) and biochemical (single-molecule fluorescence resonance energy transfer (FRET)) studies will provide greater insights into the mechanism by which eIF5A and its hypusine modification interact with the ribosome or diprolyl-tRNA in the ribosomal P site to promote peptide bond formation.

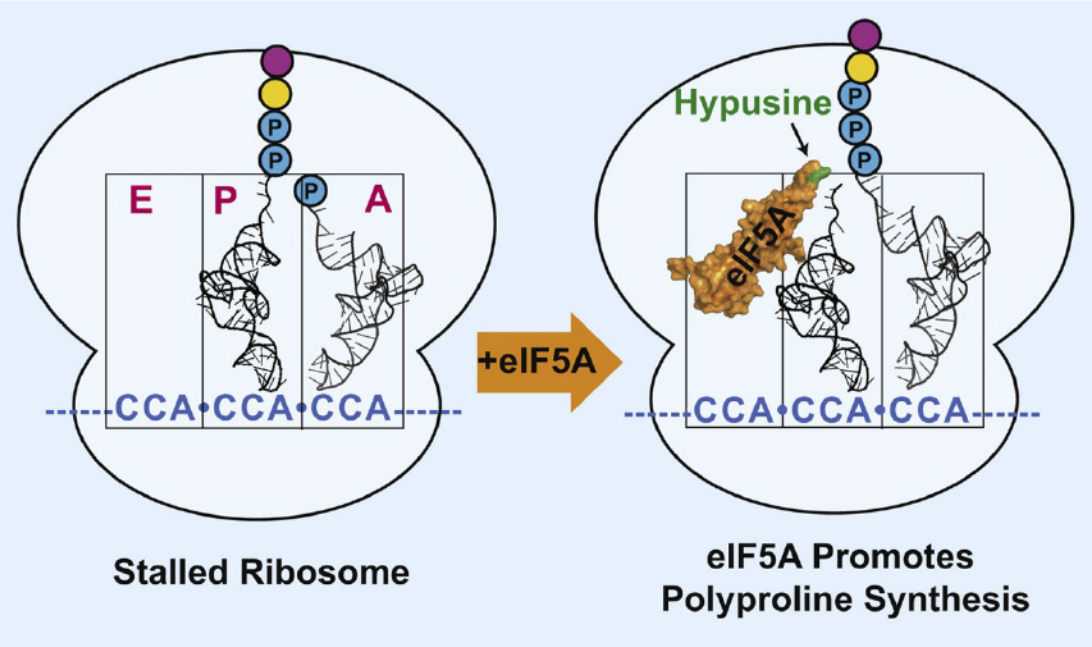

Figure 28. Model of eIF5A stimulating polyproline synthesis.

Model of ribosome stalled on polyproline sequence with di-proline attached to the P-site tRNA and Pro-tRNA^{Pro} in the A site (left). (Right) Binding of eIF5A near the E site places the hypusine side chain (Lys51, green) adjacent to the peptidyl-tRNA in the PTC of the ribosome where it helps promote peptide bond formation with the amino acid attached to the A-site tRNA. Figure taken from Gutierrez et al. (Gutierrez et al., 2013).

After formation of Pro-Pro peptide bonds, we presume that tRNAs move into hybrid P/E and A/P states and that eEF2 promotes translocation of the tRNAs and mRNA on the ribosome. This results in the deacylated tRNA and the peptidyl-tRNA in the E and P sites, respectively. Before the start of the next elongation cycle or entry into the translation termination phase, I propose that eIF5A vacates the ribosomal P/E site, thus freeing the E site for the next round of translocation. Future structural and biochemical studies will illuminate the dynamics of eIF5A on the ribosome with poor substrates like diprolyl-tRNA in the P site. It will also be interesting to determine whether eIF5A contributes to elongation regardless of the substrate (e.g. prolyl-tRNA or phenylalynyl-tRNA) in the P and A site. Notably, incorporation of phenylalanine into peptide bonds is stimulated by eIF5A *in vitro* (Fig. 12B).

6.4 eIF5A/EF-P: the third universally conserved elongation factor

Whereas eIF5A was thought to function as translation initiation factor based on its activity in Met-Pmn assays, puromycin, an aminoacyl analog that reacts well with most peptidyl-tRNA substrates, reacts poorly with fMet-tRNA^{fMet} and with peptidyl-tRNA substrates with a C-terminal proline (Wohlgemuth et al., 2008). In contrast, these latter substrates react well with authentic aminoacyl-tRNAs (Wohlgemuth et al., 2008). The poor reactivity with puromycin has been attributed to poor substrate positioning in the active site of the ribosome (Wohlgemuth et al., 2008; Youngman et al., 2004). Thus, the Met-Pmn synthesis assay is likely not a good mimic of first peptide bond formation, and the eIF5A stimulation of Met-Pmn synthesis might reflect activities of the factor distinct from first peptide bond synthesis. Consistent with this notion, the k_{obs} (data not shown)

and the Y_{max} for M-P or M-F synthesis were only modestly affected by adding eIF5A (Fig. 12); and recent studies, likewise, showed that EF-P does not stimulate dipeptide formation (Bullwinkle et al., 2013; Doerfel et al., 2013). These results argue that eIF5A and EF-P do not have a specific function in first peptide bond synthesis. However, it is noteworthy that consistent with a function in translation elongation, inactivation of eIF5A/EF-P (Bullwinkle et al., 2013; Saini et al., 2009) (Fig. 8) mimics the effects of elongation inhibitors and causes polysome retention. Taken together, the puromycin, peptide synthesis and polysome analyses indicate that the primary function of eIF5A and EF-P is to promote peptide bond formation, especially for poor substrates like polyproline.

In addition to the universally conserved translation factors, eEF1A/EF-Tu and eEF2/EF-G, three other factors have been implicated in translation elongation. However, these latter factors are not universally conserved. The factor eEF3 is proposed to coordinate E-site tRNA release with eEF1A–aminoacyl-tRNA binding to the A site of the ribosome in some fungi including *S. cerevisiae* (Anand et al., 2006; Triana-Alonso et al., 1995). Bacterial EF4 (LepA) is proposed to maintain rapid protein synthesis under stress conditions such as high ionic strength and low temperature (Pech et al., 2011), and SelB/eEFsec is an EF-Tu ortholog required for the delivery of selenocysteinyl-tRNA to the ribosome (Driscoll and Copeland, 2003). Our results studying eIF5A concur with the findings on EF-P (Doerfel et al., 2013; Ude et al., 2013) and demonstrate that eIF5A/EF-P is required for translation of polyproline sequences. This conservation of eIF5A/EF-P in all bacteria, archaea, and eukaryotes that have been examined, combined with the common function of these factors, leads us to conclude that eIF5A/EF-P is the third

universally conserved translation elongation factor. Based on its clarified role in protein synthesis, we propose that eIF5A be appropriately renamed as an elongation factor: eukaryotic elongation factor 5 (eEF5). As many advances have been achieved in the study of eIF5A/EF-P over the past four years, it will be interesting to follow as newer technologies present opportunities to gain additional insights into the function and mechanism of this enigmatic translation factor.

7. References

7.1 Appendix: Glossary of Abbreviations

5-FOA	5-fluoroorotic acid
AEBSF	4-(2-aminoethyl) benzenesulfonyl fluoride hydrochloride
ATP	adenosine-5'-triphosphate
CHO	chinese hamster ovary
CHX	cycloheximide
CTP	cytidine-5'-triphosphate
DHS	deoxyhypusine synthase
dHyp	deoxyhypusinated
DOHH	deoxyhypusine hydroxylase
eEF	eukaryotic elongation factor
EF	elongation factor
eIF	eukaryotic initiation factor
ESI QTOF MS	ElectroSpray-Ionization Quadrupole-Time-of-Flight Mass Spectrometry
fMet	formylmethionyl
IF	initiation factor
GC7	N1-guanyl-1,7-diaminoheptane
GTP	guanosine-5'-triphosphate
Hyp	hypusinated
Met-Pmn	methionyl-puromycin
Met-tRNA$_i^{Met}$	initiator methionyl-tRNA
MW	molecular weight
ORF	open reading frame

PBS	phosphate-buffered saline
P_i	inorganic phosphate
P/M	polysome to monosome
PTC	peptidyl transferase center
SC	synthetic complete
SILAC	stable isotope labeling by amino acids in cell culture
TBS	tris-buffered saline
TCA	trichloroacetic acid
TLC	thin-layer chromatography
ts$^-$	temperature-sensitive
UTR	untranslated region
WCE	whole-cell extract
YNB	yeast nitrogen base
YPD	yeast peptone dextrose
YPGAL	yeast peptone galactose

7.2 Bibliography

Abbruzzese, A., Park, M.H., and Folk, J.E. (1986). Deoxyhypusine hydroxylase from rat testis. Partial purification and characterization. The Journal of biological chemistry *261*, 3085-3089.

Acker, M.G., Kolitz, S.E., Mitchell, S.F., Nanda, J.S., and Lorsch, J.R. (2007). Reconstitution of yeast translation initiation. Methods in enzymology *430*, 111-145.

Anand, M., Balar, B., Ulloque, R., Gross, S.R., and Kinzy, T.G. (2006). Domain and nucleotide dependence of the interaction between Saccharomyces cerevisiae translation elongation factors 3 and 1A. The Journal of biological chemistry *281*, 32318-32326.

Anand, M., Chakraburtty, K., Marton, M.J., Hinnebusch, A.G., and Kinzy, T.G. (2003). Functional interactions between yeast translation eukaryotic elongation factor (eEF) 1A and eEF3. The Journal of biological chemistry *278*, 6985-6991.

Andersen, C.F., Anand, M., Boesen, T., Van, L.B., Kinzy, T.G., and Andersen, G.R. (2004). Purification and crystallization of the yeast translation elongation factor eEF3. Acta crystallographica Section D, Biological crystallography *60*, 1304-1307.

Aoki, H., Xu, J., Emili, A., Chosay, J.G., Golshani, A., and Ganoza, M.C. (2008). Interactions of elongation factor EF-P with the Escherichia coli ribosome. The FEBS journal *275*, 671-681.

Bailly, M., and de Crecy-Lagard, V. (2010). Predicting the pathway involved in post-translational modification of elongation factor P in a subset of bacterial species. Biology direct *5*, 3.

Bartig, D., Lemkemeier, K., Frank, J., Lottspeich, F., and Klink, F. (1992). The archaebacterial hypusine-containing protein. Structural features suggest common ancestry with eukaryotic translation initiation factor 5A. European journal of biochemistry / FEBS *204*, 751-758.

Bartig, D., Schumann, H., and Klink, F. (1990). The Unique Posttranslational Modification Leading to Deoxyhypusine or Hypusine Is a General Feature of the Archaebacterial Kingdom. Systematic and applied microbiology *13*, 112-116.

Benne, R., Brown-Luedi, M.L., and Hershey, J.W.B. (1978). Purification and characterization of protein synthesis initiation factors eIF-1, eIF-4C, eIF-4D, and eIF-5 from rabbit reticulocytes. Journal of Biological Chemistry *253*, 3070-3077.

Benne, R., and Hershey, J.W.B. (1978). The mechanism of action of protein synthesis initiation factors from rabbit reticulocytes. The Journal of biological chemistry *253*, 3078-3087.

Bevec, D., Jaksche, H., Oft, M., Wohl, T., Himmelspach, M., Pacher, A., Schebesta, M., Koettnitz, K., Dobrovnik, M., Csonga, R., *et al.* (1996). Inhibition of HIV-1 replication in lymphocytes by mutants of the Rev cofactor eIF-5A. Science *271*, 1858-1860.

Blaha, G., Stanley, R.E., and Steitz, T.A. (2009). Formation of the first peptide bond: the structure of EF-P bound to the 70S ribosome. Science *325*, 966-970.

Boeke, J.D., Trueheart, J., Natsoulis, G., and Fink, G.R. (1987). 5-fluoroorotic acid as a selective agent in yeast molecular genetics. Methods in enzymology *154*, 164-175.

Brar, G.A., Yassour, M., Friedman, N., Regev, A., Ingolia, N.T., and Weissman, J.S. (2012). High-resolution view of the yeast meiotic program revealed by ribosome profiling. Science *335*, 552-557.

Bullwinkle, T.J., Zou, S.B., Rajkovic, A., Hersch, S.J., Elgamal, S., Robinson, N., Smil, D., Bolshan, Y., Navarre, W.W., and Ibba, M. (2013). (R)-beta-Lysine-modified Elongation Factor P Functions in Translation Elongation. The Journal of biological chemistry *288*, 4416-4423.

Cano, V.S., Jeon, G.A., Johansson, H.E., Henderson, C.A., Park, J.H., Valentini, S.R., Hershey, J.W., and Park, M.H. (2008). Mutational analyses of human eIF5A-1--identification of amino acid residues critical for eIF5A activity and hypusine modification. The FEBS journal *275*, 44-58.

Chatterjee, I., Gross, S.R., Kinzy, T.G., and Chen, K.Y. (2006). Rapid depletion of mutant eukaryotic initiation factor 5A at restrictive temperature reveals connections to actin cytoskeleton and cell cycle progression. Molecular genetics and genomics : MGG *275*, 264-276.

Chattopadhyay, M.K., Park, M.H., and Tabor, H. (2008). Hypusine modification for growth is the major function of spermidine in Saccharomyces cerevisiae polyamine auxotrophs grown in limiting spermidine. Proceedings of the National Academy of Sciences of the United States of America *105*, 6554-6559.

Chen, K.Y., and Dou, Q.P. (1988). NAD+ stimulated the spermidine-dependent hypusine formation on the 18 kDa protein in cytosolic lysates derived from NB-15 mouse neuroblastoma cells. FEBS letters *229*, 325-328.

Cooper, H.L., Park, M.H., and Folk, J.E. (1982). Posttranslational formation of hypusine in a single major protein occurs generally in growing cells and is associated with activation of lymphocyte growth. Cell *29*, 791-797.

Cooper, H.L., Park, M.H., Folk, J.E., Safer, B., and Braverman, R. (1983). Identification of the hypusine-containing protein hy+ as translation initiation factor eIF-4D. Proceedings of the National Academy of Sciences of the United States of America *80*, 1854-1857.

Dever, T.E., and Green, R. (2012). The elongation, termination, and recycling phases of translation in eukaryotes. Cold Spring Harbor perspectives in biology *4*, a013706.

Dever, T.E., Gutierrez, E., and Shin, B.S. (2014). The hypusine-containing translation factor eIF5A. Critical reviews in biochemistry and molecular biology, 1-13.

Dias, C.A., Cano, V.S., Rangel, S.M., Apponi, L.H., Frigieri, M.C., Muniz, J.R., Garcia, W., Park, M.H., Garratt, R.C., Zanelli, C.F., *et al.* (2008). Structural modeling and mutational analysis of yeast eukaryotic translation initiation factor 5A reveal new critical residues and reinforce its involvement in protein synthesis. The FEBS journal *275*, 1874-1888.

Doerfel, L.K., Wohlgemuth, I., Kothe, C., Peske, F., Urlaub, H., and Rodnina, M.V. (2013). EF-P is essential for rapid synthesis of proteins containing consecutive proline residues. Science *339*, 85-88.

Driscoll, D.M., and Copeland, P.R. (2003). Mechanism and regulation of selenoprotein synthesis. Annu Rev Nutr *23*, 17-40.

Duncan, R.F., and Hershey, J.W. (1986). Changes in eIF-4D hypusine modification or abundance are not correlated with translational repression in HeLa cells. The Journal of biological chemistry *261*, 12903-12906.

Elgamal, S., Katz, A., Hersch, S.J., Newsom, D., White, P., Navarre, W.W., and Ibba, M. (2014). EF-P dependent pauses integrate proximal and distal signals during translation. PLoS genetics *10*, e1004553.

Eyler, D.E., and Green, R. (2011). Distinct response of yeast ribosomes to a miscoding event during translation. RNA *17*, 925-932.

Foiani, M., Cigan, A.M., Paddon, C.J., Harashima, S., and Hinnebusch, A.G. (1991). GCD2, a translational repressor of the *GCN4* gene, has a general function in the initiation of protein synthesis in *Saccharomyces cerevisiae*. Molecular and cellular biology *11*, 3203-3216.

Frigieri, M.C., Joao Luiz, M.V., Apponi, L.H., Zanelli, C.F., and Valentini, S.R. (2008). Synthetic lethality between eIF5A and Ypt1 reveals a connection between translation and the secretory pathway in yeast. Molecular genetics and genomics : MGG *280*, 211-221.

Galvao, F.C., Rossi, D., Silveira Wda, S., Valentini, S.R., and Zanelli, C.F. (2013). The deoxyhypusine synthase mutant dys1-1 reveals the association of eIF5A and Asc1 with cell wall integrity. PloS one *8*, e60140.

Ganoza, M.C., and Aoki, H. (2000). Peptide bond synthesis: function of the efp gene product. Biological chemistry *381*, 553-559.

Gelperin, D.M., White, M.A., Wilkinson, M.L., Kon, Y., Kung, L.A., Wise, K.J., Lopez-Hoyo, N., Jiang, L., Piccirillo, S., Yu, H., *et al.* (2005). Biochemical and genetic analysis of the yeast proteome with a movable ORF collection. Genes & development *19*, 2816-2826.

Gietz, R.D., Willems, A.R., and Woods, R.A. (1995). Studies on the transformation of intact yeast cells by the LiAc/SS-DNA/PEG procedure. Yeast *11*, 355-560.

Glick, B.R., Chladek, S., and Ganoza, M.C. (1979). Peptide bond formation stimulated by protein synthesis factor EF-P depends on the aminoacyl moiety of the acceptor. European journal of biochemistry / FEBS *97*, 23-28.

Glick, B.R., and Ganoza, M.C. (1975). Identification of a soluble protein that stimulates peptide bond synthesis. Proceedings of the National Academy of Sciences of the United States of America *72*, 4257-4260.

Goldstein, A.L., and McCusker, J.H. (1999). Three new dominant drug resistance cassettes for gene disruption in Saccharomyces cerevisiae. Yeast *15*, 1541-1553.

Gordon, E.D., Mora, R., Meredith, S.C., Lee, C., and Lindquist, S.L. (1987a). Eukaryotic initiation factor 4D, the hypusine-containing protein, is conserved among eukaryotes. The Journal of biological chemistry *262*, 16585-16589.

Gordon, E.D., Mora, R., Meredith, S.C., and Lindquist, S.L. (1987b). Hypusine formation in eukaryotic initiation factor 4D is not reversed when rates or specificity of protein synthesis is altered. The Journal of biological chemistry *262*, 16590-16595.

Gregio, A.P., Cano, V.P., Avaca, J.S., Valentini, S.R., and Zanelli, C.F. (2009). eIF5A has a function in the elongation step of translation in yeast. Biochemical and biophysical research communications *380*, 785-790.

Gutierrez, E., Shin, B.S., Woolstenhulme, C.J., Kim, J.R., Saini, P., Buskirk, A.R., and Dever, T.E. (2013). eIF5A promotes translation of polyproline motifs. Molecular cell *51*, 35-45.

Guttman, M., Russell, P., Ingolia, N.T., Weissman, J.S., and Lander, E.S. (2013). Ribosome profiling provides evidence that large noncoding RNAs do not encode proteins. Cell *154*, 240-251.

Guydosh, N.R., and Green, R. (2014). Dom34 rescues ribosomes in 3' untranslated regions. Cell *156*, 950-962.

Hanawa-Suetsugu, K., Sekine, S., Sakai, H., Hori-Takemoto, C., Terada, T., Unzai, S., Tame, J.R., Kuramitsu, S., Shirouzu, M., and Yokoyama, S. (2004). Crystal structure of elongation factor P from Thermus thermophilus HB8. Proceedings of the National Academy of Sciences of the United States of America *101*, 9595-9600.

Hartwell, L.H., and McLaughlin, C.S. (1969). A mutant of yeast apparently defective in the initiation of protein synthesis. Proc Natl Acad Sci USA *62*, 468-474.

Hatfield, L., Beelman, C.A., Stevens, A., and Parker, R. (1996). Mutations in trans-acting factors affecting mRNA decapping in Saccharomyces cerevisiae. Molecular and cellular biology *16*, 5830-5838.

Henderson, A., and Hershey, J.W. (2011). Eukaryotic translation initiation factor (eIF) 5A stimulates protein synthesis in Saccharomyces cerevisiae. Proceedings of the National Academy of Sciences of the United States of America *108*, 6415-6419.

Hersch, S.J., Wang, M., Zou, S.B., Moon, K.M., Foster, L.J., Ibba, M., and Navarre, W.W. (2013). Divergent protein motifs direct elongation factor P-mediated translational regulation in Salmonella enterica and Escherichia coli. mBio *4*, e00180-00113.

Hinnebusch, A.G., and Lorsch, J.R. (2012). The mechanism of eukaryotic translation initiation: new insights and challenges. Cold Spring Harbor perspectives in biology *4*.

Hofmann, W., Reichart, B., Ewald, A., Muller, E., Schmitt, I., Stauber, R.H., Lottspeich, F., Jockusch, B.M., Scheer, U., Hauber, J., *et al.* (2001). Cofactor requirements for nuclear export of Rev response element (RRE)- and constitutive transport element (CTE)-containing retroviral RNAs. An unexpected role for actin. The Journal of cell biology *152*, 895-910.

Ingolia, N.T., Brar, G.A., Rouskin, S., McGeachy, A.M., and Weissman, J.S. (2012). The ribosome profiling strategy for monitoring translation in vivo by deep sequencing of ribosome-protected mRNA fragments. Nature protocols *7*, 1534-1550.

Ingolia, N.T., Ghaemmaghami, S., Newman, J.R., and Weissman, J.S. (2009). Genome-wide analysis in vivo of translation with nucleotide resolution using ribosome profiling. Science *324*, 218-223.

Ingolia, N.T., Lareau, L.F., and Weissman, J.S. (2011). Ribosome profiling of mouse embryonic stem cells reveals the complexity and dynamics of Mammalian proteomes. Cell *147*, 789-802.

Jao, D.L., and Chen, K.Y. (2006). Tandem affinity purification revealed the hypusine-dependent binding of eukaryotic initiation factor 5A to the translating 80S ribosomal complex. J Cell Biochem *97*, 583-598.

Jayaprakash, A.D., Jabado, O., Brown, B.D., and Sachidanandam, R. (2011). Identification and remediation of biases in the activity of RNA ligases in small-RNA deep sequencing. Nucleic acids research *39*, e141.

Joe, Y.A., and Park, M.H. (1994). Structural features of the eIF-5A precursor required for posttranslational synthesis of deoxyhypusine. The Journal of biological chemistry *269*, 25916-25921.

Johansson, M.J., Esberg, A., Huang, B., Bjork, G.R., and Bystrom, A.S. (2008). Eukaryotic wobble uridine modifications promote a functionally redundant decoding system. Molecular and cellular biology *28*, 3301-3312.

Jorgensen, R., Carr-Schmid, A., Ortiz, P.A., Kinzy, T.G., and Andersen, G.R. (2002). Purification and crystallization of the yeast elongation factor eEF2. Acta crystallographica Section D, Biological crystallography *58*, 712-715.

Kaiser, A. (2012). Translational control of eIF5A in various diseases. Amino acids *42*, 679-684.

Kang, H.A., and Hershey, J.W. (1994). Effect of initiation factor eIF-5A depletion on protein synthesis and proliferation of *Saccharomyces cerevisiae*. The Journal of biological chemistry *269*, 3934-3940.

Kang, H.A., Schwelberger, H.G., and Hershey, J.W. (1993). Translation initiation factor eIF-5A, the hypusine-containing protein, is phosphorylated on serine in Saccharomyces cerevisiae. The Journal of biological chemistry *268*, 14750-14756.

Kang, K.R., Kim, Y.S., Wolff, E.C., and Park, M.H. (2007). Specificity of the deoxyhypusine hydroxylase-eukaryotic translation initiation factor (eIF5A) interaction: identification of amino acid residues of the enzyme required for binding of its substrate, deoxyhypusine-containing eIF5A. The Journal of biological chemistry *282*, 8300-8308.

Kang, K.R., Wolff, E.C., Park, M.H., Folk, J.E., and Chung, S.I. (1995). Identification of *YHR068w* in *Saccharomyces cerevisiae* chromosome VIII as a gene for deoxyhypusine synthase. Expression and characterization of the enzyme. The Journal of biological chemistry *270*, 18408-18412.

Kemper, W.M., Berry, K.W., and Merrick, W.C. (1976). Purification and properties of rabbit reticulocyte protein synthesis initiation factors M2Balpha and M2Bbeta. The Journal of biological chemistry *251*, 5551-5557.

Kim, K.K., Hung, L.W., Yokota, H., Kim, R., and Kim, S.H. (1998). Crystal structures of eukaryotic translation initiation factor 5A from Methanococcus jannaschii at 1.8 A resolution. Proc Natl Acad Sci USA *95*, 10419-10424.

Kim, Y.S., Kang, K.R., Wolff, E.C., Bell, J.K., McPhie, P., and Park, M.H. (2006). Deoxyhypusine hydroxylase is a Fe(II)-dependent, HEAT-repeat enzyme. Identification of amino acid residues critical for Fe(II) binding and catalysis [corrected]. The Journal of biological chemistry *281*, 13217-13225.

Klier, H., Wohl, T., Eckerskorn, C., Magdolen, V., and Lottspeich, F. (1993). Determination and mutational analysis of the phosphorylation site in the hypusine-containing protein Hyp2p. FEBS letters *334*, 360-364.

Kyrpides, N.C., and Woese, C.R. (1998). Universally conserved translation initiation factors. Proc Natl Acad Sci USA *95*, 224-228.

Lau, N.C., Lim, L.P., Weinstein, E.G., and Bartel, D.P. (2001). An abundant class of tiny RNAs with probable regulatory roles in Caenorhabditis elegans. Science *294*, 858-862.

Letzring, D.P., Dean, K.M., and Grayhack, E.J. (2010). Control of translation efficiency in yeast by codon-anticodon interactions. RNA *16*, 2516-2528.

Li, C.H., Ohn, T., Ivanov, P., Tisdale, S., and Anderson, P. (2010). eIF5A promotes translation elongation, polysome disassembly and stress granule assembly. PloS one *5*, e9942.

Li, G.W., Oh, E., and Weissman, J.S. (2012). The anti-Shine-Dalgarno sequence drives translational pausing and codon choice in bacteria. Nature *484*, 538-541.

Li, T., Belda-Palazon, B., Ferrando, A., and Alepuz, P. (2014). Fertility and Polarized Cell Growth Depends on eIF5A for Translation of Polyproline-Rich Formins in Saccharomyces cerevisiae. Genetics *197*, 1191-1200.

Liao, D.I., Wolff, E.C., Park, M.H., and Davies, D.R. (1998). Crystal structure of the NAD complex of human deoxyhypusine synthase: an enzyme with a ball-and-chain mechanism for blocking the active site. Structure *6*, 23-32.

Lobanov, A.V., Turanov, A.A., Hatfield, D.L., and Gladyshev, V.N. (2010). Dual functions of codons in the genetic code. Critical reviews in biochemistry and molecular biology *45*, 257-265.

Longtine, M.S., McKenzie III, A., Demarini, D.J., Shah, N.G., Wach, A., Brachat, A., Philippsen, P., and Pringle, J.R. (1998). Additonal modules for versatile and economical PCR-based gene deletion and modification in *Saccharomyces cerevisiae*. Yeast *14*, 953-961.

Lowry, C.V., Weiss, J.L., Walthall, D.A., and Zitomer, R.S. (1983). Modulator sequences mediate oxygen regulation of CYC1 and a neighboring gene in yeast. Proceedings of the National Academy of Sciences of the United States of America *80*, 151-155.

Magdolen, V., Klier, H., Wohl, T., Klink, F., Hirt, H., Hauber, J., and Lottspeich, F. (1994). The function of the hypusine-containing proteins of yeast and other eukaryotes is well conserved. Molecular & general genetics : MGG *244*, 646-652.

Mehta, K.D., Leung, D., Lefebvre, L., and Smith, M. (1990). The ANB1 locus of Saccharomyces cerevisiae encodes the protein synthesis initiation factor eIF-4D. The Journal of biological chemistry *265*, 8802-8807.

Merrick, W.C. (1979a). Assays for eukaryotic protein synthesis. Methods Enzymol *60*, 108-123.

Merrick, W.C. (1979b). Purification of protein synthesis initiation factors from rabbit reticulocytes. Methods in enzymology *60*, 101-108.

Morgan, A.A., and Rubenstein, E. (2013). Proline: the distribution, frequency, positioning, and common functional roles of proline and polyproline sequences in the human proteome. PloS one *8*, e53785.

Murphey, R.J., and Gerner, E.W. (1987). Hypusine formation in protein by a two-step process in cell lysates. The Journal of biological chemistry *262*, 15033-15036.

Muto, H., and Ito, K. (2008). Peptidyl-prolyl-tRNA at the ribosomal P-site reacts poorly with puromycin. Biochemical and biophysical research communications *366*, 1043-1047.

Navarre, W.W., Zou, S.B., Roy, H., Xie, J.L., Savchenko, A., Singer, A., Edvokimova, E., Prost, L.R., Kumar, R., Ibba, M., *et al.* (2010). PoxA, yjeK, and elongation factor P coordinately modulate virulence and drug resistance in Salmonella enterica. Molecular cell *39*, 209-221.

Nishimura, K., Lee, S.B., Park, J.H., and Park, M.H. (2012). Essential role of eIF5A-1 and deoxyhypusine synthase in mouse embryonic development. Amino acids *42*, 703-710.

Oh, E., Becker, A.H., Sandikci, A., Huber, D., Chaba, R., Gloge, F., Nichols, R.J., Typas, A., Gross, C.A., Kramer, G., *et al.* (2011). Selective ribosome profiling reveals the cotranslational chaperone action of trigger factor in vivo. Cell *147*, 1295-1308.

Ortiz, P.A., Ulloque, R., Kihara, G.K., Zheng, H., and Kinzy, T.G. (2006). Translation elongation factor 2 anticodon mimicry domain mutants affect fidelity and diphtheria toxin resistance. The Journal of biological chemistry *281*, 32639-32648.

Park, J.H., Aravind, L., Wolff, E.C., Kaevel, J., Kim, Y.S., and Park, M.H. (2006). Molecular cloning, expression, and structural prediction of deoxyhypusine hydroxylase: a HEAT-repeat-containing metalloenzyme. Proceedings of the National Academy of Sciences of the United States of America *103*, 51-56.

Park, J.H., Dias, C.A., Lee, S.B., Valentini, S.R., Sokabe, M., Fraser, C.S., and Park, M.H. (2011). Production of active recombinant eIF5A: reconstitution in E.coli of eukaryotic hypusine modification of eIF5A by its coexpression with modifying enzymes. Protein engineering, design & selection : PEDS *24*, 301-309.

Park, J.H., Johansson, H.E., Aoki, H., Huang, B.X., Kim, H.Y., Ganoza, M.C., and Park, M.H. (2012). Post-translational modification by beta-lysylation is required for activity of Escherichia coli elongation factor P (EF-P). The Journal of biological chemistry *287*, 2579-2590.

Park, J.H., Wolff, E.C., Folk, J.E., and Park, M.H. (2003). Reversal of the deoxyhypusine synthesis reaction. Generation of spermidine or homospermidine from deoxyhypusine by deoxyhypusine synthase. The Journal of biological chemistry *278*, 32683-32691.

Park, M.H. (1987). Regulation of biosynthesis of hypusine in Chinese hamster ovary cells. Evidence for eIF-4D precursor polypeptides. The Journal of biological chemistry *262*, 12730-12734.

Park, M.H. (1989). The essential role of hypusine in eukaryotic translation initiation factor 4D (eIF-4D). Purification of eIF-4D and its precursors and comparison of their activities. The Journal of biological chemistry *264*, 18531-18535.

Park, M.H. (2006). The post-translational synthesis of a polyamine-derived amino acid, hypusine, in the eukaryotic translation initiation factor 5A (eIF5A). Journal of biochemistry *139*, 161-169.

Park, M.H., Cooper, H.L., and Folk, J.E. (1981). Identification of hypusine, an unusual amino acid, in a protein from human lymphocytes and of spermidine as its biosynthetic precursor. Proceedings of the National Academy of Sciences of the United States of America *78*, 2869-2873.

Park, M.H., Joe, Y.A., and Kang, K.R. (1998). Deoxyhypusine synthase activity is essential for cell viability in the yeast Saccharomyces cerevisiae. The Journal of biological chemistry *273*, 1677-1683.

Park, M.H., Lee, Y.B., and Joe, Y.A. (1997). Hypusine is essential for eukaryotic cell proliferation. Biological signals *6*, 115-123.

Park, M.H., Liu, T.Y., Neece, S.H., and Swiggard, W.J. (1986). Eukaryotic initiation factor 4D. Purification from human red blood cells and the sequence of amino acids around its single hypusine residue. The Journal of biological chemistry *261*, 14515-14519.

Park, M.H., Nishimura, K., Zanelli, C.F., and Valentini, S.R. (2010). Functional significance of eIF5A and its hypusine modification in eukaryotes. Amino acids *38*, 491-500.

Park, M.H., Wolff, E.C., Smit-McBride, Z., Hershey, J.W., and Folk, J.E. (1991). Comparison of the activities of variant forms of eIF-4D. The requirement for hypusine or deoxyhypusine. The Journal of biological chemistry *266*, 7988-7994.

Patel, P.H., Costa-Mattioli, M., Schulze, K.L., and Bellen, H.J. (2009). The Drosophila deoxyhypusine hydroxylase homologue nero and its target eIF5A are required for cell growth and the regulation of autophagy. The Journal of cell biology *185*, 1181-1194.

Pavlov, M.Y., Watts, R.E., Tan, Z., Cornish, V.W., Ehrenberg, M., and Forster, A.C. (2009). Slow peptide bond formation by proline and other N-alkylamino acids in translation. Proceedings of the National Academy of Sciences of the United States of America *106*, 50-54.

Peat, T.S., Newman, J., Waldo, G.S., Berendzen, J., and Terwilliger, T.C. (1998). Structure of translation initiation factor 5A from Pyrobaculum aerophilum at 1.75 A resolution. Structure *6*, 1207-1214.

Pech, M., Karim, Z., Yamamoto, H., Kitakawa, M., Qin, Y., and Nierhaus, K.H. (2011). Elongation factor 4 (EF4/LepA) accelerates protein synthesis at increased Mg2+ concentrations. Proceedings of the National Academy of Sciences of the United States of America *108*, 3199-3203.

Peil, L., Starosta, A.L., Lassak, J., Atkinson, G.C., Virumae, K., Spitzer, M., Tenson, T., Jung, K., Remme, J., and Wilson, D.N. (2013). Distinct XPPX sequence motifs induce ribosome stalling, which is rescued by the translation elongation factor EF-P. Proceedings of the National Academy of Sciences of the United States of America *110*, 15265-15270.

Peil, L., Starosta, A.L., Virumae, K., Atkinson, G.C., Tenson, T., Remme, J., and Wilson, D.N. (2012). Lys34 of translation elongation factor EF-P is hydroxylated by YfcM. Nature chemical biology *8*, 695-697.

Ramachandran, G.N., and Mitra, A.K. (1976). An explanation for the rare occurrence of cis peptide units in proteins and polypeptides. Journal of molecular biology *107*, 85-92.

Roy, H., Zou, S.B., Bullwinkle, T.J., Wolfe, B.S., Gilreath, M.S., Forsyth, C.J., Navarre, W.W., and Ibba, M. (2011). The tRNA synthetase paralog PoxA modifies elongation factor-P with (R)-beta-lysine. Nature chemical biology *7*, 667-669.

Ruhl, M., Himmelspach, M., Bahr, G.M., Hammerschmid, F., Jaksche, H., Wolff, B., Aschauer, H., Farrington, G.K., Probst, H., Bevec, D., *et al.* (1993). Eukaryotic initiation factor 5A is a cellular target of the human immunodeficiency virus type 1 Rev activation domain mediating trans-activation. The Journal of cell biology *123*, 1309-1320.

Saini, P., Eyler, D.E., Green, R., and Dever, T.E. (2009). Hypusine-containing protein eIF5A promotes translation elongation. Nature *459*, 118-121.

Sasaki, K., Abid, M.R., and Miyazaki, M. (1996). Deoxyhypusine synthase gene is essential for cell viability in the yeast Saccharomyces cerevisiae. FEBS letters *384*, 151-154.

Schmeing, T.M., Voorhees, R.M., Kelley, A.C., Gao, Y.G., Murphy, F.V.t., Weir, J.R., and Ramakrishnan, V. (2009). The crystal structure of the ribosome bound to EF-Tu and aminoacyl-tRNA. Science *326*, 688-694.

Schmeing, T.M., Voorhees, R.M., Kelley, A.C., and Ramakrishnan, V. (2011). How mutations in tRNA distant from the anticodon affect the fidelity of decoding. Nat Struct Mol Biol *18*, 432-436.

Schneider-Poetsch, T., Ju, J., Eyler, D.E., Dang, Y., Bhat, S., Merrick, W.C., Green, R., Shen, B., and Liu, J.O. (2010). Inhibition of eukaryotic translation elongation by cycloheximide and lactimidomycin. Nature chemical biology *6*, 209-217.

Schnier, J., Schwelberger, H.G., Smit-McBride, Z., Kang, H.A., and Hershey, J.W.B. (1991). Translation initiation factor 5A and its hypusine modification are essential for cell viability in the yeast *Saccharomyces cerevisiae*. Molecular and cellular biology *11*, 3105-3114.

Schrader, R., Young, C., Kozian, D., Hoffmann, R., and Lottspeich, F. (2006). Temperature-sensitive eIF5A mutant accumulates transcripts targeted to the nonsense-mediated decay pathway. The Journal of biological chemistry *281*, 35336-35346.

Schreier, M.H., Erni, B., and Staehelin, T. (1977). Initiation of mammalian protein synthesis: purification and characterization of seven initiation factors. Journal of molecular biology *116*, 727-753.

Schwelberger, H.G., Kang, H.A., and Hershey, J.W. (1993). Translation initiation factor eIF-5A expressed from either of two yeast genes or from human cDNA. Functional identity under aerobic and anaerobic conditions. The Journal of biological chemistry *268*, 14018-14025.

Scuoppo, C., Miething, C., Lindqvist, L., Reyes, J., Ruse, C., Appelmann, I., Yoon, S., Krasnitz, A., Teruya-Feldstein, J., Pappin, D., *et al.* (2012). A tumour suppressor network relying on the polyamine-hypusine axis. Nature *487*, 244-248.

Shiba, T., Mizote, H., Kaneko, T., Nakajima, T., and Kakimoto, Y. (1971). Hypusine, a new amino acid occurring in bovine brain. Isolation and structural determination. Biochimica et biophysica acta *244*, 523-531.

Shin, B.S., Acker, M.G., Maag, D., Kim, J.R., Lorsch, J.R., and Dever, T.E. (2007). Intragenic suppressor mutations restore GTPase and translation functions of a eukaryotic initiation factor 5B switch II mutant. Molecular and cellular biology *27*, 1677-1685.

Shin, B.S., and Dever, T.E. (2007). Molecular genetic structure-function analysis of translation initiation factor eIF5B. Methods in enzymology *429*, 185-201.

Shin, B.S., Kim, J.R., Walker, S.E., Dong, J., Lorsch, J.R., and Dever, T.E. (2011). Initiation factor eIF2γ promotes eIF2–GTP–Met-tRNA$_i^{Met}$ ternary complex binding to the 40S ribosome. Nat Struct Mol Biol *18*, 1227-1234.

Sievert, H., Pallmann, N., Miller, K.K., Hermans-Borgmeyer, I., Venz, S., Sendoel, A., Preukschas, M., Schweizer, M., Bottcher, S., Janiesch, P.C., *et al.* (2014b). A novel mouse model for inhibition of DOHH mediated hypusine modification reveals crucial function for embryonic development, proliferation and oncogenic transformation. Disease models & mechanisms.

Silvera, D., Formenti, S.C., and Schneider, R.J. (2010). Translational control in cancer. Nat Rev Cancer *10*, 254-266.

Simonetti, A., Marzi, S., Jenner, L., Myasnikov, A., Romby, P., Yusupova, G., Klaholz, B.P., and Yusupov, M. (2009). A structural view of translation initiation in bacteria. Cellular and molecular life sciences : CMLS *66*, 423-436.

Smit-McBride, Z., Dever, T.E., Hershey, J.W., and Merrick, W.C. (1989a). Sequence determination and cDNA cloning of eukaryotic initiation factor 4D, the hypusine-containing protein. The Journal of biological chemistry *264*, 1578-1583.

Smit-McBride, Z., Schnier, J., Kaufman, R.J., and Hershey, J.W. (1989b). Protein synthesis initiation factor eIF-4D. Functional comparison of native and unhypusinated forms of the protein. The Journal of biological chemistry *264*, 18527-18530.

Steitz, J.A. (1969). Polypeptide chain initiation: nucleotide sequences of the three ribosomal binding sites in bacteriophage R17 RNA. Nature *224*, 957-964.

SternJohn, J., Hati, S., Siliciano, P.G., and Musier-Forsyth, K. (2007). Restoring species-specific posttransfer editing activity to a synthetase with a defunct editing domain.

Proceedings of the National Academy of Sciences of the United States of America *104*, 2127-2132.

Sugimoto, A. (2004). High-throughput RNAi in Caenorhabditis elegans: genome-wide screens and functional genomics. Differentiation; research in biological diversity *72*, 81-91.

Tan, S. (2001). A modular polycistronic expression system for overexpressing protein complexes in *Escherichia coli*. Protein Expr Purif *21*, 224-234.

Tanner, D.R., Cariello, D.A., Woolstenhulme, C.J., Broadbent, M.A., and Buskirk, A.R. (2009). Genetic identification of nascent peptides that induce ribosome stalling. The Journal of biological chemistry *284*, 34809-34818.

Thomas, A., Goumans, H., Amesz, H., Benne, R., and Voorma, H.O. (1979). A comparison of the initiation factors of eukaryotic protein synthesis from ribosomes and from the postribosomal supernatant. European journal of biochemistry / FEBS *98*, 329-337.

Thompson, G.M., Cano, V.S., and Valentini, S.R. (2003). Mapping eIF5A binding sites for Dys1 and Lia1: in vivo evidence for regulation of eIF5A hypusination. FEBS letters *555*, 464-468.

Tong, Y., Park, I., Hong, B.S., Nedyalkova, L., Tempel, W., and Park, H.W. (2009). Crystal structure of human eIF5A1: insight into functional similarity of human eIF5A1 and eIF5A2. Proteins *75*, 1040-1045.

Triana-Alonso, F.J., Chakraburtty, K., and Nierhaus, K.H. (1995). The elongation factor unique in higher fungi and essential for protein biosynthesis is an E site factor. The Journal of biological chemistry *270*, 20473-20478.

Ude, S., Lassak, J., Starosta, A.L., Kraxenberger, T., Wilson, D.N., and Jung, K. (2013). Translation elongation factor EF-P alleviates ribosome stalling at polyproline stretches. Science *339*, 82-85.

Umland, T.C., Wolff, E.C., Park, M.H., and Davies, D.R. (2004). A new crystal structure of deoxyhypusine synthase reveals the configuration of the active enzyme and of an enzyme.NAD.inhibitor ternary complex. The Journal of biological chemistry *279*, 28697-28705.

Valentini, S.R., Casolari, J.M., Oliveira, C.C., Silver, P.A., and McBride, A.E. (2002). Genetic interactions of yeast eukaryotic translation initiation factor 5A (eIF5A) reveal connections to poly(A)-binding protein and protein kinase C signaling. Genetics *160*, 393-405.

Weir, B.A., and Yaffe, M.P. (2004). Mmd1p, a novel, conserved protein essential for normal mitochondrial morphology and distribution in the fission yeast Schizosaccharomyces pombe. Molecular biology of the cell *15*, 1656-1665.

Wohl, T., Klier, H., Ammer, H., Lottspeich, F., and Magdolen, V. (1993). The HYP2 gene of Saccharomyces cerevisiae is essential for aerobic growth: characterization of different isoforms of the hypusine-containing protein Hyp2p and analysis of gene disruption mutants. Molecular & general genetics : MGG *241*, 305-311.

Wohlgemuth, I., Brenner, S., Beringer, M., and Rodnina, M.V. (2008). Modulation of the rate of peptidyl transfer on the ribosome by the nature of substrates. The Journal of biological chemistry *283*, 32229-32235.

Wolff, E.C., Folk, J.E., and Park, M.H. (1997). Enzyme-substrate intermediate formation at lysine 329 of human deoxyhypusine synthase. The Journal of biological chemistry *272*, 15865-15871.

Wolff, E.C., Lee, Y.B., Chung, S.I., Folk, J.E., and Park, M.H. (1995). Deoxyhypusine synthase from rat testis: purification and characterization. The Journal of biological chemistry *270*, 8660-8666.

Wolff, E.C., Park, M.H., and Folk, J.E. (1990). Cleavage of spermidine as the first step in deoxyhypusine synthesis. The role of NAD. The Journal of biological chemistry *265*, 4793-4799.

Woolstenhulme, C.J., Parajuli, S., Healey, D.W., Valvarde, D.P., Ptersen, E.N., Starosta, A.L., Guydosh, N.R., Johnson, W.E., Wilson, D.N., and Buskirk, A.R. (2013). Nascent peptides that block protein synthesis in bacteria. Proceedings of the National Academy of Sciences of the United States of America *In press*.

Yanagisawa, T., Sumida, T., Ishii, R., Takemoto, C., and Yokoyama, S. (2010). A paralog of lysyl-tRNA synthetase aminoacylates a conserved lysine residue in translation elongation factor P. Nat Struct Mol Biol *17*, 1136-1143.

Yao, M., Ohsawa, A., Kikukawa, S., Tanaka, I., and Kimura, M. (2003). Crystal structure of hyperthermophilic archaeal initiation factor 5A: a homologue of eukaryotic initiation factor 5A (eIF-5A). Journal of biochemistry *133*, 75-81.

Yokogawa, T., Kitamura, Y., Nakamura, D., Ohno, S., and Nishikawa, K. (2010). Optimization of the hybridization-based method for purification of thermostable tRNAs in the presence of tetraalkylammonium salts. Nucleic acids research *38*, e89.

Youngman, E.M., Brunelle, J.L., Kochaniak, A.B., and Green, R. (2004). The active site of the ribosome is composed of two layers of conserved nucleotides with distinct roles in peptide bond formation and peptide release. Cell *117*, 589-599.

Zanelli, C.F., Maragno, A.L., Gregio, A.P., Komili, S., Pandolfi, J.R., Mestriner, C.A., Lustri, W.R., and Valentini, S.R. (2006). eIF5A binds to translational machinery components and affects translation in yeast. Biochemical and biophysical research communications *348*, 1358-1366.

Zanelli, C.F., and Valentini, S.R. (2005). Pkc1 acts through Zds1 and Gic1 to suppress growth and cell polarity defects of a yeast eIF5A mutant. Genetics *171*, 1571-1581.

Zender, L., Xue, W., Zuber, J., Semighini, C.P., Krasnitz, A., Ma, B., Zender, P., Kubicka, S., Luk, J.M., Schirmacher, P., *et al.* (2008). An oncogenomics-based in vivo RNAi screen identifies tumor suppressors in liver cancer. Cell *135*, 852-864.

Zuk, D., and Jacobson, A. (1998). A single amino acid substitution in yeast eIF-5A results in mRNA stabilization. The EMBO journal *17*, 2914-2925.

8. Curriculum Vitae

8.1 Curriculum Vitae

Erik Niko Espiritu Gutierrez

Employment History

2009 – 2014 Pre-Doctoral IRTA Fellow. Graduate Partnership Program between Johns Hopkins University and National Institutes of Health.

2004 – 2009 Scientific Associate II. Novartis Institutes for Biomedical Research. Cambridge, MA. Center for Proteomic Chemistry.

2002 – 2004 Associate Scientist. Schering-Plough Research Institute. Kenilworth, NJ. New Leads Discovery.

Education

2014 Ph.D. Candidate in Cellular, Molecular, Developmental Biology, and Biophysics. Johns Hopkins University, Baltimore, MD and National Institutes of Health, Bethesda, MD.

2002 B.S. in Biochemistry. Boston College. Chestnut Hill, MA.

Publications

1. Dever, T.E., Gutierrez, E., and Shin, B.S. (2014). The hypusine-containing translation factor eIF5A. Critical reviews in biochemistry and molecular biology *49*, 413-425.

2. Rodrigo-Brenni, M.C., Gutierrez, E., and Hegde, R.S. (2014). Cytosolic quality control of mislocalized proteins requires RNF126 recruitment to Bag6. Molecular cell *55*, 227-237.

3. Gutierrez, E., Shin, B.S., Woolstenhulme, C.J., Kim, J.R., Saini, P., Buskirk, A.R., and Dever, T.E. (2013). eIF5A promotes translation of polyproline motifs. Molecular cell *51*, 35-45.

4. Hessa, T., Sharma, A., Mariappan, M., Eshleman, H.D., Gutierrez, E., and Hegde, R.S. (2011). Protein targeting and degradation are coupled for elimination of mislocalized proteins. Nature *475*, 394-397.

Selected Oral and Poster Presentations

1. Gutierrez, E. (2014). eIF5A promotes translation of polyproline motifs. National Institute of Child Health and Human Development Graduate Student Seminar.

2. Gutierrez, E. Shin, B.S., Woolstenhulme, C.J., Kim, J.R., Buskirk, A.R., and Dever, T.E. (2014). Translation factor eIF5A promotes peptide bond synthesis of consecutive proline sequences. National Institutes of Health Graduate Student Symposium.

3. Gutierrez, E. (2013). eIF5A promotes translation of polyproline motifs. National Institutes of Health Graduate Student Seminar Series (GS3).

4. Gutierrez, E. Shin, B.S., and Dever, T.E. (2012). The role of eIF5A and its hypusine modification in protein synthesis. New England Science Symposium.

Graduate Laboratory Rotations

Winter 2011	Section on Protein Biosynthesis, Laboratory of Thomas Dever, National Institutes of Health. Bethesda, MD. Role of eIF5A and its hypusine modification in protein synthesis.
Summer 2010	Section on Protein Biogenesis, Laboratory of Ramanujan Hegde. National Institutes of Health. Bethesda, MD. Mechanism of substrate triage by a cytosolic chaperone for membrane proteins.
Fall 2009	Department of Biophysics, Laboratory of Sarah Woodson, Johns Hopkins University. Baltimore, MD. Characterization of the interactions between ribosomal protein S4 and 16S rRNA.
Fall 2009	Department of Biology, Laboratory of Yixian Zheng, Johns Hopkins University and Carnegie Institute of Washington. Baltimore, MD. Cell morphogenesis and mitotic spindle assembly.
Summer 2009	Section on Organelle Biology, Laboratory of Jennifer Lippincott-Schwartz. National Institutes of Health. Bethesda, MD. Hedgehog signaling during intraflagellar transport in primary cilia.

8.2 Papers published as a member of the Ramanujan Hegde laboratory

From June of 2009 to March of 2010, I was a member of the Hegde laboratory where I studied the mechanisms of cytosolic quality control of membrane proteins. My work in the Hegde lab has contributed to the publication of two papers:

1. Cytosolic quality control of mislocalized proteins requires RNF126 recruitment to Bag6. Rodrigo-Brenni, M.C., Gutierrez, E., and Hegde, R.S. (2014). Molecular cell *55*, 227-237.

Abstract: Approximately 30% of eukaryotic proteins contain hydrophobic signals for localization to the secretory pathway. These proteins can be mislocalized in the cytosol due to mutations in their targeting signals, certain stresses, or intrinsic inefficiencies in their translocation. Mislocalized proteins (MLPs) are protected from aggregation by the Bag6 complex and degraded by a poorly characterized proteasome-dependent pathway. Here, we identify the ubiquitin ligase RNF126 as a key component of the MLP degradation pathway. In vitro reconstitution and fractionation studies reveal that RNF126 is the primary Bag6-dependent ligase. RNF126 is recruited to the N-terminal Ubl domain of Bag6 and preferentially ubiquitinates juxtahydrophobic lysine residues on Bag6-associated clients. Interfering with RNF126 recruitment in vitro prevents ubiquitination, and RNF126 depletion in cells partially stabilizes a Bag6 client. Bag6-dependent ubiquitination can be recapitulated with purified components, paving the way for mechanistic analyses of downstream steps in this cytosolic quality control pathway.

2. Protein targeting and degradation are coupled for elimination of mislocalized proteins. Hessa, T., Sharma, A., Mariappan, M., Eshleman, H.D., Gutierrez, E., and Hegde, R.S. (2011). Nature *475*, 394-397.

Abstract: A substantial proportion of the genome encodes membrane proteins that are delivered to the endoplasmic reticulum by dedicated targeting pathways. Membrane proteins that fail targeting must be rapidly degraded to avoid aggregation and disruption of cytosolic protein homeostasis. The mechanisms of mislocalized protein (MLP) degradation are unknown. Here we reconstitute MLP degradation in vitro to identify factors involved in this pathway. We find that nascent membrane proteins tethered to ribosomes are not substrates for ubiquitination unless they are released into the cytosol. Their inappropriate release results in capture by the Bag6 complex, a recently identified ribosome-associating chaperone4. Bag6-complex-mediated capture depends on the presence of unprocessed or non-inserted hydrophobic domains that distinguish MLPs from potential cytosolic proteins. A subset of these Bag6 complex 'clients' are transferred to TRC40 for insertion into the membrane, whereas the remainder are rapidly ubiquitinated. Depletion of the Bag6 complex selectively impairs the efficient ubiquitination of MLPs. Thus, by its presence on ribosomes that are synthesizing nascent membrane proteins, the Bag6 complex links targeting and ubiquitination pathways. We propose that such coupling allows the fast tracking of MLPs for degradation without futile engagement of the cytosolic folding machinery.